**Determination of the Rate of Contaminant Oxidations by Permanganate:
Implications for In Situ Chemical Oxidation (ISCO)**

Rachel H. Waldemer
B.S., Iowa State University, 2000

A thesis presented to the faculty of
OGI School of Science & Engineering
at Oregon Health & Science University
in partial fulfillment of the requirements for the degree
Master of Science
in
Environmental Science and Engineering

October 2004

The thesis "Determination of the Rate of Contaminant Oxidations by Permanganate: Implications for In Situ Chemical Oxidation (ISCO)" has been examined and approved by the following Examination Committee:

_____
Dr. Paul Tratnyek, Thesis Advisor
Associate Professor

_____
Dr. Phillip Vella
Manager of Technical Support, Carus Chemical Company

_____
Dr. Richard Johnson
Associate Professor

Acknowledgments

First, I would like to thank my thesis advisor, Paul Tratnyek. He provided a nice balance of allowing me to make my own decisions and conclusions while providing great support when needed. In addition to Paul, my lab-mates, Jim, Joel, Jaimie, Vaish, and Bae, deserve thanks for their input and ideas as I struggled with some of the more difficult aspects of my project. I also want to thank the faculty of the EBS department, who are great educators and have given me a lot of encouragement and support throughout my time at OGI. Furthermore, I thank my mom, Judi Bange, for her professional help in editing this document, and I want to thank both of my parents for their encouragement of my educational goals.

Finally, I could not have done this program without the support of my husband, Jim. I especially appreciate his enduring many a conversation about the exciting world of permanganate chemistry and being a great sounding board to bounce ideas off of. I also want to thank him for his calming influence during the most stressful times of research and writing.

Table of Contents

List of Figures

List of Tables

List of Abbreviations

1,1,1-TCA	1,1,1-Trichloroethane
1,2-DCA	1,2-Dichloroethane
BTEX	Benzene, Toluene, Ethylbenzene, and Xylenes
cis-DCE	cis-1,2-dichloroethylene
COC	Contaminant of concern
DDT	p,p'-Dichlorodiphenyltrichloroethane
DNAPL	Dense non-aqueous phase liquid
ETBE	Ethyl tert-butyl ether
ISCO	In situ chemical oxidation
k''	Second-order rate constant
$KMnO_4$	Potassium permanganate
k_{obs}	Pseudo-first-order rate constant
LNAPL	Light non-aqueous phase liquid
MnO_2	Manganese dioxide
MnO_4^-	Permanganate
MTBE	Methyl tert-butyl ether
$NaMnO_4$	Sodium permanganate
NAPL	Non-aqueous phase liquid
NOD	Natural oxidant demand
NOM	Natural organic matter
PAH	Polycyclic aromatic hydrocarbon
PCB	Polychlorinated biphenyl
PCE	Perchloroethylene
PRB	Permeable reactive barrier
QSAR	Quantitative structure activity relationship
RDX	hexahydro-1,3,5-trinitro-1,3,5-triazine
TCE	Trichloroethylene
TNT	2,4,6-Trinitrotoluene
trans-DCE	trans-1,2-dichloroethylene
UV	Ultra-Violet

Abstract

Determination of the Rate of Contaminant Oxidations by Permanganate:
Implications for In Situ Chemical Oxidation (ISCO)
Rachel H. Waldemer, B.S.

M.S., OGI School of Science & Engineering
October 2004

Thesis Advisor: Paul Tratnyek

When assessing the feasibility of in situ chemical oxidation (ISCO) for treatment of a contaminated site, knowledge of the oxidation rates of the contaminants to be treated is critical. While kinetic data for the reactions of permanganate (MnO_4^-) with chlorinated solvents such as trichloroethylene (TCE) and perchloroethylene (PCE) are available, there is a lack of kinetic data for the reactions of MnO_4^- with many other environmental contaminants. To help fill these data gaps, an efficient method of determining rate constants for oxidation of contaminants by MnO_4^- was developed. This method uses UV spectroscopy to analyze decreasing concentrations of MnO_4^- at 525 nm (an absorbance maximum of MnO_4^-) in the presence of excess contaminant. A complication of this method is that colloidal manganese dioxide (MnO_2), a product of MnO_4^- reduction, also absorbs at 525 nm. It is shown here that (for the reaction times of interest) the colloidal MnO_2 particles are small enough that they behave according to Beer's Law of absorbance. Because the particles follow Beer's Law, it was possible to separate the absorbance of MnO_2 from the absorbance of MnO_4^-.

Rate constants of four chlorinated ethylenes—PCE, TCE, cis-1,2-dichloroethylene (cis-DCE), and trans-1,2-dichloroethylene (trans-DCE)—obtained with this method fall within the range of previously published rate constants, many of which were obtained by using gas chromatography to analyze decreasing concentrations of the chlorinated ethylenes in the presence of excess MnO_4^-. After this validation, the UV spectroscopy based method was used to determine oxidation rate constants for 22 other contaminants from the chemical classes of chlorinated alkanes, oxygenates, fuels, phenols, and pesticides. It was determined that many of the phenols and some pesticides have reactivities with MnO_4^- that are similar to (or faster than) the chlorinated ethylenes.

Because chlorinated ethylenes have been treated successfully in the field using ISCO technology with MnO_4^-, it is likely that phenols and some pesticides could also be treated successfully with this technology.

To provide a basis for predicting rate constants for compounds not studied, kinetic data generated from this study along with kinetic data obtained from the published literature were analyzed to determine whether quantitative structure-activity relationships (QSARs) exist for the reaction of compounds with MnO_4^-. A general descriptor that characterizes the reactivity of MnO_4^- with all compounds—regardless of chemical structure—was not found. Within chemical classes, however, the reactivity of the chlorinated ethylenes with MnO_4^- correlated strongly to reactivity of these compounds with ozone, possibly indicating similar mechanisms of oxidation for the two oxidants. Satisfactory descriptors were not found for compounds belonging to the BTEX or oxygenate classes. Because the training set of the QSARs developed for the substituted phenols consists of both phenolate ions and protonated phenols, the correlations cannot be used for predictive purposes outside the pH condition studied.

Chapter 1: Introduction

In situ chemical oxidation (ISCO) is a widely used method of remediation for many contaminated sites. In order to design an effective ISCO system, knowledge of the rate of oxidation of the contaminants to be treated is critical. Although permanganate (MnO_4^-) has become a popular oxidant for ISCO, the only contaminant class for which there are extensive rate data is the chlorinated ethylenes [1-10]. As a result, there are very few data for the rate at which MnO_4^- oxidizes important contaminants of other chemical classes, such as fuels, oxygenates, explosives, and phenols. To overcome this, a protocol that enables the efficient determination of rate constants for these contaminants is needed.

UV spectroscopy is a convenient way to measure MnO_4^- oxidation rates. Permanganate absorbs strongly at 525 nm; therefore, we can use low concentrations of MnO_4^- and maintain pseudo-first-order conditions even with contaminants of concern (COCs) that are only moderately water-soluble (COC solutions with concentrations as low as 1 mM can be analyzed with this method).   Unlike gas chromatography, UV spectroscopy does not require the development of new methods for analyzing chemicals of different chemical classes. This allows rate constants for the oxidation of many COCs to be determined using the same method.

Chapter 2: Background

2.1 Principles of in situ chemical oxidation (ISCO)

The number of contaminated sites in the United States is estimated to be in the hundreds of thousands [11]. About 80% of these sites have contaminated groundwater [12]. The conventional remediation method for contaminated groundwater has been "pump-and-treat," which involves extracting the water for treatment and then discharging or re-injecting the treated water. This method can be costly due to the long operation times (30 years or more in some cases [12]), and the cost of disposing the extracted COCs. Monitored natural attenuation is another popular method of groundwater treatment. While relatively inexpensive, this monitored natural attenuation often requires a longer time frame than active remediation methods to reach the maximum contaminant levels (MCLs) set by the U.S. Environmental Protection Agency (US EPA) [13].

Innovative alternatives to pump-and-treat and natural attenuation include in situ chemical oxidation (ISCO) and permeable reactive barriers (PRBs). ISCO is a technique in which a chemical oxidant is injected into the subsurface at the point of contamination, and PRBs are physical barriers made of a reactive material placed in the groundwater flow path downstream of the source zone. One advantage of treating the COCs in place is that it avoids generating large volumes of water requiring treatment and disposal [14]. These technologies are also advantageous in that they often can achieve the desired level of remediation long before pump-and-treat and natural attenuation [14]. Although there is often a large initial capital cost for both of these methods, it is possible for both to be less expensive than the traditional methods due to the shorter time period of active involvement and monitoring, the lower operational and maintenance costs, and the lack of cost associated with disposal of contaminated waste [14]. An advantage of ISCO over PRBs is that ISCO can be used at sites where it is impractical or impossible to use PRBs,

such as sites where the contamination is very deep within the subsurface. Furthermore, almost all PRBs employ reductive processes [15]; however, not all COCs are degradable by reduction, while most COCs can be oxidized [15].

A disadvantage of ISCO technologies is that they have the potential to oxidize heavy metals, which are often less hazardous in their reduced states. Examples of such metals are uranium, which can be oxidized from U(IV) to U(VI), and chromium, which can be oxidized from Cr(III) to Cr(VI).   Both of these metals are more toxic and mobile in their oxidized states, making ISCO a poor remediation choice where these metals are present in high concentrations. Other sites where ISCO is not advised are sites with large amounts of natural organic matter (NOM), which competes with the COCs for the oxidant [16, 17].

2.2 Pros and cons of MnO_4^- compared with other ISCO technologies

The most common oxidants used for ISCO are MnO_4^-, ozone, and Fenton's Reagent (hydrogen peroxide catalyzed by Fe^{2+} to form ·OH). Sodium persulfate is also gaining interest as an oxidant for ISCO [18, 19], but is still in the initial stages of development.

The other ISCO oxidants react with many COCs more quickly than MnO_4^-. However, because they also react with NOM more quickly, these oxidants are depleted within days, while MnO_4^- can last in the subsurface for several months before being consumed [20]. That MnO_4^- is more stable compared with the other oxidants means fewer injection wells are required because MnO_4^- can be injected further from the point of contamination. In addition, while the Fenton's reaction requires acidic conditions (pH 2 to 4) [21], MnO_4^- is effective over a pH range of 4.0 to 8.0 [4].

A disadvantage of MnO_4^- is that manganese dioxide (MnO_2), the product of MnO_4^- reduction, precipitates. Precipitation of MnO_2 has been shown to reduce permeability of the aquifer in some cases [22-24], and it may also reduce the ability of MnO_4^- to effectively oxidize dense non-aqueous phase liquid (DNAPL) sources by forming a crust on the outside of the DNAPL and thus limit mass transfer from the

DNAPL to the aqueous phase [24]. Unlike MnO_4^-, the other oxidants do not form any insoluble reaction products. However, Fenton's reagent oxidations generate significantly more gas than MnO_4^- oxidation reactions, which increases safety concerns for workers installing the remediation systems.

Another disadvantage of MnO_4^- is that it contains trace amounts of impurities such as chromium (0.5 mg/kg to 13 mg/kg), copper (<0.1 mg/kg to 15 mg/kg), and mercury (N.D to 0.06 mg/kg) [21]. Furthermore, EPA has a secondary quality standard for manganese with an MCL in drinking water of 0.05 mg/L. Secondary quality standards are based on nontoxic effects such as potential discoloration and staining; as such, they are only recommended—not required—by EPA. However, individual states may choose to enforce these standards, which would limit the amount of MnO_4^- that could be injected into the groundwater.

2.3 Sodium vs. potassium permanganate

Permanganate is available commercially in two forms, potassium permanganate ($KMnO_4$) and sodium permanganate ($NaMnO_4$). According to a recent study, the efficiency and kinetics of TCE degradation are essentially the same with $NaMnO_4$ and $KMnO_4$ [25]. However, according to Carus Chemical Company, the largest manufacturer of permanganates worldwide, the amount of $NaMnO_4$ injected for ISCO applications in 2003 was about twice that of $KMnO_4$ [20]. A big advantage of $NaMnO_4$ is that it has ~50% by weight water solubility while the water solubility of $KMnO_4$ is only 6% by weight [26]. In addition, $NaMnO_4$ is sold in liquid form while $KMnO_4$ is only available as a solid that must be mixed with water on-site. Thus, the $KMnO_4$ requires more complex equipment and has the potential for exposing workers to hazardous dust particulates [20].

2.4 Reaction mechanism for MnO_4^- and the chlorinated ethylenes

Most sites using MnO_4^- for ISCO technology are contaminated with chlorinated ethylenes [12]. The generally accepted mechanism of oxidation of alkenes with MnO_4^- is

electrophilic attack by MnO_4^- on the carbon-carbon double bond, forming a cyclic hypomanganate diester [4, 5, 21, 27-29]. The formation of this cyclic hypomanganate diester is the rate-limiting step of the reaction of MnO_4^- and TCE [5]. After the cyclic hypomanganate diester is formed, it quickly degrades into one of four carboxylic acids (the pH of the reaction determines which one) [5]. All four carboxylic acids can then be oxidized by a second MnO_4^- to form carbon dioxide [5]. This reaction scheme is shown in Figure 1.
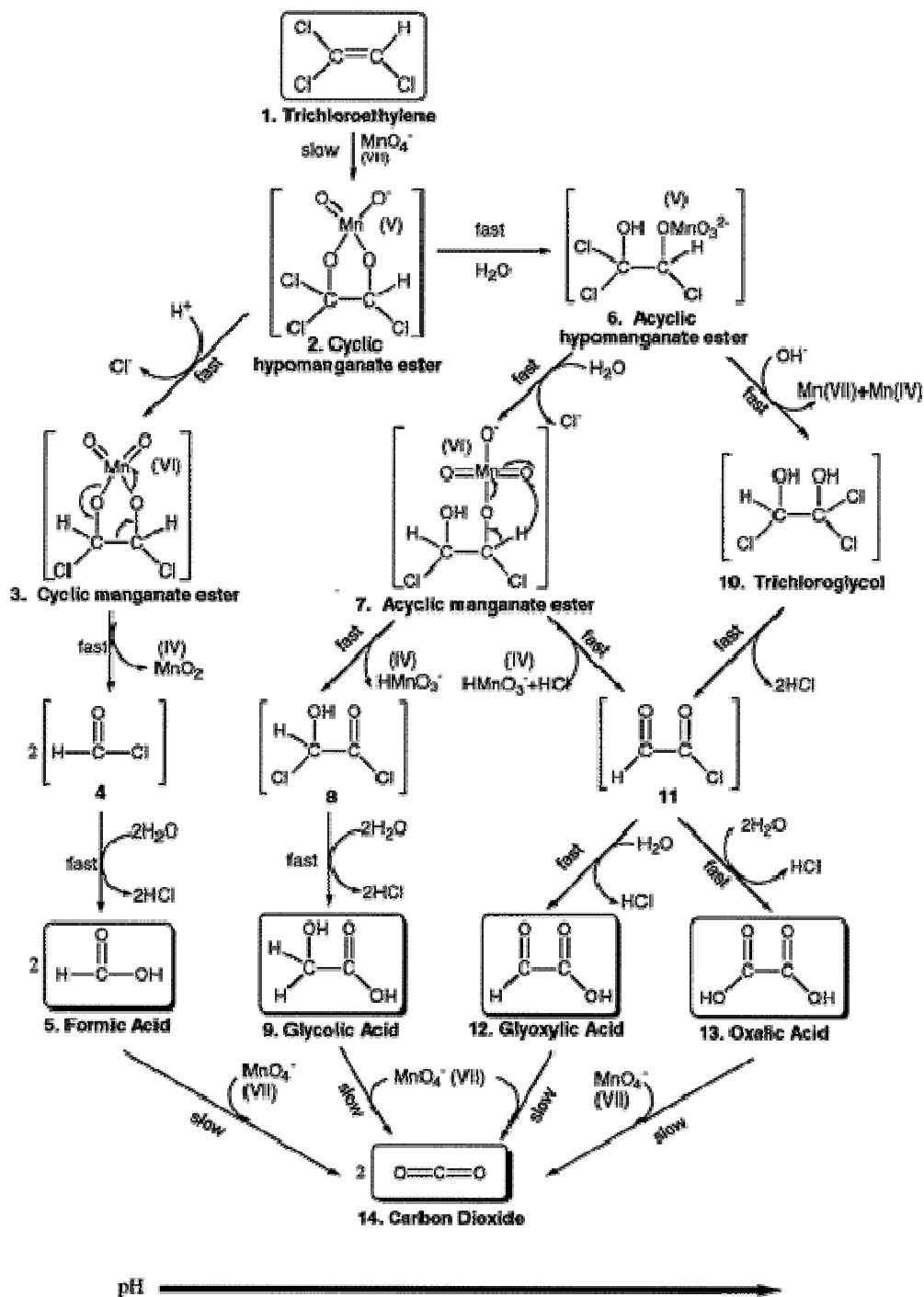
Figure 1: Reaction scheme for the oxidation of TCE by permanganate proposed by Yan and Schwartz (*Environmental Science and Technology, 34,* 2535-2541). Reprinted with permission from *Environmental Science and Technology*. Copyright 2000 American Chemical Society.

Chapter 3: Experimental Methods

3.1 Chemical reagents

All chemicals were obtained in high purity from either Sigma-Aldrich (St. Louis, MO) or ChemService (West Chester, PA) and used without further purification. For the chlorinated ethylenes, stock solutions were prepared as saturated solutions: 1 ml of a chlorinated ethylene was added to 20 ml of water, shaken vigorously, and allowed to equilibrate overnight. The stock solution for toluene was also prepared as a saturated solution; however, as toluene is a LNAPL, the solution was inverted overnight, and the aqueous phase was drawn with a syringe from the upturned vial to avoid contamination with pure phase toluene. The other stock solutions were made by dissolving the COC in water or directly into phosphate buffer to obtain the desired concentration for the stock solution.

Potassium permanganate of 99% purity was obtained from Sigma-Aldrich (St. Louis, MO). The MnO_4^- crystals were dissolved in deionized water[1] to make 5 mM stock solutions.

A 50 mM phosphate buffer was used to control pH (all experiments were done at pH 6.5 or 7.0). A secondary purpose of the phosphate buffer was to inhibit flocculation of the colloidal particles of MnO_2 [30]. For some experiments, 50 mM phosphate buffer was not concentrated enough to prevent flocculation of the MnO_2, so the buffer concentration was increased to 100 mM. Data to show this was effective are given in Chapter 4.

MnO_2 residues can build up on the inside of a cuvette during a reaction; therefore, the cuvettes were cleaned daily with a 6% hydrogen peroxide, 2% sulfuric acid solution.

---

[1] The water was deionized using Millipore's Milli-Q purification system.

The values of the energies of the highest occupied molecular orbital (E_{HOMO}) and the lowest unoccupied molecular orbital (E_{LUMO}) used in Chapter 6 were calculated using molecular modeling software (CAChe, version 6.1). The calculations were performed with the semiempirical method MOPAC using the PM5 parameter set [31] and the Conductor-like Screening Model (COSMO), which was used to incorporate solvent effects [32].

3.2 Stopped-flow vs. static methods

Pseudo-first-order conditions were maintained by using at least a 5:1 ratio of COC to MnO_4^-. A UV/VIS spectrophotometer (Perkin-Elmer model Lambda 20) was used to measure decreasing absorbance at 525 nm, an absorption maximum for MnO_4^-.

Two experimental methods, designated as *stopped-flow* and *static*, were used to analyze the COCs. Advantages of the static method are that it is simple and gives less run-to-run variability. However, many fast-reacting COCs have half-lives less than the ~30 seconds required to set up the static method—these COCs in addition to the other COCs that took less than an hour for the reaction to reach completion were analyzed by the stopped-flow method.

The static method involved premixing the MnO_4^- and the COC in a 1-cm pathlength, 5-ml quartz cuvette with a screw cap seal. This method was used for slow reactions (reactions that took 60 minutes or longer to reach completion). The stopped-flow apparatus consisted of two gas-tight syringes (one for the MnO_4^- and one for the COC stock solution) that were connected to a mixing cell (2 µl dead volume) that lead to a quartz flow-through cuvette with a 1-cm pathlength. A syringe pump enabled quick delivery (~1 sec) from the mixing cell to the cuvette. Second-order rate constants obtained for TCE with the two methods are comparable (0.67 ± 0.05 $M^{-1}s^{-1}$ for the stopped flow method and 0.76 ± 0.03 $M^{-1}s^{-1}$ for the static method).

3.3 Method limitations

An important limitation of the UV-based method of determining rate constants is that while many compounds are sufficiently water soluble to obtain concentrations of 1 mM, compounds of several important chemical classes are not. These include compounds in the dioxin and polyaromatic hydrocarbon (PAH) classes and most explosives, such as 2,4,6-trinitrotoluene (TNT), hexahydro-1,3,5-trinitro-1,3,5-triazine (RDX), and CL-20.

Chapter 4: Data Analysis

4.1 Determination of Beer's Law regime

It has been shown by others that the product of MnO_4^- oxidation is a colloidal form of MnO_2, which also absorbs at 525 nm [4, 30, 33-35]. The colloidal particles have both absorbing and scattering properties; however, their absorbance obeys Beer's Law until the colloidal particles flocculate and scattering becomes dominant. Beer's Law of absorbance states that:

$$A = \mathcal{E}bc \qquad [1]$$

where A is absorbance, $\mathcal{E}$ is absorptivity, b is path-length, and c is concentration. Because Beer's Law also applies to mixtures [36], the absorbance at any wavelength for this reaction is equal to:

$$A_\lambda = [MnO_4^-] \times \mathcal{E}_{MnO_4^-}^\lambda + [MnO_2] \times \mathcal{E}_{MnO_2}^\lambda \qquad [2]$$

where λ is the wavelength of interest, $\mathcal{E}_{MnO_4^-}^\lambda$ is the absorptivity of MnO_4^- at wavelength λ, and $\mathcal{E}_{MnO_2}^\lambda$ is the absorptivity of MnO_2 at wavelength λ. When successive scans of a reaction in which both the reactant and the product absorb light are plotted together (Figure 2A), a sharp isosbestic point indicates that MnO_2 behaves according to Beer's Law. (The isosbestic point is the wavelength at which all molar absorptivities are equal [37].) It follows that the absorbance at that wavelength should not change unless other effects, such as light scattering, become important.

Figure 2B shows the variation of absorbance at 525 nm (where both MnO_4^- and MnO_2 absorb) with absorbance at 418 nm (where only MnO_2 absorbs). A linear relationship between the two provides additional evidence that Beer's Law holds [30, 33]. For reactions that were too fast to be measured with successive scans, a sharp isosbestic

point could not be used to verify that Beer's Law was obeyed. These reactions required replicate experiments, one monitored at 525 nm and the other at 418 nm. As can be seen in Figure 3, this relationship is initially linear, and then has a characteristic curvature. This curvature is most likely a result of flocculation of the colloidal MnO_2 particles. Because the linear region is difficult to define exactly, only 75% of the time for which MnO_2 follows Beer's Law was used in the analysis of the psuedo-first-order rate constant, k_{obs} (as described in Chapter 5).
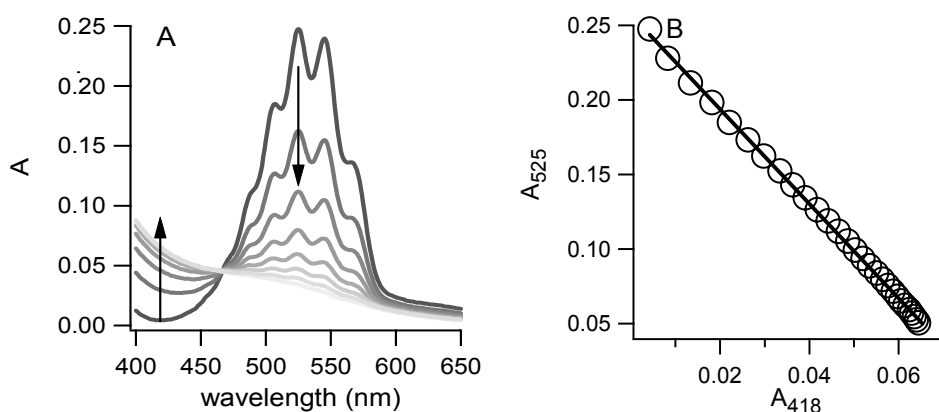
Figure 2: A) Successive scans (in 12-minute intervals) of the reaction between 0.1 mM MnO_4^- and 1.0 mM TCE. Absorbance decreases at 525 nm and increases at 418 nm as the MnO_4^- is reduced by TCE and MnO_2 is produced. Note the sharp isosbestic point at 467 nm. B) A linear relationship between the A_{525} vs. A_{418} data provides additional verification that colloidal MnO_2 follows Beer's Law. Experimental conditions: pH 7, 25°C, 50 mM phosphate buffer.
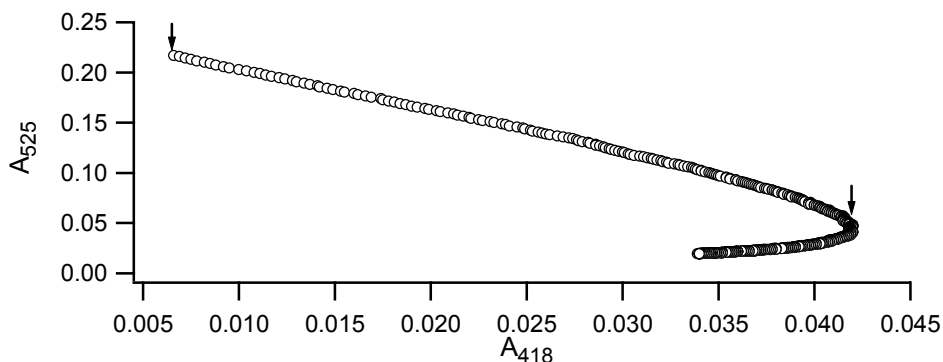
Figure 3: A_{525} for the reaction of 1 mM m-cresol and 0.1 mM $KMnO_4$ is plotted against A_{418} for a reaction set up under identical conditions. The graph is linear, and therefore MnO_2 follows Beer's Law for the initial part of the reaction. The time corresponding to the first 75% of the linear region is used to determine k_{obs}. Experimental conditions: pH 7, 25°C, 50 mM phosphate buffer.

4.2 A special case: COCs that absorb light

Several COCs, most notably the nitrophenols, absorb significantly in the same wavelength range as MnO_4^-. This complicated the application of Beer's Law. Picric acid, and some of the other absorbing COCs still gave an isosbestic point—the main difference from other COCs being that the wavelength of the isosbestic point for nitrophenols shifted from ~467 nm to ~461 nm (see Figure 4).
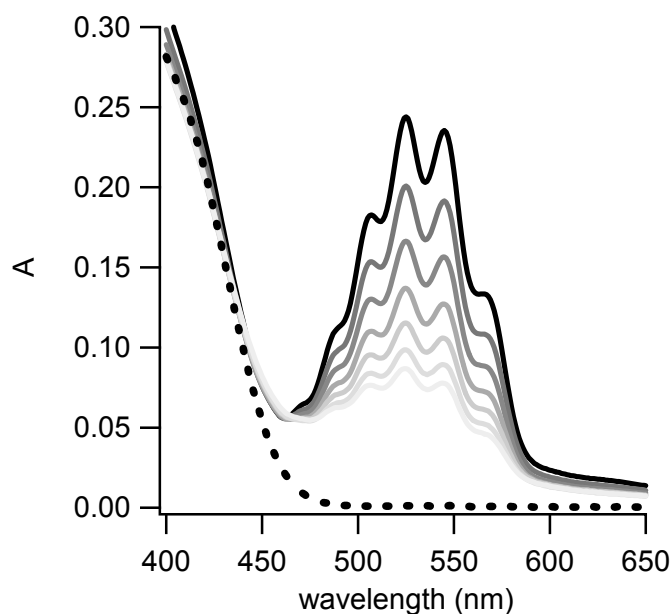
Figure 4: Successive scans (separated by 24 hours) for the reaction of 0.1 mM $KMnO_4$ and 5 mM picric acid.   The absorptive properties of the picric acid cause a shift in the isosbestic point from ~467 nm to ~461 nm.   The dashed line is the spectrum of 5 mM picric acid. Experimental conditions: pH 7, 25°C, 50 mM phosphate buffer.

Other COCs, such as 2,4-dinitrophenol, have such high absorbance in this range that it is difficult to determine an isosbestic point. As shown in Figure 5, the reaction appears to behave according to Beer's Law for up to 5 hours, with the absorbance between 600 and 650 nm decreasing as usual. After 5 hours, however, the absorbance in this region increases. This may be due to light scattering, so only the data for the first 5 hours of the reaction were used to determine k_{obs}.
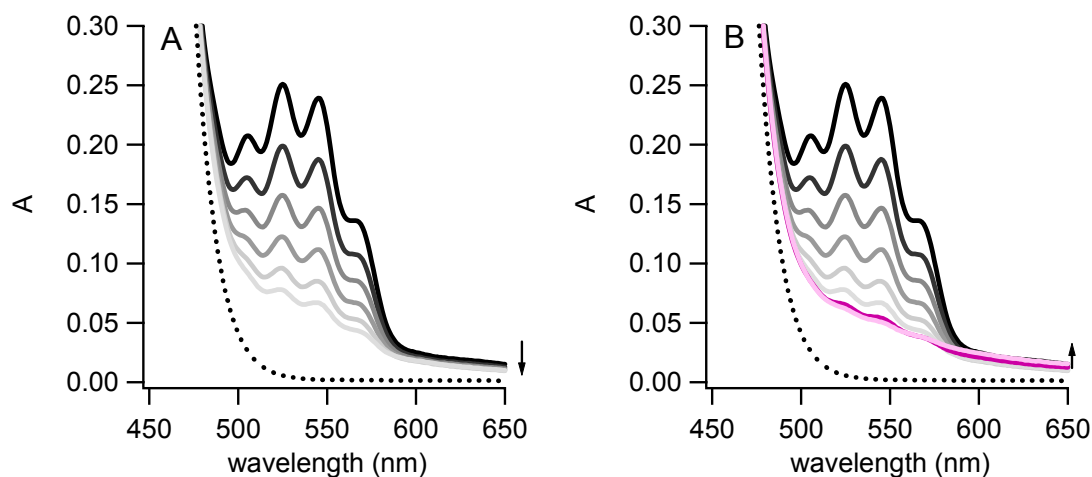
Figure 5: Successive scans (1 hour apart) for the reaction of 0.1 mM MnO_4^- and 1 mM 2,4-dinitrophenol. 5A shows the first 5 hours of the reaction. 5B is identical to 5A with the addition of the last 2 hours of the reaction shown in shades of pink. After the 5th hour, the absorbance in the range of 600 to 650 nm increased over time, when initially the absorbance in this range decreased as the reaction progressed. This was designated to be the point in the reaction where the colloidal MnO_2 no longer followed Beer's Law, so the data used to estimate k_{obs} for 2,4-dinitrophenol were taken from only the first 5 hours. The dashed line is the spectrum of 1 mM 2,4-dinitrophenol. Experimental conditions: pH 7, 25°C, 50 mM phosphate buffer.

4.3 Determining the amount of phosphate buffer to use in a reaction

As mentioned in Chapter 3, the amount of phosphate buffer required to inhibit flocculation of the colloidal manganese dioxide is somewhat reaction-dependent. For most reactions, a 50 mM concentration of phosphate buffer was sufficient for this purpose, as determined by a sharp isosbestic point that is maintained for the majority of the reaction. However, for some of the slower reactions, the isosbestic point is lost early in the reaction when a 50 mM concentration of phosphate buffer was used (Figure 6). For these cases, increasing the phosphate buffer concentration to 100 mM restores the isosbestic point. Appendix A shows the experimental conditions, including phosphate buffer concentration, for all reactions studied.
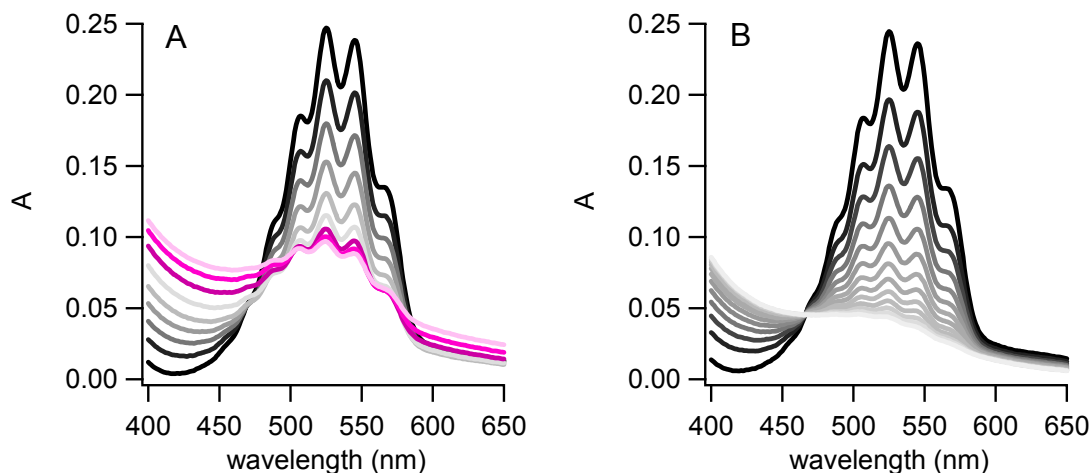
Figure 6: Successive scans (2 hours apart) for the reduction of 0.1 mM KMnO$_4$ by 30 mM methyl ethyl ketone (MEK). A) This reaction with 50 mM phosphate buffer—note that the isosbestic point degrades after 10 hours (the lightest gray spectrum). B) This reaction with 100 mM phosphate buffer—note that the isosbestic point is maintained for all of the reaction (24 hours). Experimental conditions: pH 7, 25°C.

4.4 Derivation of the fitting equation

Assuming that MnO$_4^-$ and MnO$_2$ are the only species absorbing light at 525 nm, for any point in the reaction:

$$A_{525} = [MnO_4^-] \times \mathcal{E}_{MnO_4^-}^{525} + [MnO_2] \times \mathcal{E}_{MnO_2}^{525} \qquad [3]$$

where $\mathcal{E}_{MnO_4^-}^{525}$ is the absorptivity of MnO$_4^-$ at 525 nm and $\mathcal{E}_{MnO_2}^{525}$ is the effective absorptivity of the colloidal MnO$_2$ at 525 nm. While $\mathcal{E}_{MnO_4^-}^{525}$ can be determined from the slope of an absorbance vs. concentration plot (see Figure 7), the colloidal nature of the MnO$_2$ makes it difficult to determine either the concentration of MnO$_2$ or $\mathcal{E}_{MnO_2}^{525}$.

In addition to showing when Beer's Law is obeyed, a sharp isosbestic point also implies that no long-lived absorptive intermediates are formed during the reaction. Therefore, the total concentration (C_T) of MnO$_4^-$ and MnO$_2$ must be equal to the initial amount of MnO$_4^-$ used:

$$C_T = [MnO_4^-]_o = [MnO_4^-] + [MnO_2] \qquad [4]$$
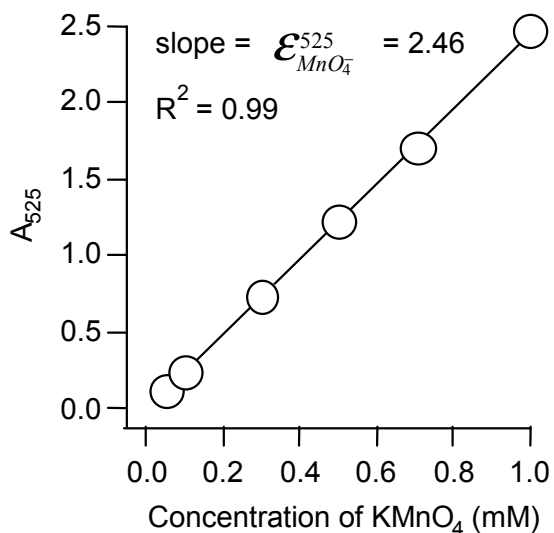
Figure 7: The absorptivity of MnO_4^- was determined from the slope of this absorbance vs. concentration plot.

Mechanistic studies of the chlorinated solvents (PCE, TCE, cis-DCE, and trans-DCE), toluene, and MTBE have been shown to be first-order with regard to both COC and MnO_4^- [4, 35, 38, 39]. As these COCs represent several different chemical classes, it is reasonable to assume that MnO_4^- will follow first-order degradation kinetics with most COCs. Because MnO_2 is the only species that absorbs at 418 nm, this assumption can be verified by fitting a first-order appearance curve to the MnO_2 absorbance data, which is shown in Figure 8. Using the assumption of first-order degradation kinetics, Equation 3 can be rewritten as:

$$A_{525} = [C_T e^{-k_{obs}t}] \times \varepsilon_{MnO_4^-}^{525} + [C_T - C_T e^{-k_{obs}t}] \times \varepsilon_{MnO_2}^{525} \qquad [5]$$

where k_{obs} is the pseudo-first-order rate constant. Equation 5 can be applied to the A_{525} vs. time data to obtain fitted values for both k_{obs} and $\varepsilon_{MnO_2}^{525}$. Chi-squared values for data fitted with Equation 5 are smaller than 0.001 in all cases (see Chapter 5).
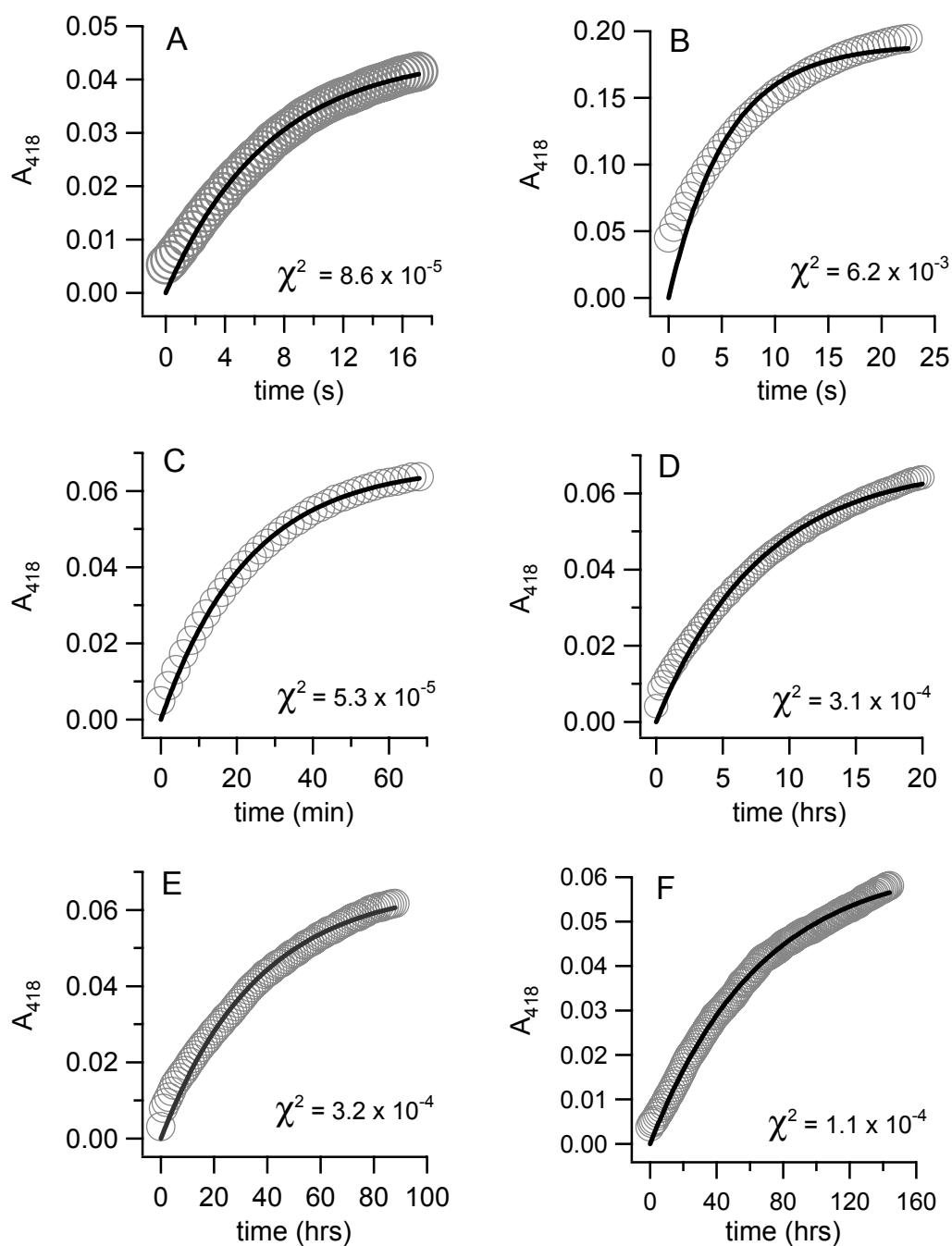
Figure 8: Representative examples of first-order appearance curves for MnO_2 (the product of MnO_4^- oxidation reactions) analyzed at 418 nm. The concentration of MnO_4^- used in these reactions was 0.1 mM. The fast reactions (occur on the order of seconds) include A) 1 mM m-cresol and B) 1 mM 2-chlorophenol. The intermediate reactions (occur on the order of minutes to hours) include C) 1 mM TCE and D) 1 mM PCE. The slow reactions (occur on the order of days) include E) 50 mM MTBE and F) 4 mM toluene. Experimental conditions: pH 7, 25°C, 50 mM phosphate buffer, with the exception that 100 mM phosphate buffer was used in the reaction of MTBE and MnO_4^-.

4.5 Variability in the effective absorptivity of MnO₂

It is reasonable to expect that the effective absorptivity of the colloidal MnO_2 particles would not be constant over the range of reaction rates studied, because it seems likely that many colloidal properties (such as size) would vary depending on how quickly the particles are generated. It is interesting to note that the majority of fitted values for $\varepsilon_{MnO_2}^{525}$ obtained from Equation 5 cluster in a roughly normal distribution with a mean centered at ~0.4 (see Figure 9). In fact, all of the outlying values of $\varepsilon_{MnO_2}^{525}$ (-1.3, -1.7, -2.7, -3.5) are from reactions of MnO_4^- with ethyl tert-butyl ether (ETBE). Indeed, this clear identification of an outlier provides support for using Equation 5 to obtain both k_{obs} and $\varepsilon_{MnO_2}^{525}$ simultaneously.
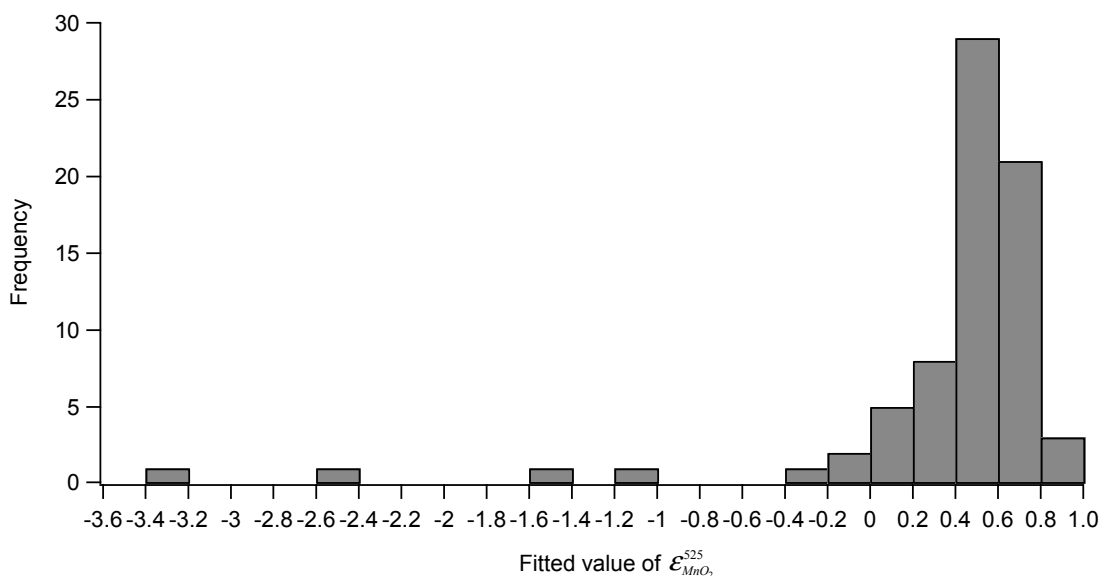
Figure 9: Frequency distribution for fitted values of the effective aborptivity of MnO₂. All of the large deviations are from fits with the same COC (ETBE).

It seems unlikely that the colloid produced in the reaction of MnO_4^- with ethyl tert-butyl ether (ETBE) is so different from that of methyl tert-butyl ether (MTBE), for example, especially when ETBE has an intermediate reaction rate compared with the large range of molecules analyzed in this study. Instead, it seems more likely that the first-order model is inappropriate for this reaction. Figure 10A shows a reaction that

generated a value of -3.5 for $\mathcal{E}^{525}_{MnO_2}$. In Figure 10B, the same data is plotted, but $\mathcal{E}^{525}_{MnO_2}$ was fixed to a value of 0.376 (the mean of positive $\mathcal{E}^{525}_{MnO_2}$ values).

χ^2 = 3.7 x 10^{-4}

$\mathcal{E}^{525}_{MnO_4^-}$ = 2.46 ± 0

$\mathcal{E}^{525}_{MnO_2}$ = -3.5 ± 0.5

C_T = 0.1 ± 0

k_{obs} = 0.073 ± 0.008 hrs^{-1}

40 mM ETBE + 0.1 mM KMnO$_4$
50 mM Phosphate Buffer, pH 7, 25°C

χ^2 = 9.1 x 10^{-3}

$\mathcal{E}^{525}_{MnO_4^-}$ = 2.46 ± 0

$\mathcal{E}^{525}_{MnO_2}$ = 0.376 ± 0

C_T = 0.1 ± 0

k_{obs} = 0.31 ± 0.01 hrs^{-1}

40 mM ETBE + 0.1 mM KMnO$_4$
50 mM Phosphate Buffer, pH 7, 25°C
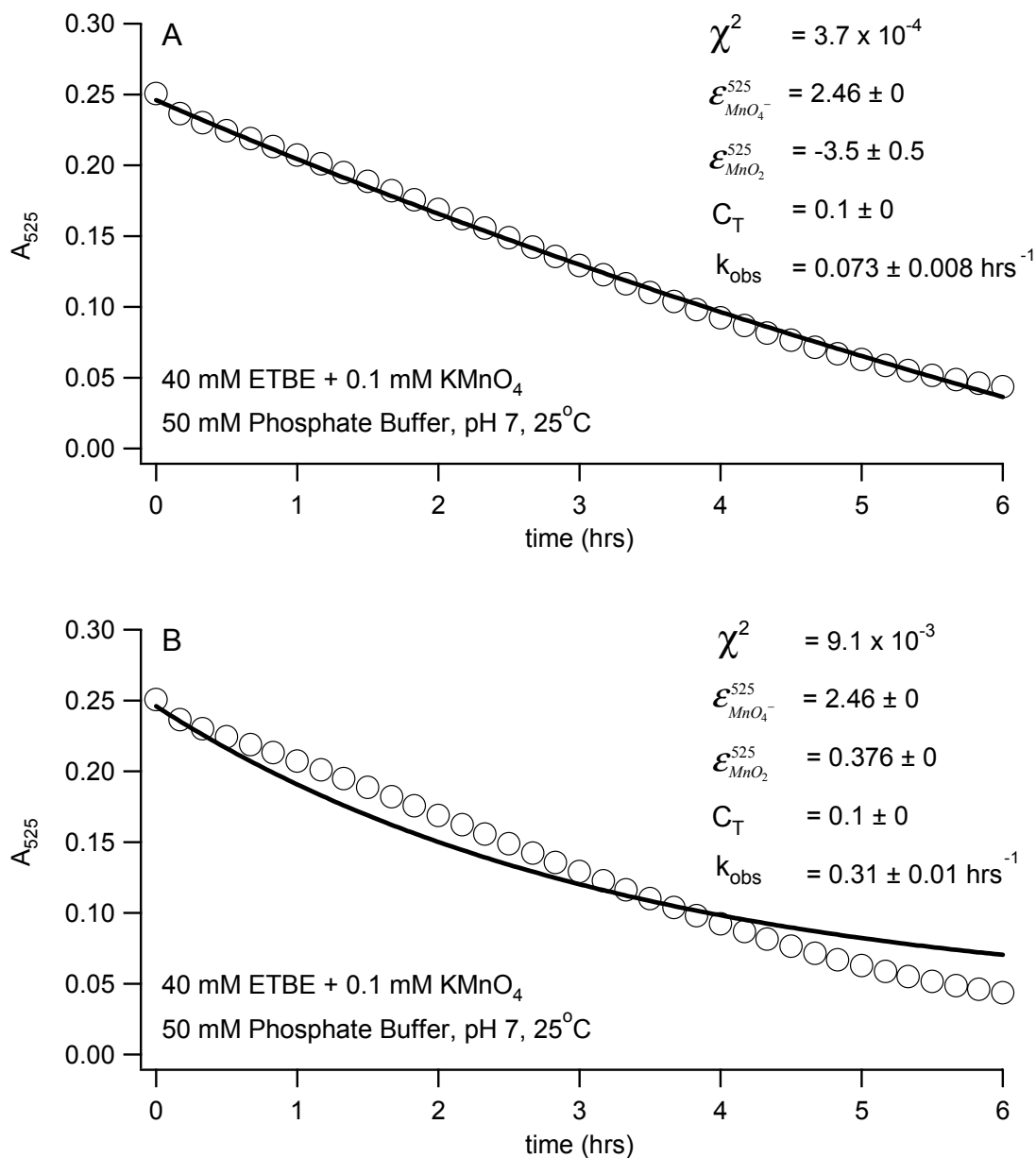
Figure 10: Reaction of 1 mM KMnO$_4$ and 40 mM ETBE. A) Equation 5 fit to A$_{525}$ vs. time data allowing the effective absorptivity of MnO$_2$ to be unrestrained. B) Equation 5 fit to A$_{525}$ vs. time data with the effective absorptivity of MnO$_2$ forced to be 0.376 (the mean of positive values of effective absorptivities of MnO$_2$ obtained from Equation 5). Experimental conditions: pH 7, 25°C, 50 mM phosphate buffer.

As can be seen from this comparison, the best-fit curve in Figure 10B provides a poor description of the reaction. Indeed, the reaction appears to be closer to zero-order with respect to MnO_4^-. This is somewhat surprising given how well the data for the very similar MTBE molecule fit the first-order kinetic model (Figure 11). One potential explanation could be a steric effect. Damm et al. [38] detected tert-butyl formate and tert-butyl alcohol in reactions of MTBE and MnO_4^-; therefore, it is likely that the reaction center occurs at the ether bonds. These bonds are protected more by the ethyl group of ETBE than the methyl group of MTBE, so it may be that the rate-limiting step of the reaction is finding the proper orientation of the reactants rather than the diffusion of MnO_4^-. Because the reaction of ETBE and MnO_4^- does not seem to fit the first-order kinetics model with respect to MnO_4^-, a second-order rate constant was not calculated for this compound.

$$\chi^2 = 2.4 \times 10^{-5}$$
$$\varepsilon_{MnO_4^-}^{525} = 2.46 \pm 0$$
$$\varepsilon_{MnO_2}^{525} = 0.192 \pm 0.006$$
$$C_T = 0.097 \pm 8.5 \times 10^{-5}$$
$$k_{obs} = 0.0186 \pm 0.0001 \text{ hrs}^{-1}$$
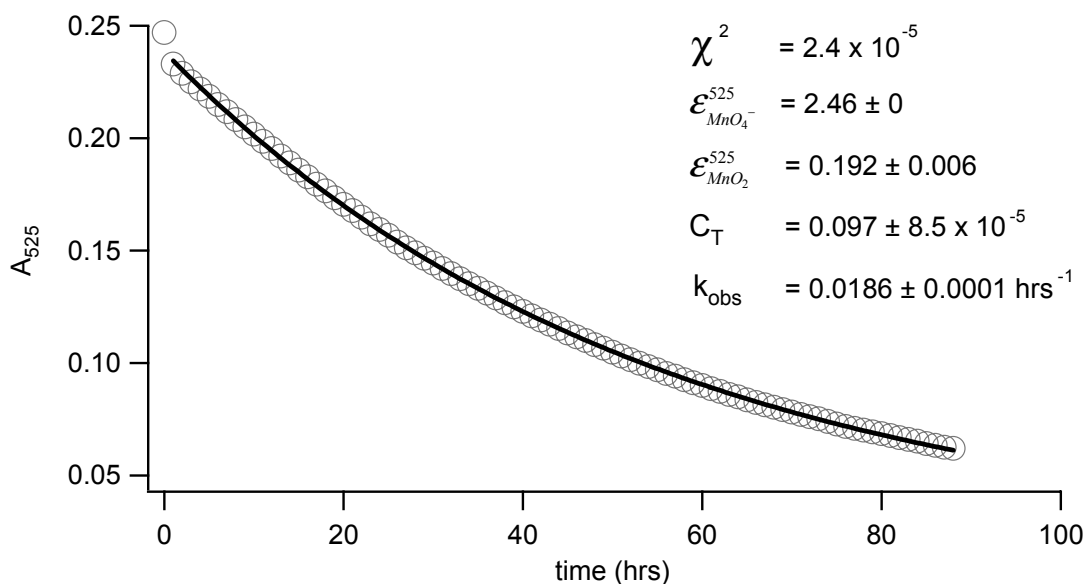
Figure 11: The reaction of 0.1 mM $KMnO_4$ and 50 mM MTBE fit with Equation 5. Experimental conditions: pH 7, 25°C, 100 mM phosphate buffer.

Although they deviate less from the mean, the other negative values of $\varepsilon_{MnO_2}^{525}$ shown in Figure 9 (those between -0.5 and 0) are also difficult to explain, and are likely an artifact of allowing flexibility in the $\varepsilon_{MnO_2}^{525}$ value for Equation 5. It is interesting to note that the majority of these negative values are obtained from fits of the nitrophenols;

as mentioned earlier, these compounds absorb light in the wavelength range of interest, which may contribute to error in the fitting process. However, even with the most negative $\mathcal{E}^{525}_{MnO_2}$ value of -0.44, the best-fit curve seems to fit the model reasonably well, and k_{obs} changes by less than a factor of two (see Figure 12).

$$\chi^2 = 3.3 \times 10^{-5}$$
$$\mathcal{E}^{525}_{MnO_4^-} = 2.46 \pm 0$$
$$\mathcal{E}^{525}_{MnO_2} = -0.44 \pm 0.06$$
$$C_T = 0.1 \pm 0$$
$$k_{obs} = 0.00168 \pm 5 \times 10^{-5}$$

$$\chi^2 = 5.8 \times 10^{-5}$$
$$\mathcal{E}^{525}_{MnO_4^-} = 2.46 \pm 0$$
$$\mathcal{E}^{525}_{MnO_2} = 0.376 \pm 0$$
$$C_T = 0.1 \pm 0$$
$$k_{obs} = 0.00273 \pm 4 \times 10^{-5}$$
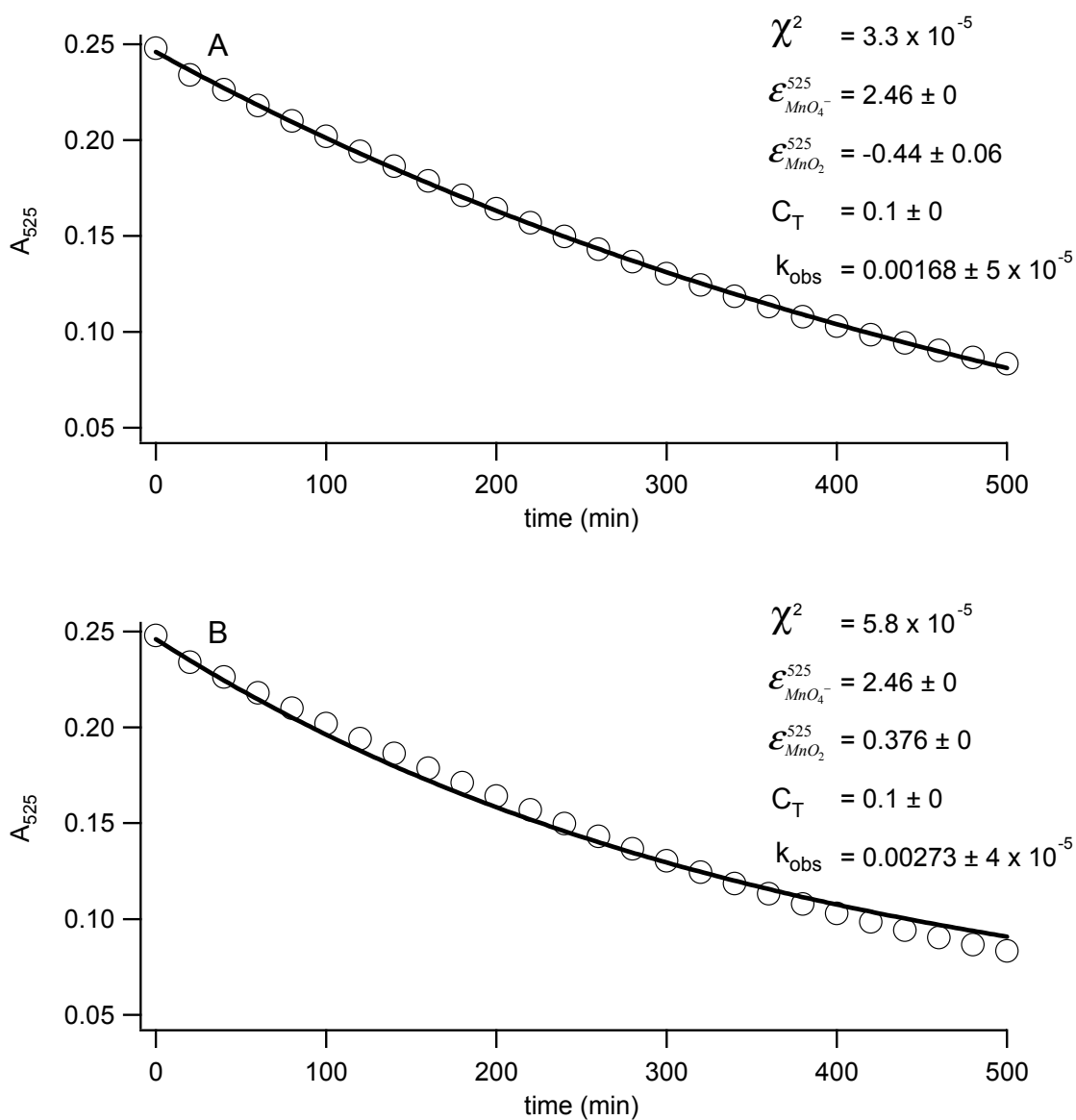
Figure 12: The reaction of 1 mM 2,4-dinitrophenol and 0.1 mM $KMnO_4$. A) Equation 5 fit to A_{525} vs. time data allowing the effective absorptivity of MnO_2 to be unrestrained. B) Equation 5 fit to A_{525} vs. time data with effective absorptivity of MnO_2 forced to be 0.376 (the mean of positive values of effective absorptivities of MnO_2 obtained from Equation 5). Experimental conditions: pH 7, 25°C, 50 mM phosphate buffer.

4.3 Alternative methods

A review of the literature uncovered two alternative methods of calculating the concentration of MnO_4^- that also take into account the absorbance of MnO_2 at 525 nm. Both methods are similar in that they also incorporate Beer's Law of absorbance, but they differ in their assumptions.

4.3.1 Lee and Perez-Benito Method

The method devised by Lee and Perez-Benito [34] involves running successive scans of the reaction until the reaction reaches completion, defined as when none of the characteristic absorption peaks of the MnO_4^- spectrum appear in the scan, as shown in Figure 13. If the final absorbances at 418 nm and 525 nm are known, it is possible to obtain the concentration of MnO_4^- without having a value for $\varepsilon_{MnO_2}^{525}$. This is illustrated with Equations 6-8, which are progressive rearrangements of Equation 3 [34]. In these equations the superscripts indicate wavelengths, and the subscripts i, f, and v, represent initial, final, and variable times respectively.

$$[MnO_4^-]_v = (A_v^{525} - \varepsilon_{MnO_2}^{525}[MnO_2]_v)/\varepsilon_{MnO_4^-}^{525} \qquad [6]$$

$$[MnO_4^-]_v = (A_v^{525} - \varepsilon_{MnO_2}^{525}A_v^{418}/\varepsilon_{MnO_2}^{418})/\varepsilon_{MnO_4^-}^{525} \qquad [7]$$

$$[MnO_4^-]_v = (A_v^{525} - A_f^{525}A_v^{418}/A_f^{418})/\varepsilon_{MnO_4^-}^{525} \qquad [8]$$

One problem in applying the Lee and Perez-Benito method for this study was that the instrument requires ~30 seconds to scan the range encompassing the wavelengths 400 nm to 650 nm, making it impossible to use this method for the fast reactions that have half-lives on the order of 30 seconds. At the alternate end of the time spectrum, many of the longest reactions lose their isosbestic points before the reaction is complete (in the sense that there are no more MnO_4^- peaks visible in the spectrum). An example of such a reaction is shown in Figure 14. Because of these factors, the Lee and Perez-Benito method is not adequate for the purposes of this project.
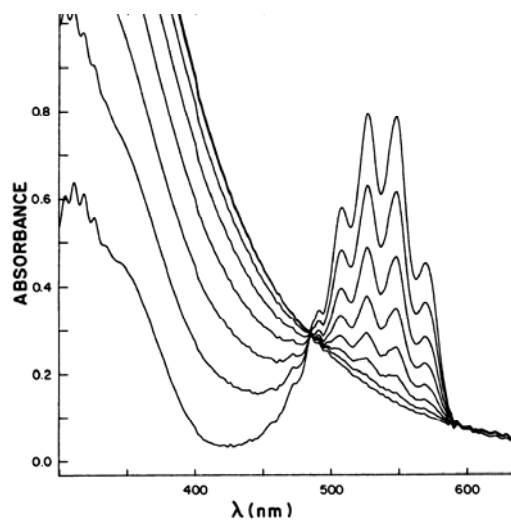
Figure 13: Successive scans obtained by Lee and Perez-Benito (*Canadian Journal of Chemistry*, 1985, *63*, 1275-1279) for the oxidation of 1-tetradecene (7.89E-3 M) by methyltributylammonium permanganate (3.02E-4 M) in methylene chloride at 25°C. Reprinted with permission of the publisher.
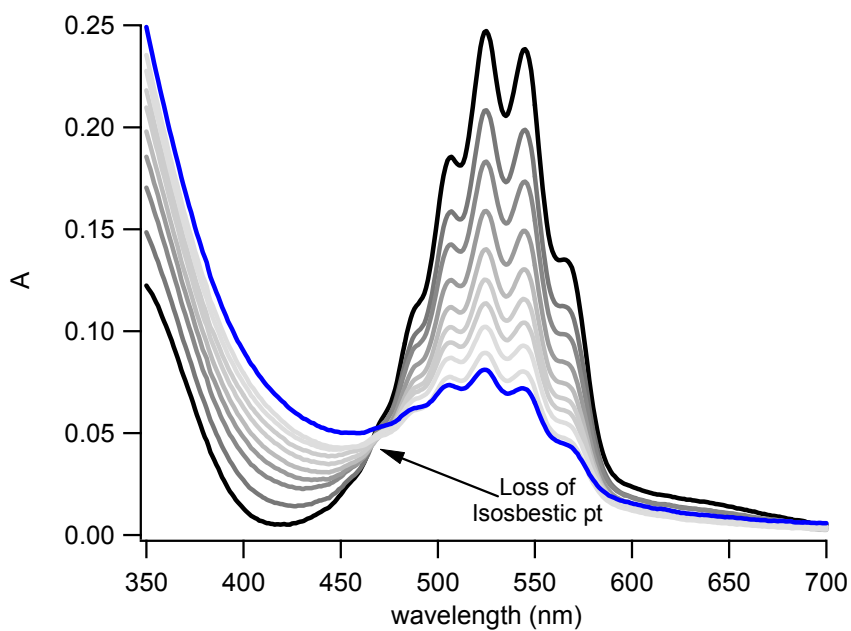
Figure 14: Reaction between 50 mM 1,4-dioxane and 0.1 mM $KMnO_4$. Time between scans is 12 hours, except for the last 2 scans, which are separated by 18 hours. The isosbestic point is lost during the time period between 96 hours and 114 hours. Experimental conditions: pH 7, 25°C, 50 mM phosphate buffer.

4.2.2 Gardner Method

Kimberly Gardner's [35] solution to the undefined nature of both [MnO_2] and $\mathcal{E}_{MnO_2}^{525}$ was to calculate the [MnO_4^-] at two different wavelengths, so that only the relative absorbance of MnO_2 at the two wavelengths is required for the calculation, as shown in Equations 9 and 10:

$$[MnO_4^-] = \frac{A_{MnO_2}^x - Q \times A_{MnO_2}^y}{\mathcal{E}_{MnO_2}^x - Q \times \mathcal{E}_{MnO_4^-}^y} \qquad\qquad [9]$$

$$\text{where } Q = \frac{\mathcal{E}_{MnO_2}^y}{\mathcal{E}_{MnO_2}^x} = \frac{A_{MnO_2}^y}{A_{MnO_2}^x} \qquad\qquad [10]$$

For the reactions that Gardner studied (MnO_4^- oxidations of aromatic hydrocarbons such as toluene and ethylbenzene), a final spectrum of MnO_2 could not be used to calculate Q because "toward the end of most reactions, [the MnO_2 colloid] begins to change spectroscopically due to coagulation." (This is the same problem that prevented use of the Lee and Perez-Benito method for this study.) Thus, Gardner calculated this ratio before the reaction reached completion. In order to calculate Q, Gardner also had to devise a method of separating the absorbance due to MnO_4^- from the absorbance due to MnO_2. She accomplished this by estimating an absorption spectrum of MnO_2 by assuming that all the absorbance in the ranges 438 – 478 nm and 598 – 638 nm at all time points in the reaction was due to MnO_2, and then fitting a third-order polynomial to these data. She showed good fitting results with this method after the reaction completed 2-3 half-lives (see Figure 15).

Gardner's method and the method described in Section 4.4 incorporate similar assumptions. While her method involves first estimating the absorbance of MnO_2 with a fitting equation and calculating k_{obs} in a separate step, the method used in this study involves estimating $\mathcal{E}_{MnO_2}^{525}$ with a fitting equation that gives values for both $\mathcal{E}_{MnO_2}^{525}$ and k_{obs} in the same step. It is possible to use Gardner's method for experiments done with the static method; however, it cannot be used for the reactions that require analysis by the stopped-flow method. Furthermore, some modifications would have to be made because the spectra for reactions at the conditions used in this study (25°C and 50 mM phosphate buffer) are different enough from the spectra at her conditions (75°C and 4 mM

phosphate buffer) that the range over which the absorbance can be said to be due entirely to MnO_2 is different (see Figures 15 and 16). (Figure 17 shows it is possible to replicate Gardner's results with the method devised for this study when using her experimental conditions of 75°C and 4 mM phosphate buffer.)   It should be noted that both methods give similar results for k'' for the reaction of $KMnO_4$ and toluene—Gardner obtained a value of 7.0 x 10^{-4} $M^{-1}s^{-1}$ for k'' vs. the value of 8.3 x 10^{-4} $M^{-1}s^{-1}$ obtained from this study.
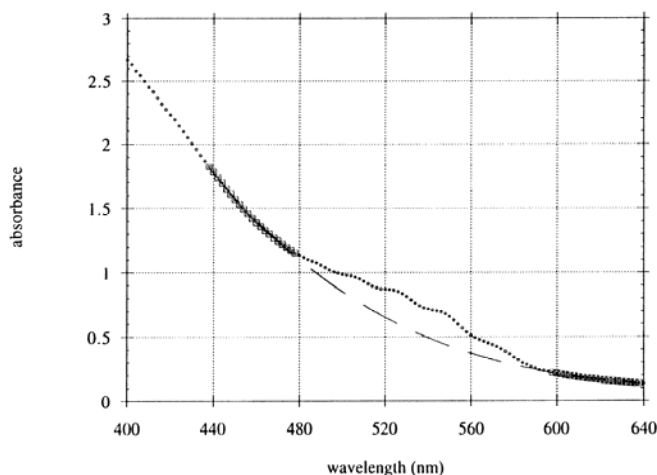
Figure 15: From [35]: "UV/vis spectrum for the reaction of MnO_4^- and toluene in water after 2 half-lives. The small dots are the full UV/vis spectrum, the large squares are the segments used to model the MnO_2, and the dashed line is the third-order polynomial fit" (reprinted with permission from the author).
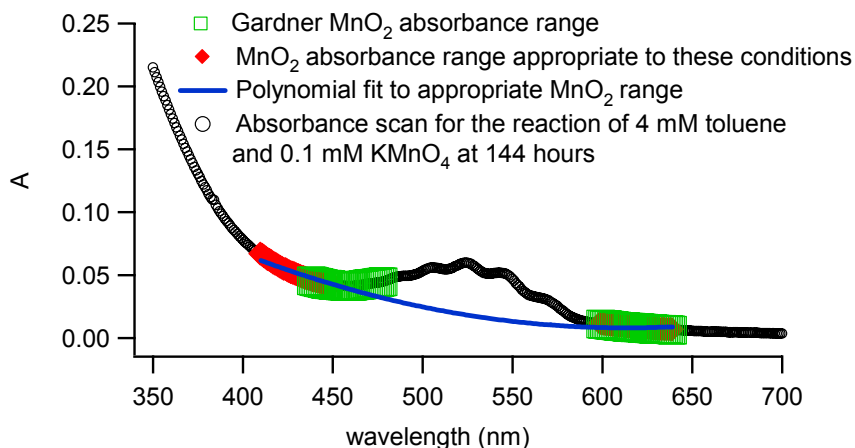
Figure 16: For reaction with the same COC (toluene) at the conditions used in this study: 4 mM toluene, 0.1 mM $KMnO_4$, and 50 mM phosphate buffer at 25°C, the wavelength range over which the absorbance can be said to be due entirely to MnO_2 is different from Gardner's.
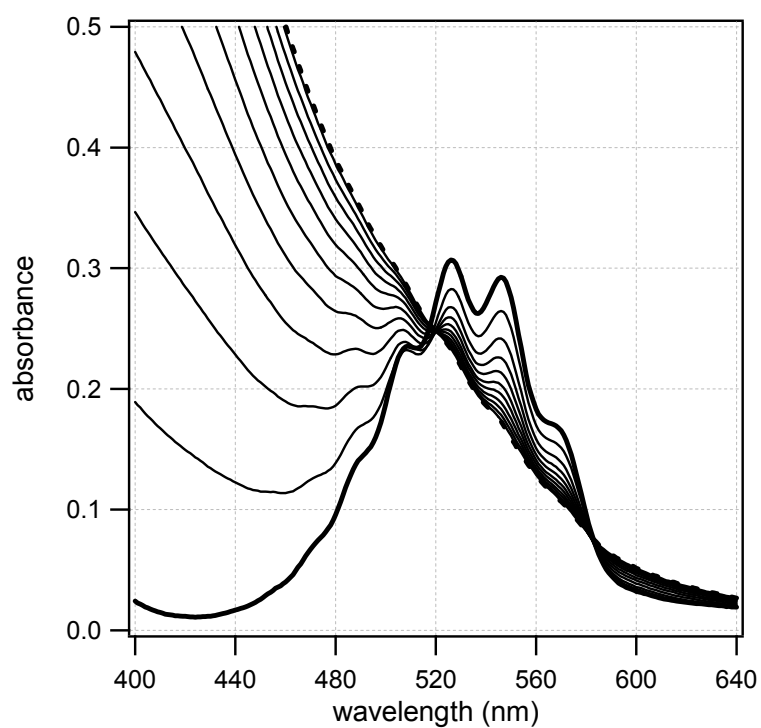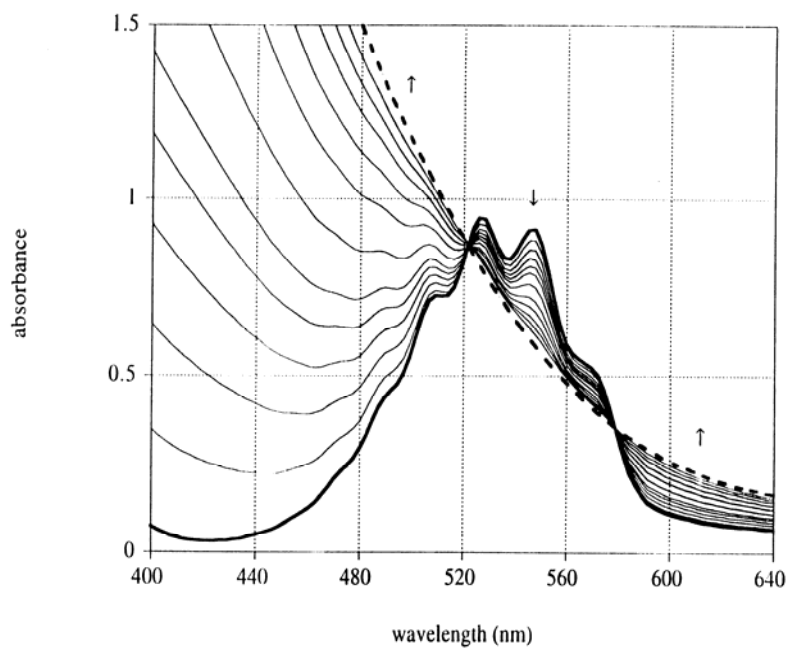
Figure 17: A comparison of the successive scans of the oxidation of toluene by KMnO$_4$ obtained by Gardner at 75°C and 4 mM phosphate buffer [35] (top) (reprinted with permission from the author) and successive scans obtained at these conditions (but with different amounts of toluene and KMnO$_4$) with the method from this study (bottom).

Chapter 5: Kinetic Data

5.1 Determination of pseudo-first-order rate constants (k_{obs})

As mentioned in Chapter 4, k_{obs} was determined from the fit of Equation 5 to experimental data. Multiple experiments with the same concentration of the COC were done only for reactions where the experiment was completed in 24 hours or less. When determining k_{obs} for replicate reactions, the data were plotted and fit with $\mathcal{E}_{MnO_2}^{525}$ held constant, the rationale being that colloidal particles generated under identical conditions should have the same effective absorptivity. However, because the colloidal particles may have different properties based on the rate of their formation, $\mathcal{E}_{MnO_2}^{525}$ was not held constant over varying concentrations of COC. Figure 18 shows how well Equation 5 fit a wide array of reactions with time frames ranging from 17 seconds to 144 hours (6 days). Where fits for multiple replicates are shown (Figure 18a and 18b), the fits were obtained by keeping $\mathcal{E}_{MnO_2}^{525}$ constant, optimized to give the best result for all replicates.

5.2 Determination of second-order rate constants (k'')

The k_{obs} values obtained by fitting Equation 5 to experimental data were used to determine second-order rate constants, k''. When the solubilities of the COC were low, or for some of the reactions that occurred on the order of days, k'' was calculated from Equation 11:

$$k'' = \frac{k_{obs}}{[COC]} \qquad [11]$$

For these COCs, the treatment effectively assumes the order of reaction with respect to COC to be first-order. The COCs for which k'' was determined this way are MTBE, ETBE, toluene, PCE, picric acid, and 2,4-dinitrophenol (See Figure 20). MTBE, PCE,

and toluene have been shown by others to be first-order with respect to COC [4, 35, 38, 39]. Picric acid and 2,4-dinitrophenol are likely to be first-order with respect to COC based on their structural similarity to the mononitrophenols.

When COC solubilities made it possible to do experiments over a range of concentrations, k'' values were obtained from the slope of k_{obs} vs. COC concentration. If we rearrange Equation 11, it can be seen that a linear plot of k_{obs} vs. COC concentration indicates that the reaction with respect to the COC is first-order (only a value of 1 for n results in a straight line). Figure 19 shows many representative k_{obs} vs. COC concentration plots, all of which are linear.

$$k_{obs} = k''[\text{COC}]^n \qquad\qquad [12]$$

The second-order rate constants obtained for all experiments are summarized in Figure 20 along with k'' values obtained from an extensive literature search of MnO_4^- rate constants. The values used in Figure 20 are listed in Appendix B. This appears to be the first comprehensive summary of all known rate constants for relevant environmental COCs in one place. It can be seen from Figure 20 that values obtained in this study are well within the range of the values for k'' obtained from previous studies. This helps validate the approach used here, because most of the other values for k'' are obtained by analyzing the oxidation of the COC with MnO_4^- in excess, which is the opposite condition of that used in this study. The correlation between rate constants obtained from this study and those obtained by using gas chromatography (GC) to analyze the oxidation of the COC with MnO_4^- in excess is further demonstrated in Figure 21. In this figure, the k'' values obtained from experiments in this study are compared with literature values of k'' obtained using GC. The good correlation between these values confirms that the rate of oxidation of daughter products for the COCs in this study can be neglected when determining k'' from the reduction of MnO_4^- with COCs in excess.
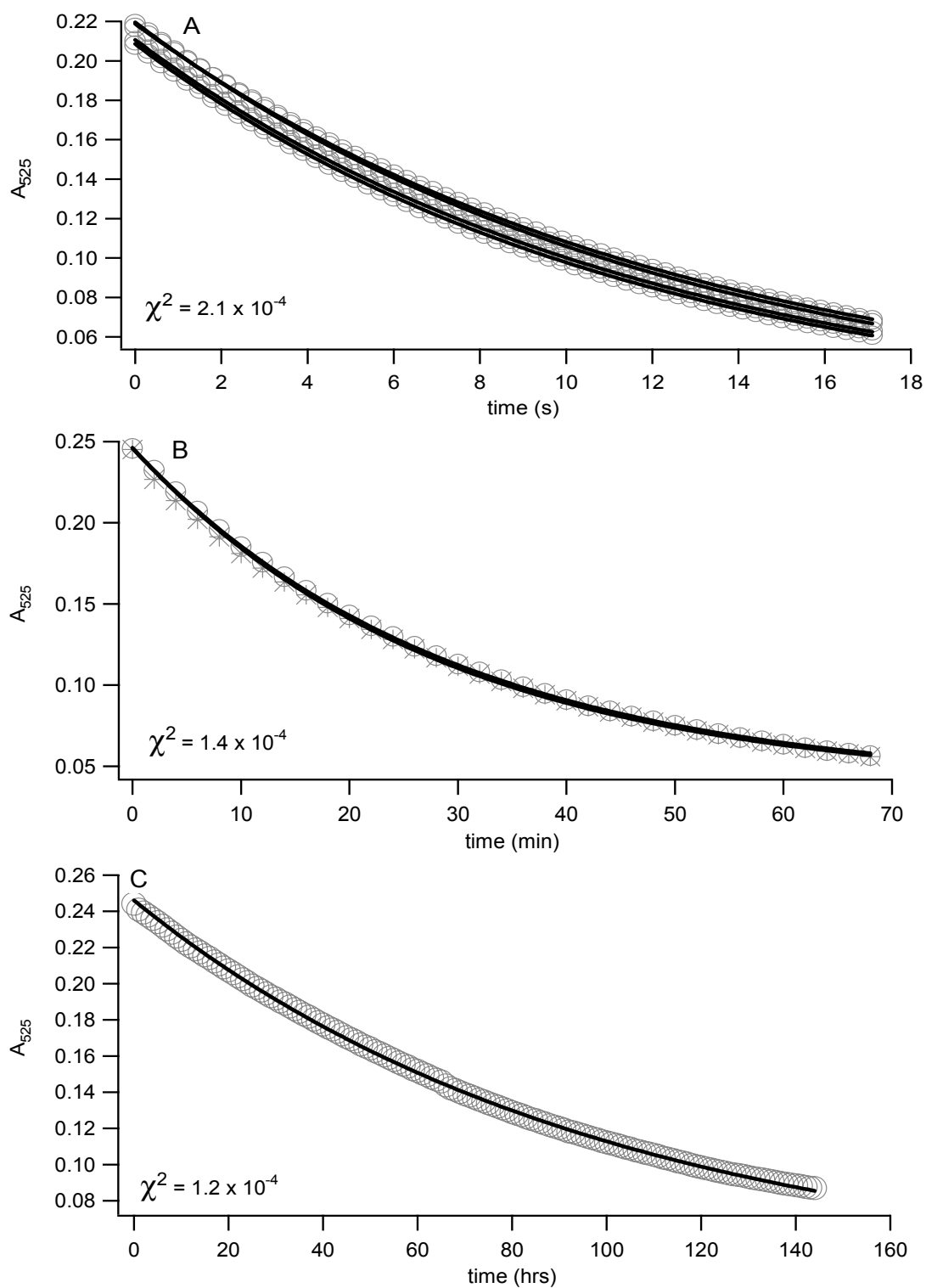
Figure 18: Reactions of varying time scales fit with Equation 5. A) 1 mM m-cresol, B) 1 mM TCE, and C) 5 mM picric acid. Experimental conditions: pH 7, 25°C, 50 mM phosphate buffer.

Included in Figure 20 are compounds with low solubilities (less than 0.5 mM) that cannot be characterized with this method. As mentioned in Chapter 3, these compounds include many of the explosives, some pesticides, polychlorinated dibenzodioxins (PCDDs), polyaromatic hydrocarbons (PAHs), and polychlorinated biphenyls (PCBs). Other compounds, such as carbon tetrachloride, dichloromethane, 1,2-dichloroethane (1,2-DCA), and 1,1,1-trichloroethane (1,1,1-TCA) have sufficient solubilities for this method, but are not reactive enough for k'' to be determined. However, by comparing psuedo-first-order reactions of 1,4-dioxane with carbon tetrachloride, dichloromethane, 1,2-DCA, and 1,1,1-TCA at comparable concentrations, it is clear that dichloromethane and 1,2-DCA have rates that are slower than 1,4-dioxane, and the rates of carbon tetrachloride and 1,1,1- TCA are no faster than 1,4-dioxane (see Figures 22 and 23). As k'' for 1,4-dioxane was shown to be $4.2 \times 10^{-5} \text{ M}^{-1}\text{s}^{-1}$, it is likely that the second-order rate constants for carbon tetrachloride, methylene chloride, 1,2-DCA, and 1,1,1-TCA are less than $10^{-4} \text{ M}^{-1}\text{s}^{-1}$.
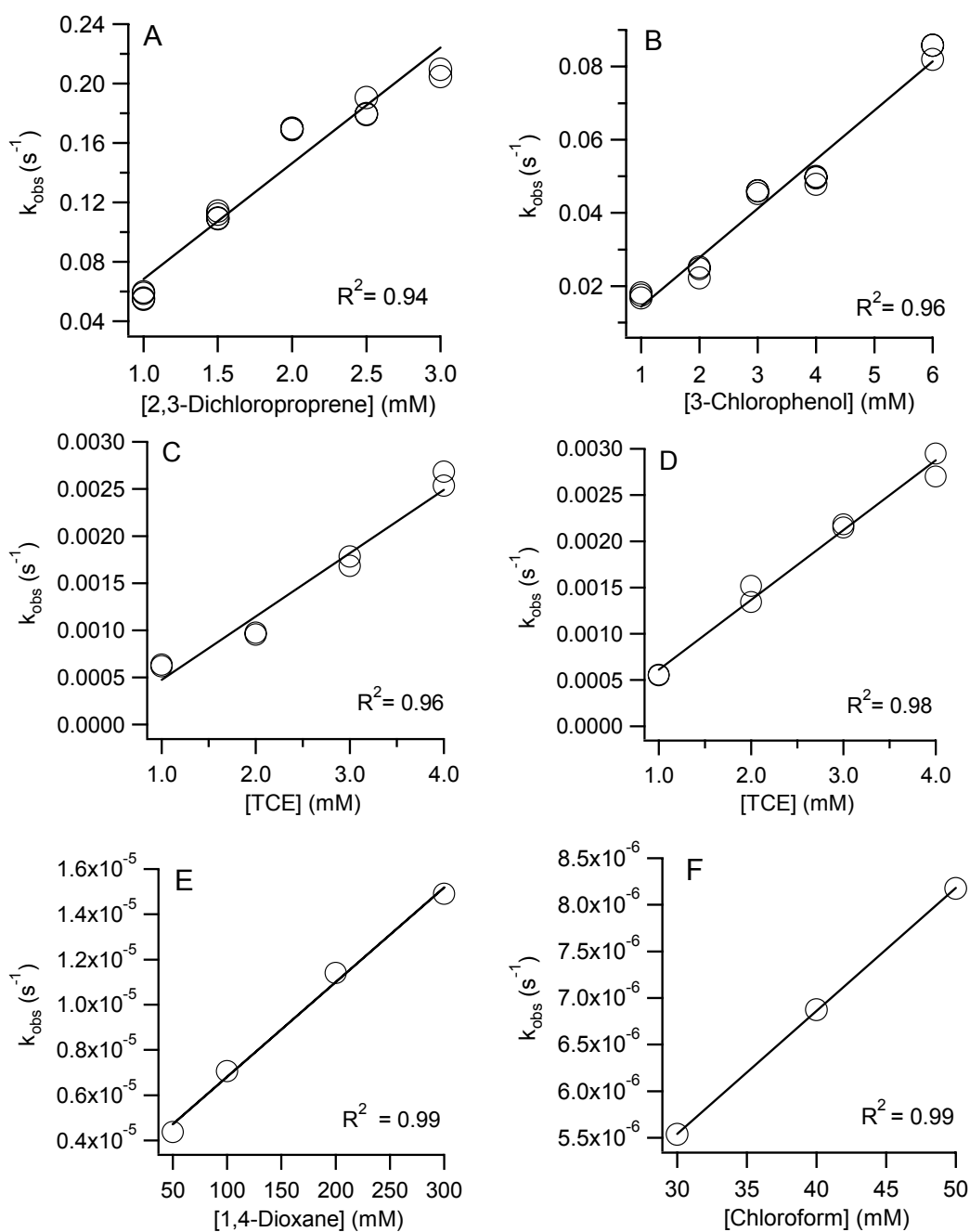
Figure 19: Selected k_{obs} vs. concentration of COC plots—the slope of the lines are k''. All reactions are done with 0.1 mM $KMnO_4$. The stopped-flow method was used to determine k'' for reactions A-C, and the static method was used to determine k'' for reactions D-E. Other experimental conditions: pH 7, 25°C, 50 mM phosphate buffer, with the exception that a 100 mM phosphate buffer was used for the reactions with chloroform.

Figure 20: Summary of second-order rate constants with MnO_4^- for compounds in all classes. Temperatures for the literature values vary from 20°C to 30°C (exceptions: k'' for benzene was determined at 70°C and k'' values for the phenols were determined at 16°C). Experimental conditions for this study: pH 7, 25°C, phosphate buffer concentrations vary (see Appendix A). The pH for the literature values of k'' ranges from 4.6 to 8.0. Abbreviations used in this table can be found in the List of Abbreviations on page ix. See Appendix B for the data on which this figure is based.
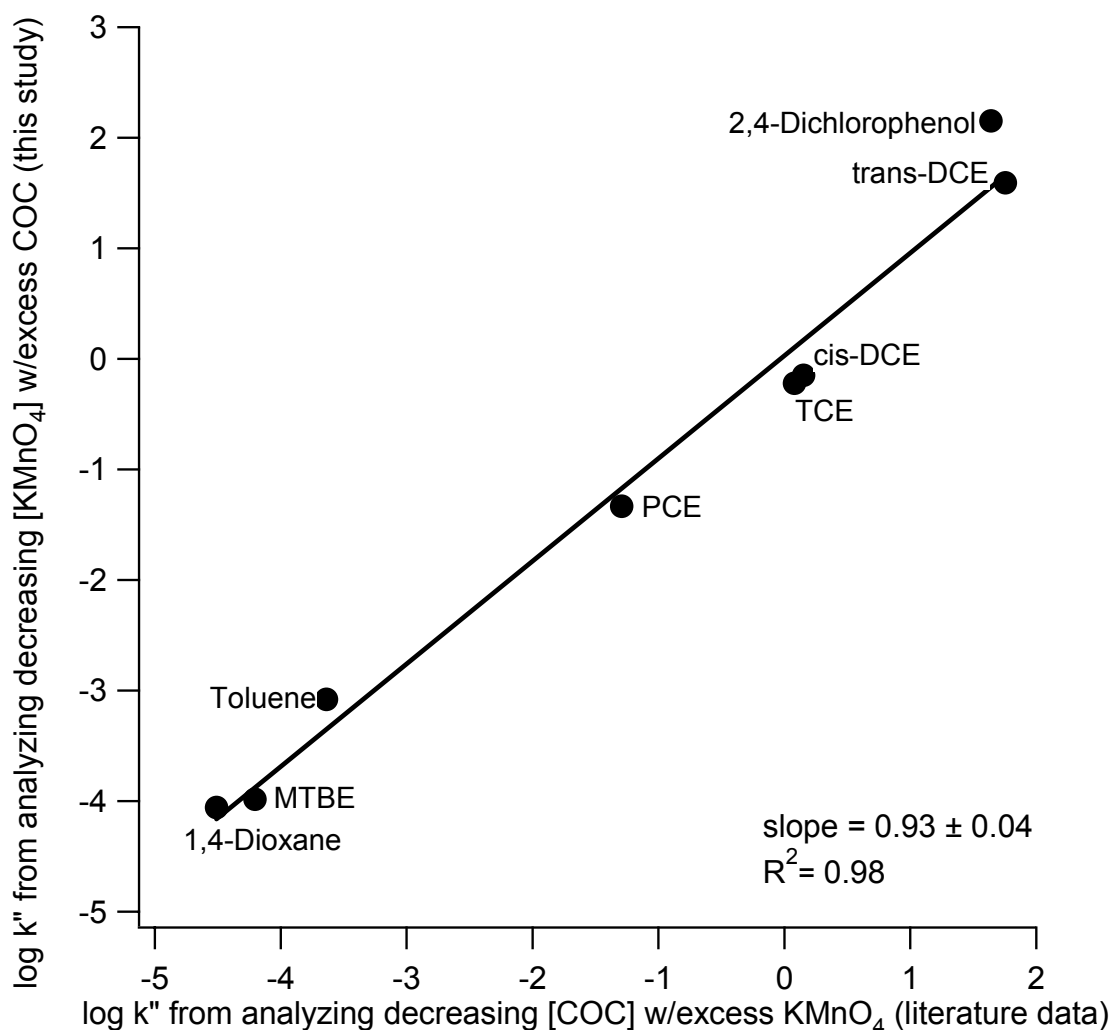
Figure 21: Correlation between k'' obtained from this study by analyzing decreasing concentrations of $KMnO_4$ in the presence of an excess COC and literature values of k'' obtained by analyzing decreasing concentrations of COC in the presence of excess $KMnO_4$. The literature values of k'' for the chlorinated ethylenes are the reactions at 25^oC from [39]. These values were chosen as the representative literature values for the chlorinated ethylenes because the conditions most closely matched those used in this study. As seen in Figure 20, only one literature value is available for MTBE, 1,4-dioxane, and 2,4-dichlorophenol, so these were the literature values used for this figure. In Figure 20, two literature values are shown for toluene; however, only one was obtained by analyzing decreasing COC concentrations—the value used in this figure. The robustness of the correlation confirms that it is reasonable to neglect reduction of $KMnO_4$ by daughter products over the reaction times used in this study. Although 2,4-dichlorophenol deviates somewhat from the correlation, it should be noted that the literature value was obtained at 16^oC while the value from this study was obtained at 25^oC.
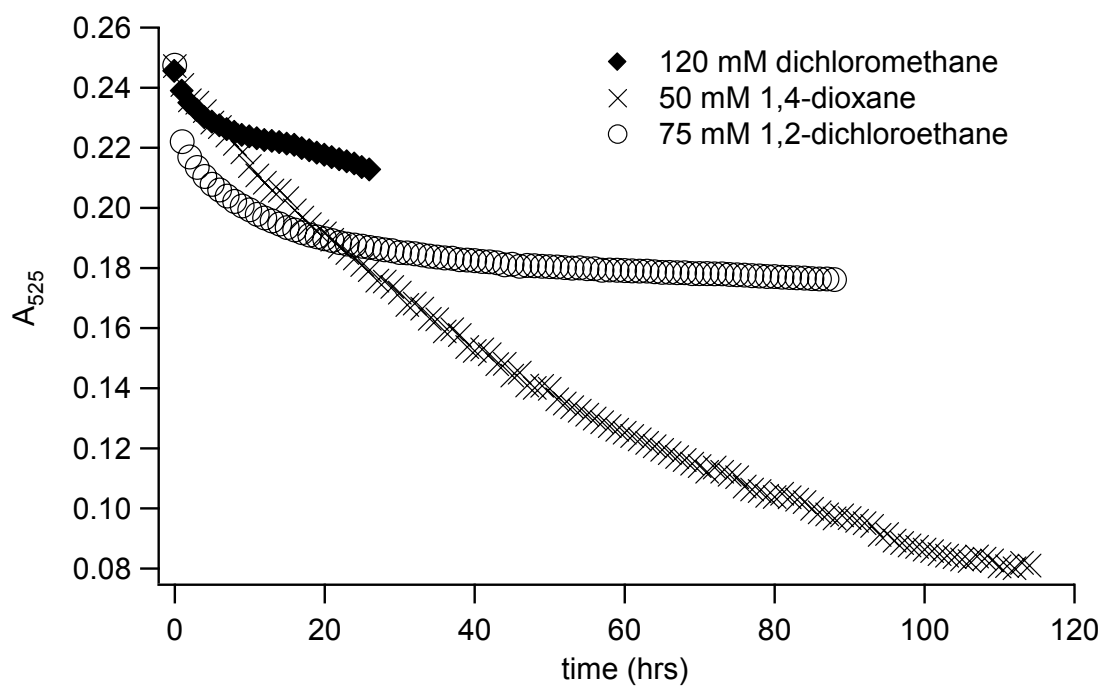
Figure 22: Comparison of the reactions of MnO_4^- with dichloromethane, 1,2-dichloroethane, and 1,4-dioxane. Although higher concentrations of 1,2-dichloroethane and dichloromethane were used, they were less reactive with MnO_4^- than 1,4-dioxane, implying that k'' for these COCs must be less than 4.2×10^{-5}, the k'' for 1,4-dioxane obtained in this study. The initial drop seen with dichloromethane and 1,2-dichloroethane is hypothesized to be due to a reactive impurity in the compounds. Experimental conditions: pH 7, $25^{\circ}C$, 50 mM phosphate buffer.
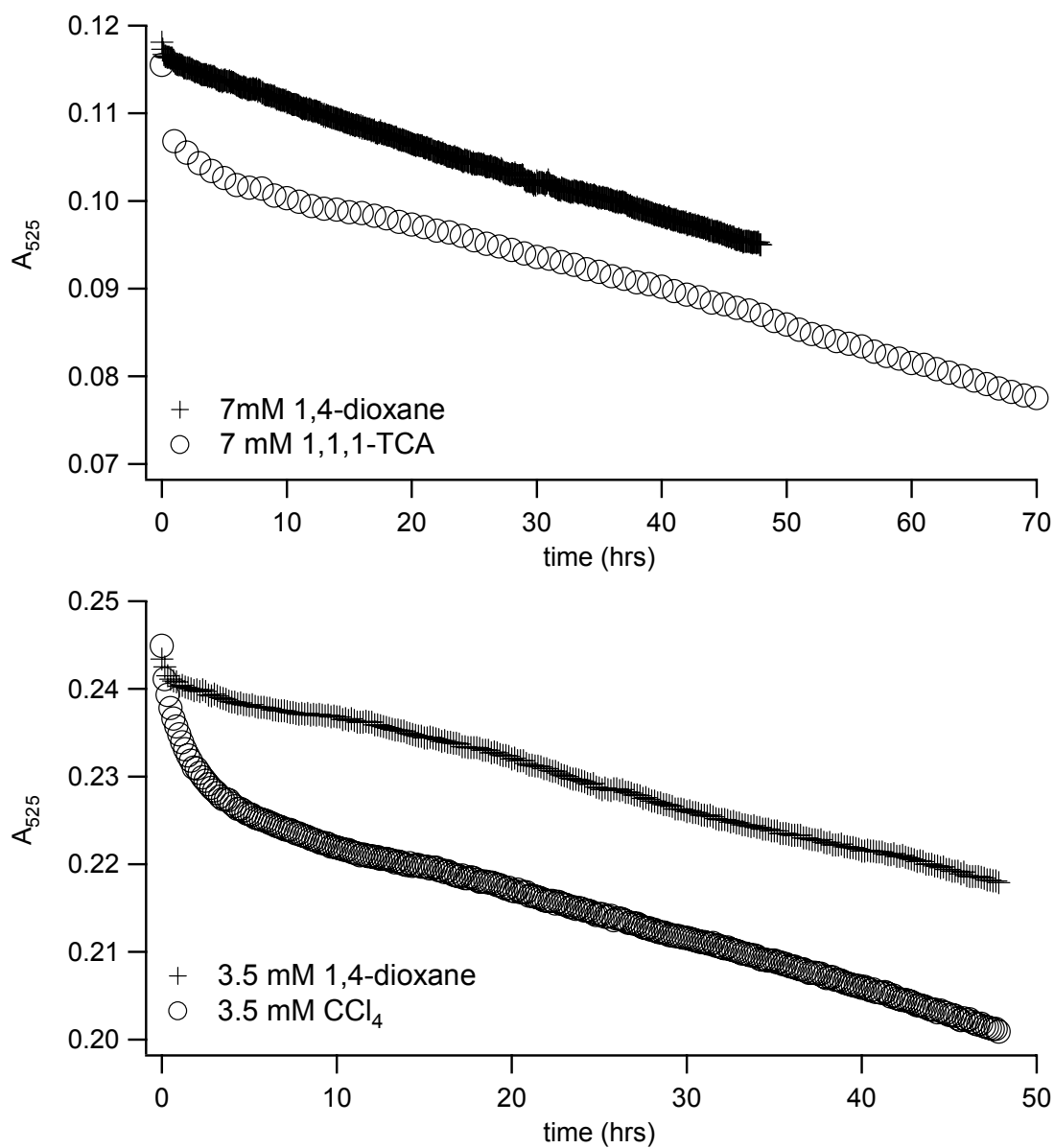
Figure 23: Comparison of reactions of $KMnO_4$ with 1,1,1-TCA and carbon tetrachloride with the reaction of $KMnO_4$ and 1,4-dioxane. Neglecting the initial drop (again, likely due to $KMnO_4$ reaction with trace impurities), both of these COCs appear to have rates that are comparable to that of 1,4-dioxane, which has a k'' value that is less than 10^{-4} $M^{-1}s^{-1}$. Experimental conditions: pH 7, 25°C, 50 mM phosphate buffer.

5.3 The effect of MnO_4^- autodecomposition

Experiments with MnO_4^- and no COC showed a slight decrease in absorbance over time, indicating that autodecomposition of MnO_4^- was occurring. Other researchers have also noted that MnO_4^- decomposes over time in aqueous solution [27, 38, 40]. Because MnO_2 is an effective catalyst for the decomposition of MnO_4^- in aqueous solution, only trace amounts of reducing materials or MnO_2 will induce the decomposition of MnO_4^- [27]. However, as shown in Figure 24, this decrease is negligible when compared with the decrease in absorbance by reaction of MnO_4^- with picric acid (the COC with the lowest value of k_{obs}—see Appendix A). Therefore, the second-order rate constants reported in this study are not corrected for any potential contribution that may be due to MnO_4^- autodecomposition. The fact that the correlation in Figure 21 is so good, even though it includes data from COCs with second-order rate constants obtained from low values of k_{obs} (such as toluene), further supports that not correcting for MnO_4^- autodecomposition is justified.
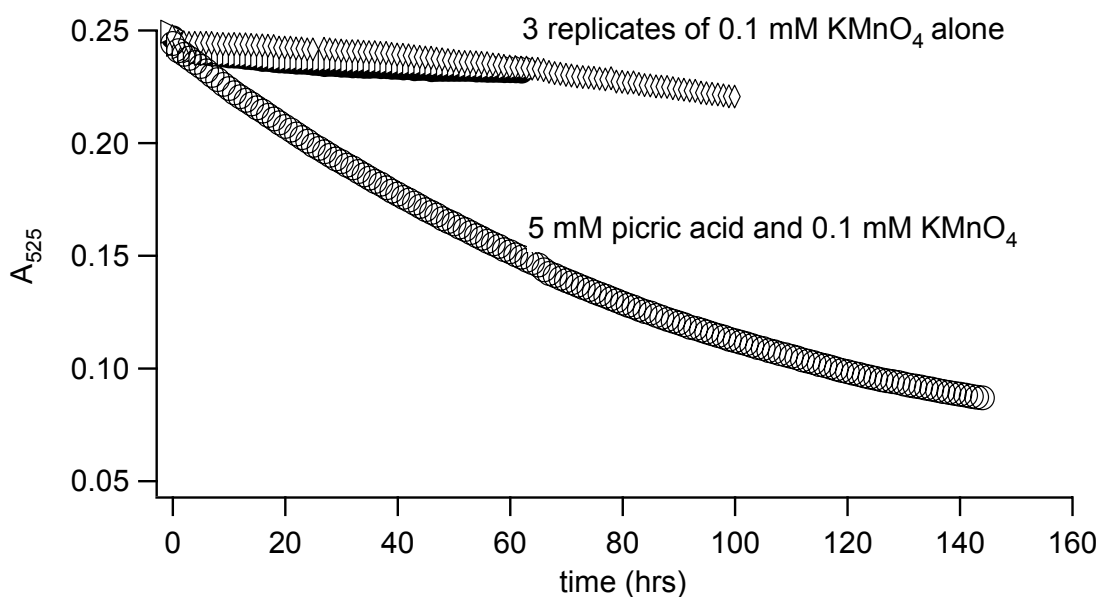
Figure 24: The decrease in absorbance due to MnO_4^- autodecomposition is negligible when compared with the decrease in absorbance due to reaction with COCs. Shown here is picric acid, the COC with the lowest value of k_{obs} (see Appendix A). Experimental conditions: pH 7, 25°C, 50 mM phosphate buffer.

5.4 The effect of common groundwater constituents

A study showing little variation in the reaction rate of TCE and MnO_4^- in both "hard" tap water and deionized water [1] implies that MnO_4^-, unlike ozone and Fenton's reagent, does not strongly react with bicarbonate and other carbonate species. This is likely because MnO_4^- reacts directly with COCs, while ozone and Fenton's reagent produce hydroxyl radicals that can be scavenged by the carbonate species [4].

The current study further characterizes the effect of bicarbonate and other common groundwater constituents on the rate of TCE and MnO_4^-. Bicarbonate in the range of 50 to 400 mg/L often occurs in groundwater, with concentrations above 1000 mg/L possible; nitrate concentrations in groundwater are mostly below 20 mg/L, but groundwater contaminated with fertilizers can have concentrations above 1000 mg/L; and sulfate concentrations in groundwater tend to range from under 15 mg/L to about 500 mg/L [41]. Therefore, 1.0 mM TCE and 0.1 mM MnO_4^- were reacted in 50 mM phosphate buffer containing nitrate, sulfate, or bicarbonate in concentrations ranging from 0 to ~1000 mg/L. As expected, the rates of oxidation of TCE by MnO_4^- show no apparent trend with increasing concentrations of any of the groundwater constituents studied (Figure 25).
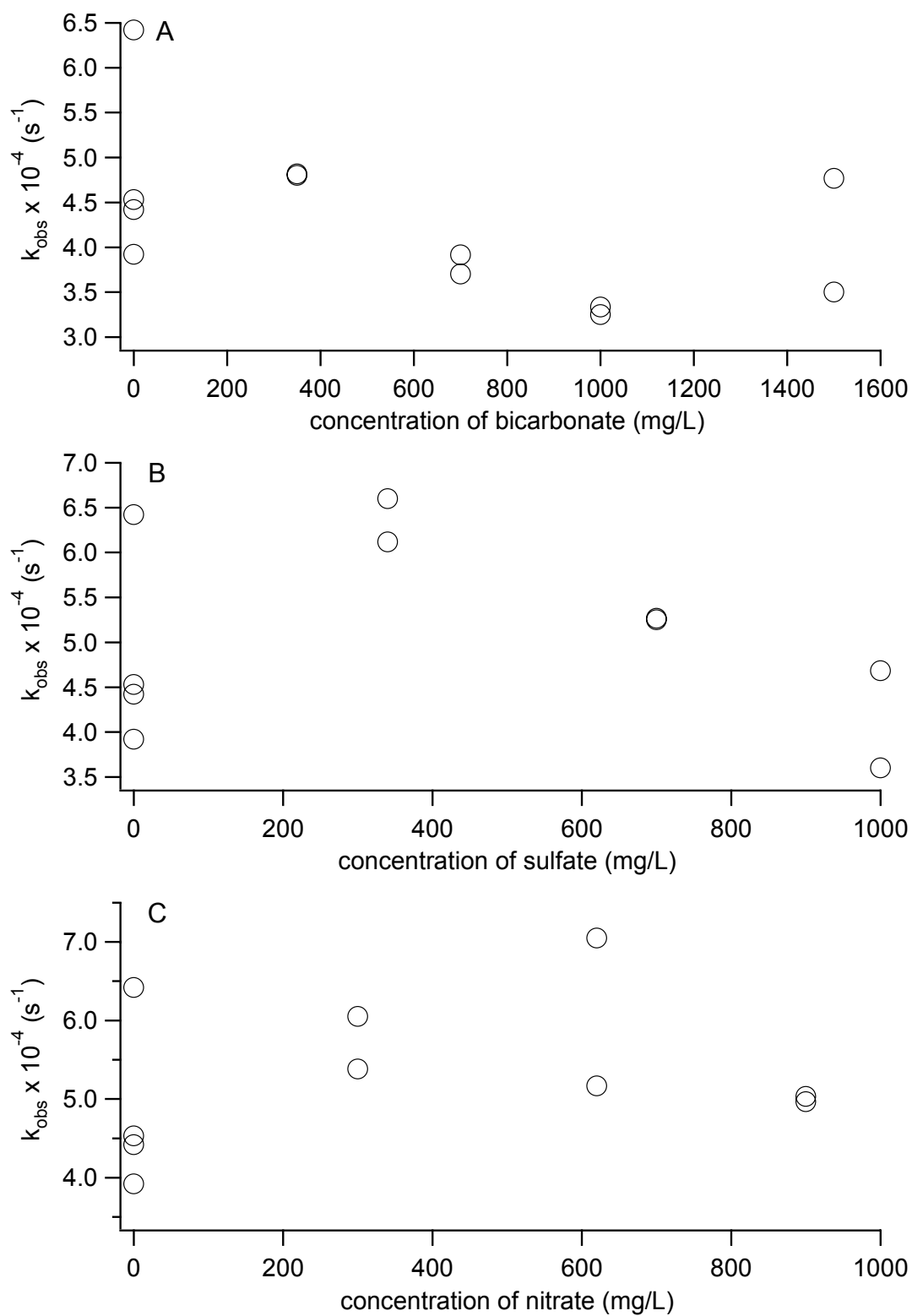
Figure 25: Reaction of 1.0 mM TCE and 0.1 mM KMnO$_4$ in the presence of A) bicarbonate, B) sulfate, and C) nitrate. None of these common groundwater constituents appear to affect the rate of the TCE and KMnO$_4$. Experimental conditions: pH 7, 25°C, 50 mM phosphate buffer.

5.5 Permanganate and NOM

As mentioned in Chapter 2, one of the potential limitations of ISCO is that the oxidant may be consumed by natural organic matter (NOM) and other reduced species in the aquifer before reacting with the COC. In many cases, this natural oxidant demand (NOD) of the aquifer is large compared with the oxidant demand of the COC [16, 17], and for high levels of NOM, the cost of the large amount of MnO_4^- required to overcome the NOD may decrease the feasibility of using this technology.

NOM is present in groundwater at concentrations of ~0.5 mg/L [42]. To determine if NOM has any effect on the rate constants for COC reaction with MnO_4^-, NOM concentrations ranging from 0.05 to 30 mg/L were added to the reaction of 1.0 mM TCE and 0.1 mM MnO_4^-. The NOM used was GT-NOM, an unfractionated total aquatic NOM (collected by reverse osmosis) from Georgetown, SC. This sample of NOM was chosen because sufficient quantities were available and its properties have been well characterized [43-49].

As can be seen in Figure 26, the presence of NOM does not affect the rate of reaction of TCE and MnO_4^- until the concentrations of NOM are above 10 mg/L. Experiments by Yan and Schwartz show a similar trend, where k'' for TCE and MnO_4^- was only slightly decreased in groundwater containing a low amount of total organic carbon (<2 mg/L), while k'' for TCE and MnO_4^- was reduced almost by 40% in groundwater containing 2% landfill leachate, which contained 10 mg/L of total organic carbon [4]. Both experiments indicate that environmental concentrations of NOM do not affect the rate of reaction between MnO_4^- and TCE. Although not tested, it is logical to extrapolate this result to other COCs.

The data in Figure 27 shows that the reaction of MnO_4^- with NOM alone is not strictly first-order—the reaction is initially fast and then levels out. Mumford et al. also saw evidence for an initial fast rate followed by a slower rate for the reaction between MnO_4^- and the oxidizable aquifer material in their system [50]. This kinetic behavior may be explained by differences in accessibility of MnO_4^- to the many potential sites of oxidation that are present in NOM.
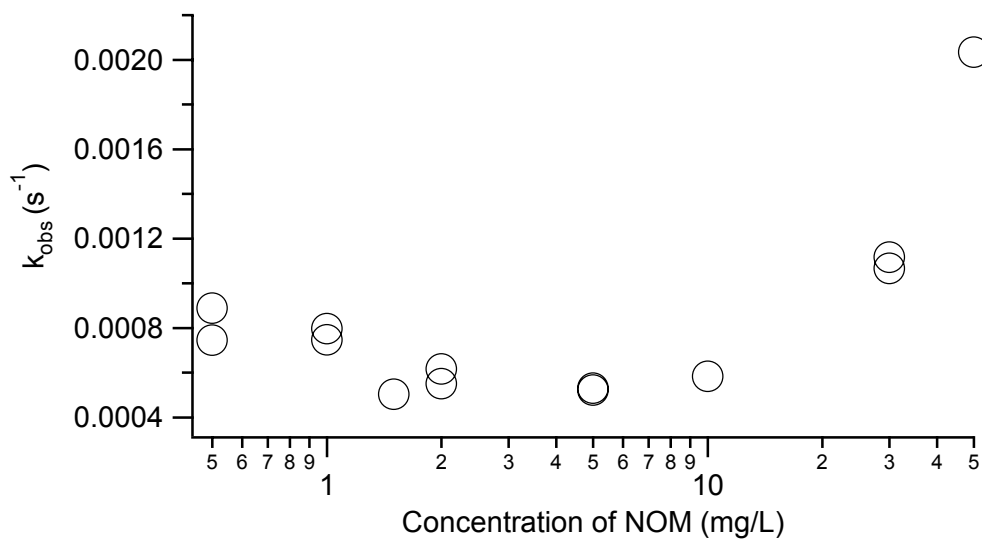
Figure 26: The reaction of 0.1 mM MnO_4^- and 1.0 mM TCE with varying amounts of NOM. The NOM does not seem to affect the reaction until the concentration increases to >10 mg/L. Experimental conditions: pH 7, 25°C, 50 mM phosphate buffer.
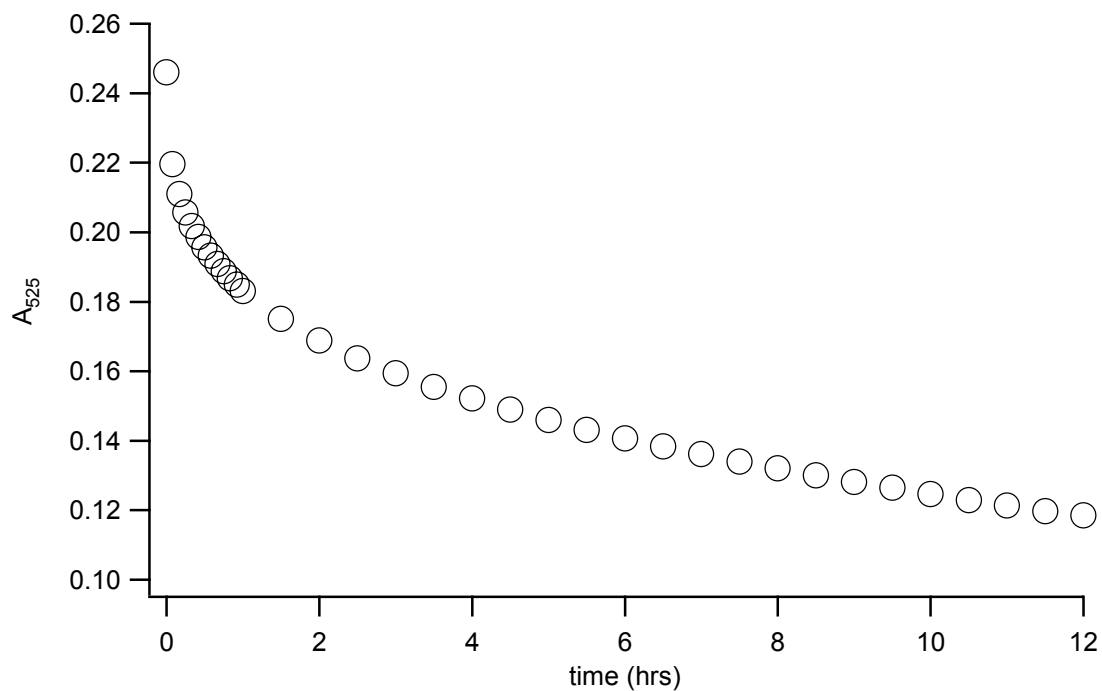
Figure 27: The reaction of 0.1 mM MnO_4^- and 10 mg/L NOM. Experimental conditions: pH 7, 25°C, 50 mM phosphate buffer.

Chapter 6: Quantitative Structure-Activity Relationships (QSARs)

6.1 QSARs of all compounds with MnO_4^-

One of the goals of this study was to investigate whether quantitative structure-activity relationships (QSARs) could be developed for oxidations of COCs by MnO_4^-. The primary motivation for developing QSARs was to provide a means of predicting the rate of MnO_4^- oxidation for compounds that have not been studied. A further benefit of developing QSARs is that evidence for a correlation (or lack of one) between chemical structure and reactivity with MnO_4^- can provide insight on the mechanism of MnO_4^- oxidation with COCs. Because outliers often are easily identified when data are shown in this format, yet another benefit of QSARs is its usefulness in determining consistency among the data [51].

In order to develop a successful QSAR among a group of compounds, the compounds must have similar reaction mechanisms or structurally similar reaction centers. In addition, a descriptor variable that relates to the reaction mechanism or reaction center must be identified. Descriptors that relate to the energetics of reaction include the half-wave potential ($E_{1/2}$), ionization potential (IP), and the energy of the highest occupied molecular orbital (E_{HOMO}). These may be preferred descriptors for oxidation reactions [51, 52].

Even though ionization potential (IP) is directly related to E_{HOMO} through Koopman's theorem (IP = $-E_{HOMO}$) [53], experimentally derived values of IP were also used as a descriptor.   As can be seen in Figure 28, the computer-calculated E_{HOMO} and the experimentally derived IP values do not perfectly follow Koopman's theorem, and the lack of a perfect correlation between them indicates that slightly different information is obtained from the two descriptors.

Another descriptor that was explored is the energy difference between the HOMO and the LUMO (E_{Gap}). This descriptor has been used as a measure of the relative stability of a compound toward chemical reaction—compounds with larger gaps are thought to have lower reactivity [53, 54]. Finally, the rate of oxidation by ozone was used as a descriptor for the rate of oxidation by MnO_4^- to determine whether a cross-correlation between the two oxidants exists. Ozone was chosen because the reaction intermediate of direct ozonation of some compounds is the cyclic ozonide, which is structurally similar to the cyclic hypomanganate ester formed in MnO_4^- oxidation of alkenes (see Figure 1); in addition, the rates of a large variety of compounds by ozone are available in the published literature.

Figure 28 shows a scatter plot matrix of all of the compounds for which data are available from either the literature or experiments from this study. Based on the lack of significant correlation to either E_{HOMO} or IP, oxidation by MnO_4^- of COCs with different chemical structures appears to be too complex to be described by a single descriptor. The stability of the COC as measured by E_{Gap} also does not appear to predict the reactivity with MnO_4^-. Interestingly, the descriptor that seems to correlate with reactivity of MnO_4^- among compounds of different chemical classes is the reactivity of these compounds with ozone. It is therefore likely that there are other effects in addition to electron transfer (perhaps steric effects) that are involved in the reaction of these compounds with MnO_4^-. If the unknown effects also affect the reactivity of compounds with ozone, these effects would be incorporated in the rate of oxidation by ozone. This may be the reason why the rate of oxidation by ozone is the best descriptor for the rate of oxidation by MnO_4^-.

6.2 QSARs of individual chemical classes

6.2.1 QSARs of chlorinated ethylenes

Figure 29 shows a negative correlation of the chlorinated ethylenes with E_{HOMO} and a positive correlation with IP. However, an organic compound is oxidized when it loses electrons to the oxidant, and as lower IP (and higher E_{HOMO}) indicates easier removal of an electron, one would expect that compounds with low IP (and high E_{HOMO})

would be the most reactive with an oxidant. Yet the apparent correlation shown in Figure 29 is the opposite, indicating that energetics are not the controlling effect in the reaction. The reason for this may be that the rate-limiting step in reaction with the chlorinated ethylenes is the formation of the cyclic hypomanganate ester (Figure 1).
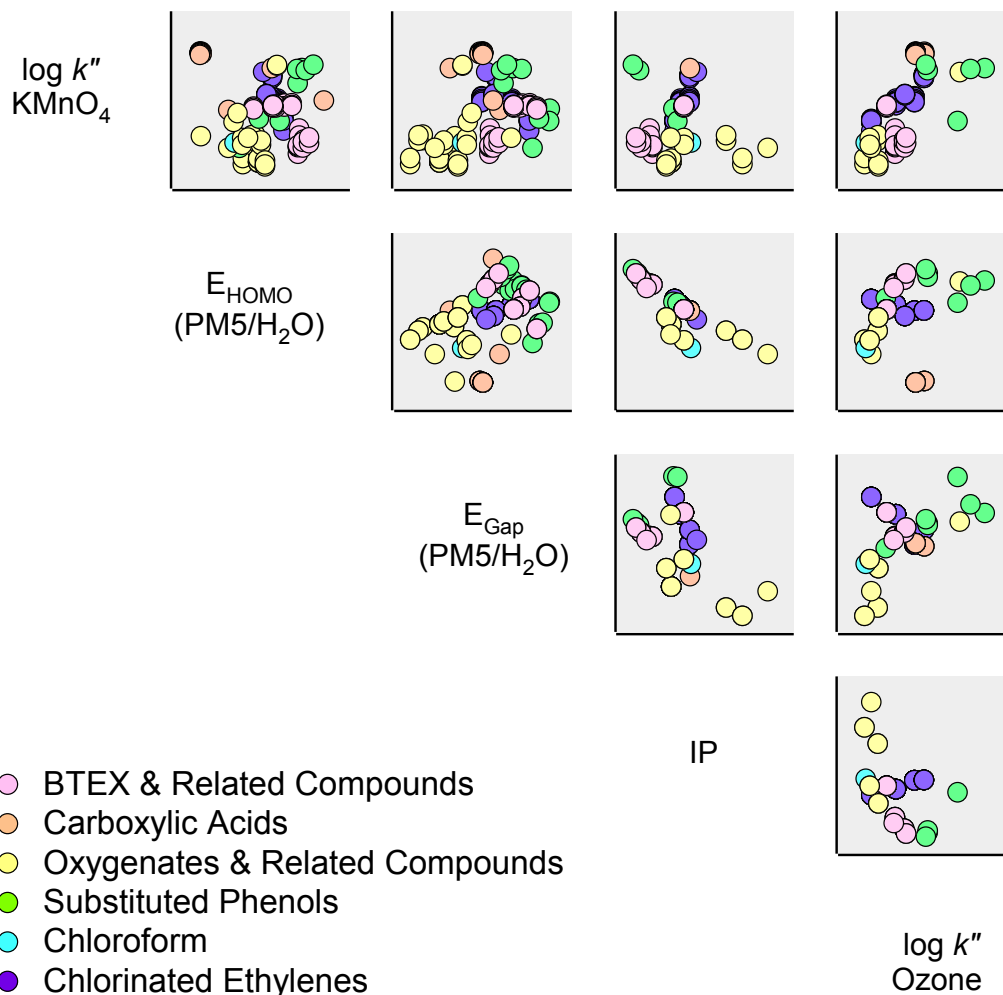
Figure 28: Scatter plot matrix of log *k″* of all compounds obtained from experiments or literature. All *k″* values were obtained at a pH between 4.0 and 8.0, at temperatures between 20°C and 30°C. E_{HOMO} and E_{Gap} were calculated with CACHe molecular modeling software. IP values were obtained from [55-57]. Ozone rate constants were obtained from [58-60]. The values used in this figure are shown in Appendix C.
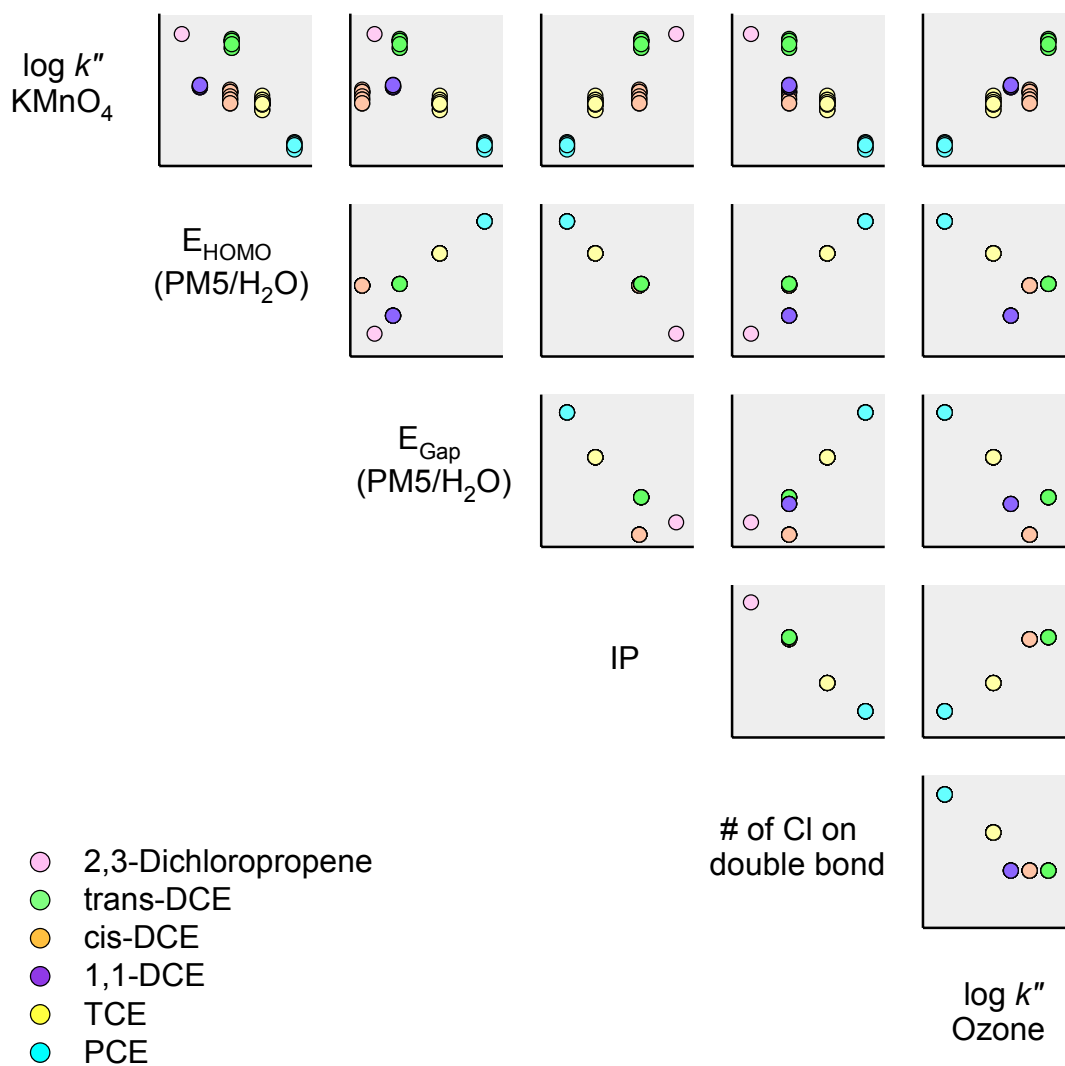
Figure 29: Scatter plot of log k'' for oxidation by MnO_4^- vs. selected descriptors for the chlorinated ethylenes. Ionization potentials (IP) are from [55]. E_{HOMO} and E_{Gap} were calculated using molecular modeling software (CAChe), and log k'' for oxidation of ethylenes by ozone is from [58]. The values used in this figure are shown in Appendix C.

Because chlorine is an electron-withdrawing substituent, and the reactivity of the chlorinated ethylenes decreases with increasing number of chlorines, MnO_4^- appears to be behaving as an electrophile in the initial rate-determining step, and it is likely that the electron density in the pi bonds of the chlorinated ethylenes, and not energetics, is controlling the reaction. In fact, the case has previously been made that energetics for the ground state of the alkene should not be controlling for any reaction where nucleophilic attack on a reversibly formed pi complex (e.g., oxymetalation) is rate determining [61].

In addition to the number of chlorine substituents, steric hindrance from the position of the chlorines also appears to be an important factor controlling the rate of reaction with MnO_4^-. This is most notably seen with cis-DCE and trans-DCE, which both have two chlorine substituents with one on each carbon, but significantly different rates. Trans isomers are generally more stable than cis isomers; thus, in reactions where steric effects are not significant, it is expected that the cis isomer would react faster than the trans isomer [61]. However, for reactions in which large cyclic activated complexes (such as the cyclic hypomanganate diester) are formed, the change in bond angles causes increased steric hindrance of the chlorines in the cis orientation, resulting in slower rates [4, 61]. The rate of 1,1-DCE is more similar to cis-DCE than trans-DCE, which indicates that chlorines on the same carbon are sterically hindered as well. A further indication of the controlling effects of steric hindrance is that TCE, cis-DCE, and 1,1-DCE all have similar rates even though TCE has three chlorines, while cis-DCE and 1,1-DCE only have two.

Direct ozonation of unsaturated compounds in low-pH aqueous media (the media used in the referenced ozone experiments) is generally agreed to occur through the formation of ozonide, another five-membered cyclic intermediate [62]; therefore, it likely incorporates many of the rate-determining effects that are not described by the other descriptors. It is not surprising, then, that the rates of oxidation between ozone and MnO_4^- correlate so well—not only is there a high value of R^2 for the correlation (0.86), but it is clear that the correlation would be even better by removing the cis-DCE outlier. That the reaction rate of oxidation of cis-DCE by MnO_4^- is over-predicted by the rate of oxidation by ozone is likely because ozonide is less bulky than the cyclic hypomanganate

diester formed by MnO_4^- oxidation, and is therefore not as greatly affected by steric hindrance from the close proximity of the chlorine atoms on cis-DCE.

6.2.2 QSARs of the substituted phenols

As seen in Figure 30, the rate of oxidation of phenols by MnO_4^- appears to correlate well with many of the descriptors: correlations with E_{HOMO} and $E_{1/2}$ both yield R^2 values higher than 0.9, and an R^2 value of 0.86 was obtained for the correlation with a specialized scale of the Hammet sigma constant, σ^-. The σ^- scale was used because it was derived from the ionization of anilines and phenols in water and more fully accounts for the ability of substituents to stabilize or destabilize the electron-rich reaction centers of the aromatic ring [52]. However, it is possible that the apparent robustness of the correlations is deceptive because the training set used in the correlation is a mixture of phenols in their ionic and molecular states. (The pK_as of the phenols varied from 0.38 for picric acid to 10.3 for p-cresol, yet the rate of oxidation by MnO_4^- was determined at pH 7 for all of them. Also, it should be noted that the compounds correlate well to pK_a, which would be expected if there were strong differences in the reactivity of the phenols vs. the phenolates.) That the training set includes both phenols and phenolates is significant because with other oxidants, the ionic forms of phenols have reactivities that are typically 1 to 2 orders of magnitude different from their corresponding molecular forms [59, 63]. Therefore, it is difficult to determine whether the correlations truly reflect the descriptor variable or whether there are large differences between the rates of phenolates and phenols with MnO_4^-. Indeed, it should be noted that the values for picric acid and 2,4-dinitrophenol drive the correlations, and not only are both of these compounds ions at pH 7 (their pK_as are 0.38 and 4.09, respectively), but experiments exploring pH effects on the rate of MnO_4^- oxidation of 2,4-dinitrophenol indicated that the molecular form is more reactive than the ionic form [40].

In order to explore this effect further, the percentages of the phenolates and phenols at pH 7 were calculated (see Table 1), and rates due to the phenolates and those due to the phenols were correlated separately. This was accomplished by making the

assumption that either the phenol (in the case of the correlation with phenolates) or the phenolate (in the case of the correlation with phenols) does not contribute at all to the rate of the oxidation at pH 7. This would be true if there was a greater than two orders of
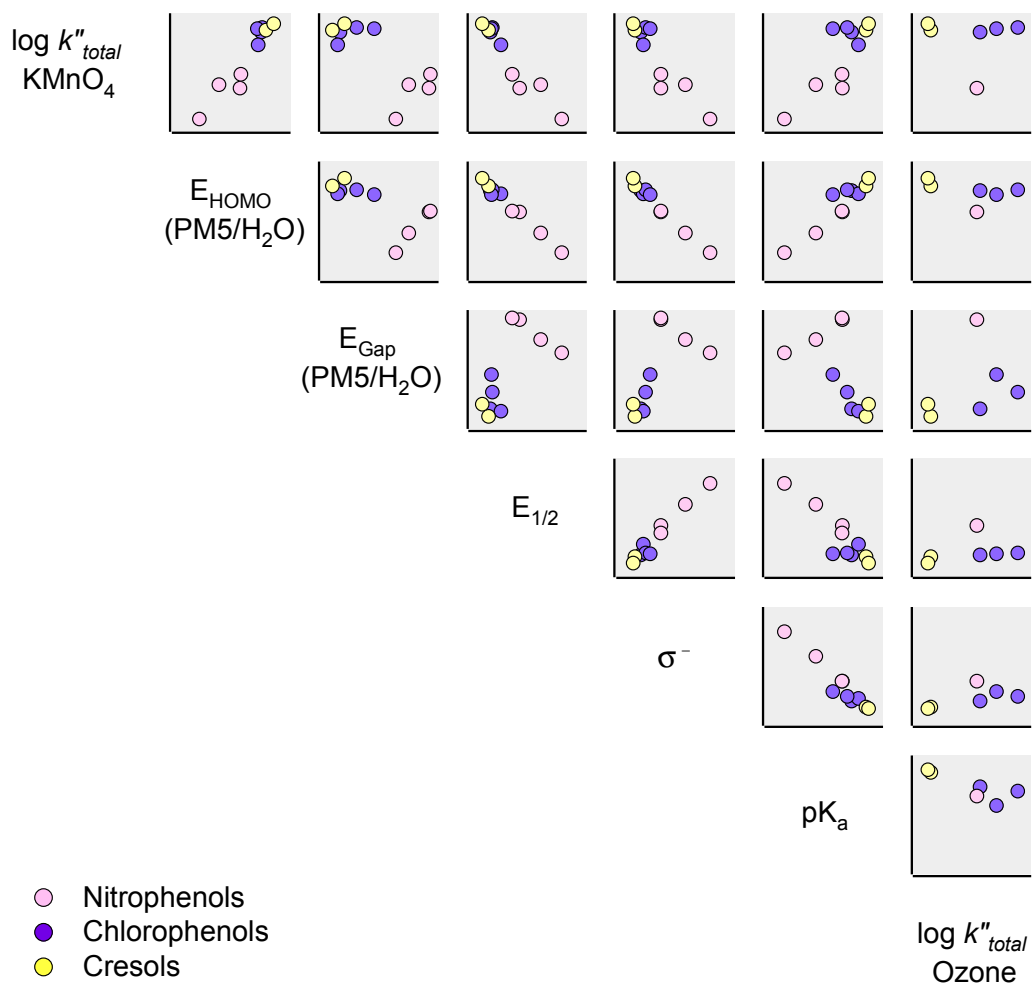
Figure 30: Scatter plot matrix of log k'' for oxidation of substituted *phenols and phenolates* at pH 7 by MnO_4^- vs. selected descriptors. Half-wave potentials ($E_{1/2}$) are from [64], Hammett constants (σ^-) are from [65], pK_a values are from [63, 66], and ozone values are from [59]. E_{HOMO} and E_{Gap} values were calculated using molecular modeling software (CAChe). The values used in this figure are shown in Appendix C.

Table 1: Comparison of the calculated k'' for phenols only and phenolates only at pH 7 to the experimental value of k'' which incorporates the combined effects of phenols and phenolates at pH 7.

Compound	pKa	Fraction of phenols at pH 7 (α_0)	Fraction of phenolates at pH 7 (α_1)	Combined k'' at pH 7[a]	k'' of phenols at pH 7[b]	k'' of phenolates at pH 7[b]
2-Chlorophenol	8.3	9.5E-01	4.8E-02	7.40E+01	7.77E+01	1.55E+03
3-Chlorophenol	9.12	9.9E-01	7.5E-03	1.34E+01	1.35E+01	1.78E+03
2,4-Dichlorophenol	7.8	8.6E-01	1.4E-01	1.42E+02	1.65E+02	1.04E+03
246-Trichlorophenol	6.1	1.1E-01	8.9E-01	1.20E+02	1.07E+03	1.35E+02
m-Cresol	10	1.0E+00	1.0E-03	9.80E+01	9.81E+01	9.81E+04
p-Cresol	10.3	1.0E+00	5.0E-04	2.37E+02	2.37E+02	4.73E+05
2-Nitrophenol	7.17	6.0E-01	4.0E-01	2.43E-01	4.07E-01	6.02E-01
4-Nitrophenol	7.2	6.1E-01	3.9E-01	3.70E-02	6.03E-02	9.56E-02
2,4-Dinitrophenol	4.09	1.2E-03	1.0E+00	6.00E-02	4.88E+01	6.01E-02
Picric Acid	0.38	2.4E-07	1.0E+00	5.63E-04	2.35E+03	5.63E-04

a) Experimental value
b) Calculated value

magnitude difference between the rates of oxidation of the phenol and of the phenolate, with the same species having the faster rate for every compound studied. If this assumption is incorrect, neither of the QSARs are meaningful. Furthermore, because both the QSARs for the phenolates and those for the phenols are created assuming that the species in the QSAR has the faster rate of oxidation, only one of the QSARs can be correct. Keeping these assumptions in mind, the analysis is as follows:

Case 1: The rate at pH 7 is due entirely to phenols

The rate of oxidation assuming the phenol is the only species determining the rate of oxidation at pH 7 was calculated using Equation 13:

$$k''_{phenol} = \frac{k''_{total, pH7}}{\alpha_0}$$

[13]

where $\alpha_0 = [H^+]/([H^+] + K_a)$ and is equal to the fraction of the phenol in the protonated form [67]. The same descriptors as those in Figure 30 were used in correlations with $k''_{phenol.}$ Because fewer than 1 in 1000 protonated forms are present at pH 7 for both picric acid and 2,4-dinitrophenol, it is doubtful the assumption that the experimental

value for the rate of oxidation at pH 7 is due entirely to the reactivity of the phenolic species is correct. If these points are thrown out, the phenols appear to correlate well to E_{HOMO} and $E_{1/2}$, while becoming less dependent on pK_a. It is also interesting to note that, as expected, the oxidation of the phenols by MnO_4^- correlates better to the oxidation of phenols by ozone than the correlations for the combined effects of both phenols and phenolates.
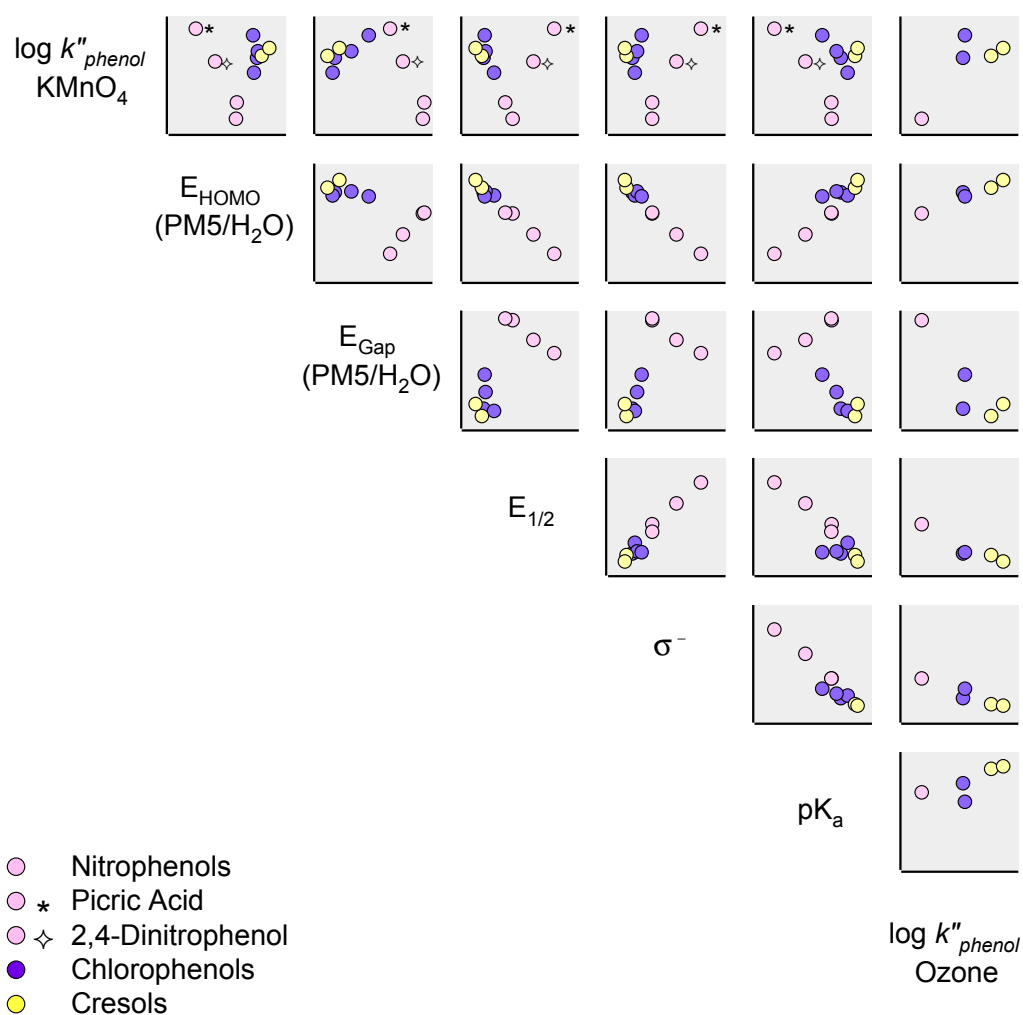
Figure 31: Scatter plot matrix of log k'' for oxidation of *phenols* by MnO_4^- vs. selected descriptors. Half-wave potentials ($E_{1/2}$) are from [64], Hammett constants (σ^-) are from [65], and pK_a values are from [63, 66]. E_{HOMO} and E_{Gap} values were calculated using molecular modeling software (CAChe). The values used in this figure are shown in Appendix C.

Case 2: The rate at pH 7 is due entirely to the phenolate

The rate of oxidation assuming the phenolate is the only species determining the rate of oxidation at pH 7 was calculated using Equation 14:

$$k''_{phenolate} = \frac{k''_{total, pH7}}{\alpha_1} \qquad [14]$$

where $\alpha_1 = K_a/([H^+] + K_a)$ and is equal to the fraction of phenols that have lost a proton (the phenolates) [67]. These correlations are also good, and do not have any obvious outliers. The reason there are no outliers is that the rates for the phenols most in question (those with phenolates present in proportions less than 1:1000) get larger (see Table 1), which increases the correlation with the descriptors.

Because it is currently unknown whether the assumption that only the phenol or the phenolate contributes to reactivity at pH 7 is valid and whether the phenol or phenolate QSAR is expected to be correct, neither QSAR should be used for predictive purposes without further study. However, because the QSARs of the phenols and phenolate ions still show correlations with E_{HOMO}, $E_{1/2}$, and σ^- while becoming less dependent on pK_a, it is clear that pK_a is not the only factor driving the original QSARs. Thus, it is possible that the original QSAR could be valid for predictions of reactivity for other phenols at pH 7. In order to fully understand these issues, more experiments are necessary. To determine whether the original QSAR can be used for predictive purposes, the rates of phenols that will further fill in the correlation should be predicted, and then obtained experimentally to see if there is agreement between the two. To further understand the pH effects of the phenols, oxidation rates for each phenol should be obtained at 2 pH units above and below the pK_a, so that the difference in rate between the phenolates and phenols can be determined with confidence.
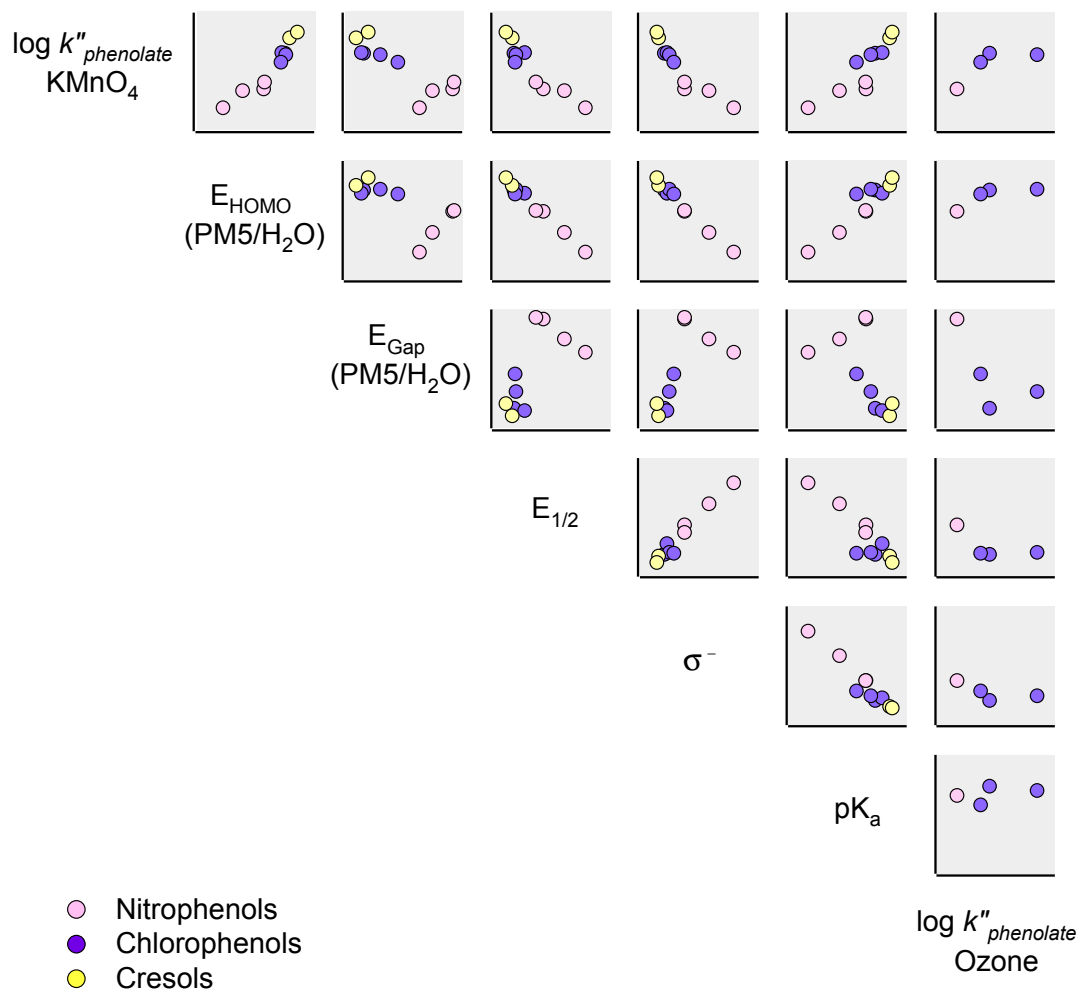
Figure 32: Scatter plot matrix of log k'', for oxidation of *phenolates* by MnO_4^- vs. selected descriptors. Half-wave potentials ($E_{1/2}$) are from [64], Hammett constants (σ^-) are from [65], and pK_a values are from [63, 66]. E_{HOMO} and E_{Gap} values were calculated using molecular modeling software (CAChe). The values used in this figure are shown in Appendix C.

6.2.3 QSARs with compounds belonging to the BTEX and oxygenate chemical classes

As shown in Figures 33 and 34, neither the compounds belonging to the BTEX class nor those belonging to the oxygenate class correlate with any of the descriptors used in this study. Although the alcohols may appear to correlate to IP, allyl alcohol, which drives the correlation, contains a double bond. Because the reactivity of allyl alcohol is much higher compared with ethanol and methanol, it is likely that MnO_4^- is actually reacting with the electron-rich double bond, and not the alcohol functional group. Therefore, an appearance of a correlation among the alcohols is probably an artifact.
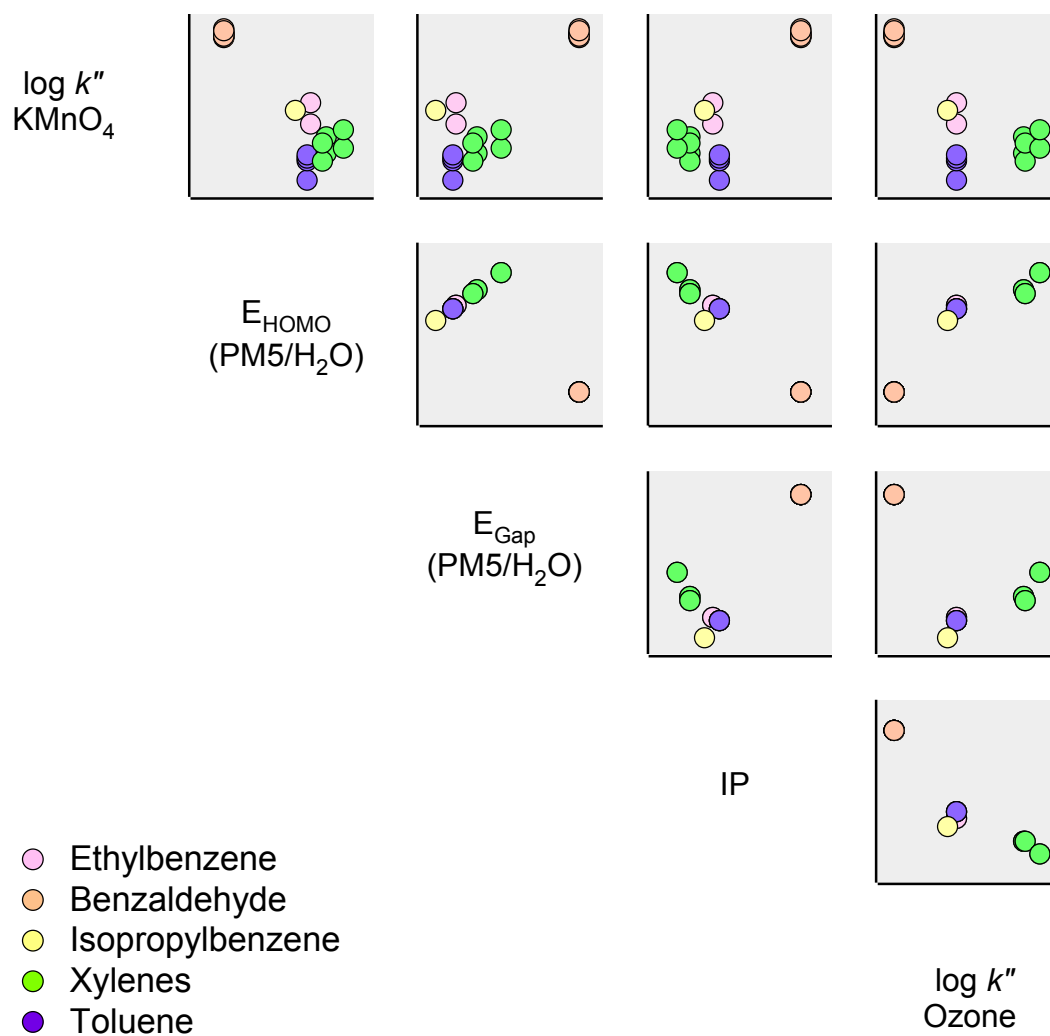
Figure 33: Scatter plot matrix of the BTEX compounds. Ionization potentials (IP) are from [55], E_{HOMO} and E_{Gap} were calculated using molecular modeling software (CAChe), and log k'' values for oxidation of ethenes by ozone are from [58]. The values used in this figure are shown in Appendix C.
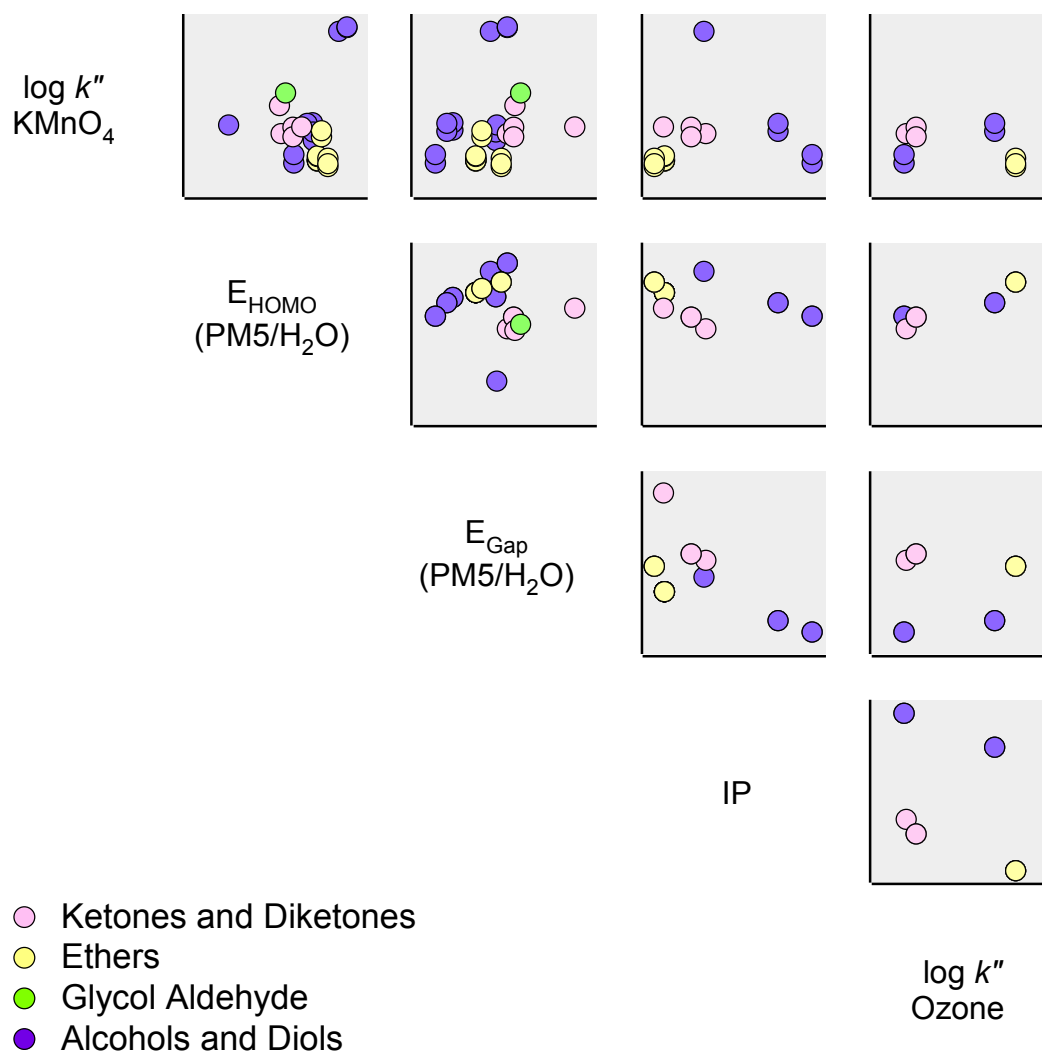
Figure 34: Scatter plot matrix of oxygenates and related compounds. Values of IP were obtained from [55, 68]. E_{HOMO} and E_{Gap} were calculated using molecular modeling software (CAChe), and log k'' values for oxidation of compounds by ozone are from [58]. The values used in this figure are shown in Appendix C.

Chapter 7: Field Application of k'' Data

7.1 Application of k'' to a plume containing a single COC

When designing an ISCO project for remediation of a COC, it is important to keep the concentration of MnO_4^- in >5-fold excess of both the NOD and the COC in order to maintain maximum degradation rates.   The determination of the concentration of MnO_4^- required should also take into account the dilution of MnO_4^- from the point of injection to the source of COC. As long as MnO_4^- remains in excess, the concentration of the COC at any point in time can be calculated with Equation 15:

$$[COC] = [COC]_i e^{-k''[MnO_4^-]t}$$ [15]

where $[COC]_i$ is the initial aqueous concentration of COC. $[COC]_i$ will remain constant at the saturation limit of the COC as long as NAPL is present, assuming that the rate of oxidation is rate-limiting (as opposed to the rate of dissolution from the NAPL). Once the NAPL has been depleted, the aqueous [COC] will decrease exponentially.

In order to use Equation 15 to determine the amount of time required to achieve a certain remediation goal, it should be noted that k'' varies with temperature, and will be lower under natural groundwater temperatures (the values of k'' shown in Figure 20 and Appendix B were obtained at temperatures ranging from $20^{\circ}C$ to $30^{\circ}C$). This temperature effect can be calculated with the Arrhenius equation:

$$k = Ae^{-E_A/RT}$$ [16]

where A is the pre-exponential factor, E_A is the activation energy, R is the universal gas constant, and T is temperature in kelvins. Activation energies for chlorinated ethyleneand BTEX compounds and the corresponding reduction factors of k'' for a 10°C decrease are given in Table 2. For these 10 compounds (with several orders of magnitude difference among their reaction rates) the reduction factors of k'' for a 10°C decrease range from 1.4 to 2.5.

Table 2: Activation energies and k'' reduction factors for chlorinated ethylenes and BTEX compounds

COC	E_A (kcal/mol)	Reference	k'' reduction factor for a 10°C decrease
trans-DCE	5.8	[39]	1.4
1,1-DCE	6.9	[39]	1.5
cis-DCE	8.8	[39]	1.7
TCE	8.9	[39]	1.7
PCE	9.3	[39]	1.7
Ethylbenzene	13.1	[69]	2.2
p-Xylene	14.6	[69]	2.4
o-Xylene	14.8	[69]	2.4
m-Xylene	15.1	[69]	2.4
Toluene	15.8	[69]	2.5

Example calculation: The following is an example calculation of the time required to reach a concentration of 0.005 mg/L, the maximum contaminant level (MCL) for TCE [70], in 15°C groundwater that has an initial aqueous concentration of 1385 mg/L TCE. The [MnO_4^-] used in this calculation is 7000 mg/L (0.044 M); because this is ~5× the TCE concentration, the use of pseudo-first-order kinetics is appropriate. This concentration does not account for dilution and is in addition to the MnO_4^- required for the NOD of the aquifer. Furthermore, it is assumed that DNAPL is not present at the site. The k'' for TCE at 25°C (static method, this study) is 0.76 $M^{-1}s^{-1}$. The adjusted k'' for TCE at 15°C is 0.45 $M^{-1}s^{-1}$ (0.76 $M^{-1}s^{-1}$ ×1.7).

$$[0.005 \, mg/L] = [1385 \, mg/L]_i \, e^{-0.45 \, M^{-1}s^{-1}[0.044 \, M]\times t} \qquad [17]$$

$$t = \frac{\ln(0.005 \, mg/L) - \ln(1385 \, mg/L)}{-0.45 \, M^{-1}s^{-1} \times 0.044 \, M} = 632 \, s = 10.5 \, min \qquad [18]$$

7.2 Application of k'' to a plume containing a mixture of COCs

Many contaminant plumes contain a mixture of COCs [71]. In this case, as long as MnO_4^- is in excess, the rate of degradation of each COC should be independent of one another. For example, if a plume contained TCE, cis-DCE, and VC, the concentration of any COC at any time can be determined by its respective rate law:

$$[TCE] = [TCE]_i e^{-k''[MnO_4^-]t} \qquad [19]$$

$$[cis-DCE] = [cis-DCE]_i e^{-k''[MnO_4^-]t} \qquad [20]$$

$$[VC] = [VC]_i e^{-k''[MnO_4^-]t} \qquad [21]$$

The total time it takes to degrade the plume is therefore limited by the COC with the lowest k'' and highest initial concentration. On the other hand, the rate of consumption of MnO_4^- is additive as shown in Equation 22:

$$\frac{\partial[MnO_4^-]}{\partial t} = [MnO_4^-] \times (k''_{TCE}[TCE] + k''_{cis-DCE}[cis-DCE] + k''_{VC}[VC]) \qquad [22]$$

Example calculation: The following is a calculation of the time required for each of the COCs to reach their respective MCL levels (0.005 mg/L for TCE, 0.070 mg/L for cis-DCE, and 0.002 mg/L for VC [70]) in 15°C groundwater that has initial aqueous concentrations of 1385 mg/L TCE (0.01 M) 5000 mg/L (0.05 M) cis-DCE, and 700 mg/L (0.01 M) VC. The [MnO_4^-] used in this calculation is 35425 mg/L (0.23 M); because this is 5× the total [COC], the use of pseudo-first-order kinetics is appropriate. This concentration does not account for dilution and is in addition to the MnO_4^- required for the NOD of the aquifer. Furthermore, it is assumed that DNAPL is not present at the site. The k'' for TCE at 25°C (static method, this study) is 0.76 $M^{-1}s^{-1}$. The adjusted k'' for TCE at 15°C is 0.45 $M^{-1}s^{-1}$ (0.76 $M^{-1}s^{-1} \times 1.7$). The k'' for cis-DCE at 25°C (static method, this study) is 0.71 $M^{-1}s^{-1}$. The adjusted k'' for cis-DCE at 15°C is 0.42 M^-s^{-1} (0.71 $M^{-1}s^{-1}$

$\times 1.7$). The k'' for VC at $25°C^2$ is 77 M^{-1}s^{-1}. The adjusted k'' for VC at $15°C^3$ is 55 M^{-1}s^{-1} (77 M^{-1}s^{-1} $\times 1.4$).

Time for TCE to reach MCL:

$$t = \frac{\ln(0.005 \, mg \, / \, L) - \ln(1385 \, mg \, / \, L)}{-0.45 \, M^{-1}s^{-1} \times 0.23 \, M} = 121 \, s = 2 \, min \qquad [23]$$

Time for cis-DCE to reach MCL:

$$t = \frac{\ln(0.070 \, mg \, / \, L) - \ln(5000 \, mg \, / \, L)}{-0.42 \, M^{-1}s^{-1} \times 0.23 \, M} = 116 \, s = 1.9 \, min \qquad [24]$$

Time for VC to reach MCL:

$$t = \frac{\ln(0.002 \, mg \, / \, L) - \ln(700 \, mg \, / \, L)}{-55 \, M^{-1}s^{-1} \times 0.23 \, M} = 1 \, s \qquad [25]$$

Rate of MnO$_4^-$ consumption:

$$\frac{\partial[MnO_4^-]}{\partial t} = [0.23 \, M] \times (0.45 \, M^{-1}s^{-1}[0.01 \, M] + 0.42 \, M^{-1}s^{-1}[0.05 \, M] + 77 M^{-1}s^{-1}[0.01 \, M]) \qquad [26]$$

$$= 0.18 \, M \, / \, s$$

As can be seen, when no NAPL is present, COCs decrease rapidly to MCL levels. Again, when NAPL is present, the times required to reach MCL will be affected by the rate of NAPL dissolution to the aqueous phase in addition to the rate of oxidation by MnO$_4^-$.

---

[2] Even though k'' for VC has not been determined experimentally, it was shown in Section 6.2.1 that k'' for chlorinated alkenes correlates strongly with the number of chlorines on the double bond; therefore, the k'' obtained for 2,3-dichloropropene (77 M^{-1}s^{-1}), should provide a good approximation for the k'' for VC.
[3] The k'' for VC is closest to k'' for trans-DCE, so the reduction factor for trans-DCE was used as an approximation of the reduction factor for VC.

Chapter 8: Conclusions

This appears to be the most comprehensive summary of kinetic data for MnO_4^- oxidation reactions of environmentally relevant compounds across a wide range of chemical classes. After completing an extensive literature search, many data gaps were filled using an efficient method of determining rate constants based on monitoring decreasing MnO_4^- concentrations with UV spectroscopy. This method was shown to give comparable results to the more traditional approach of monitoring COC concentrations with gas chromatography, which is less efficient when a large number of rate constants for compounds with different chemical structures are required.

The COCs shown to react with MnO_4^- as quickly as or faster than the chlorinated ethylenes (compounds that have been treated successfully with MnO_4^- in the field) include many of the substituted phenols and the two pesticides analyzed in this study, aldicarb and dichlorvos. COCs that had much slower reactivity with MnO_4^- include the chlorinated alkanes, BTEX compounds, and many of the compounds used as oxygenates. This indicates that ISCO with MnO_4^- may not be the preferred method for remediation of sites contaminated with gasoline, due to the high concentrations and longer time frames required.

The rate of reaction of MnO_4^- with the model compound TCE was shown to be unaffected by many common groundwater constituents such as bicarbonate, nitrate, and sulfate. In addition, natural conditions of NOM also did not affect the rate of reaction of MnO_4^- and TCE.

While the QSARs developed have limited predictive value, the QSARs with the chlorinated ethylenes provided information on the mechanism of MnO_4^- oxidation with that class of compounds. Exploratory correlation analysis with the phenols indicates that with further experimentation, satisfactory QSARs with E_{HOMO}, $E_{1/2}$, and σ^- will likely be developed.

References

1. Vella, P.A. and B. Veronda. (1993). Oxidation of trichloroethylene: A comparison of potassium permanganate and Fenton's reagent. In W.W. Eckenfelder, A.R. Bowers, and J.A. Roth (Eds.), *3rd International Symposium, Chemical Oxidation: Technology for the Nineties, Vanderbilt University, Nashville, TN, 17-19 February 1993* (pp. 62-73). Nashville, TN: Technomic, Lancaster, UK.

2. Tratnyek, P.G*., et al.* (1998). In situ treatment of organics by sequential reduction and oxidation. In G.B. Wickramanayake and R.E. Hinchee (Eds.), *Physical, Chemical, and Thermal Technologies: Proceedings of the First International Conference on Remediation of Chlorinated and Recalcitrant Compounds, 18-21 May 1998, Monterey, CA* (pp. 371-376). Monterey, CA: Battelle Press.

3. Yan, Y.E. and F.W. Schwartz. (1998). Oxidation of chlorinated solvents by permanganate. In G.B. Wickramanayake and R.E. Hinchee (Eds.), *Physical, Chemical, and Thermal Technologies: Proceedings of the First International Conference on Remediation of Chlorinated and Recalcitrant Compounds, 18-21 May 1998, Monterey, CA* (pp. 403-408). Monterey, CA: Battelle Press.

4. Yan, Y.E. and F.W. Schwartz. (1999). Oxidative degradation and kinetics of chlorinated ethylenes by potassium permanganate. *Journal of Contaminant Hydrology*. **37**(3-4): 343-365.

5. Yan, Y.E. and F.W. Schwartz. (2000). Kinetics and mechanisms for TCE oxidation by permanganate. *Environmental Science and Technology*. **34**(12): 2535-2541.

6. Huang, K.-C*., et al.* (1999). Kinetic study of oxidation of trichloroethylene by potassium permanganate. *Environmental Engineering Science*. **16**(4): 265-274.

7. Hood, E.D*., et al.* (2000). Experimental determination of the kinetic rate law for the oxidation of perchloroethylene by potassium permanganate. *Chemosphere*. **40**(12): 1383-1388.

8. Dai, Q. and S. Reitsma. (2002). Kinetic study of permanganate oxidation of tetrachloroethylene at pH 10.60 ± 0.1. In A. Gavaskar and A.S.C. Chen (Eds.), *Proceedings of the Third International Conference on Remediation of Chlorinated and Recalcitrant Compounds, 20-23 May 2002, Monterey, CA.* (2C-09). Monterey, CA: Battelle Press.

9. Poulson, S.R. and H. Naraoka. (2002). Carbon isotope fractionation during permanganate oxidation of chlorinated ethylenes (cDCE, TCE, PCE). *Environmental Science and Technology*. **36**(15): 3270-3274.

10. Hunkeler, D*., et al.* (2003). Monitoring oxidation of chlorinated ethenes by permanganate in groundwater using stable isotopes: Laboratory and field studies. *Environmental Science and Technology*. **37**(4): 798-804.

11. Committee on U.S. Geological Survey Water Resources. (1996). *Hazardous Materials in the Hydrologic Environment: The Role of Research by the U.S. Geological Survey*. Washington, D.C.: The National Academies Press.

12. U.S. Environmental Protection Agency. (1998). *Field Applications of In Situ Remediation Technologies: Chemical Oxidation* (EPA-542-R-98-008). U.S. Environmental Protection Agency, Office of Solid Waste and Emergency Response: Washington, D.C.

13. U.S. Environmental Protection Agency. (1998). *Technical Protocol for Evaluating Natural Attenuation of Chlorinated Solvents in Ground Water* (EPA/600/R-98/128). U.S. Environmental Protection Agency: Washington D.C.

14. Interstate Technology and Regulatory Cooperation Work Group (ITRC). (2001). *Technical and Regulatory Guidance for In Situ Chemical Oxidation of Contaminated Soil and Groundwater.* Interstate Technology and Regulatory Cooperation Work Group (ITRC):

15. Tratnyek, P.G.*, et al.* (2003). Permeable reactive barriers of iron and other zero-valent metals. In *Chemical Degradation Methods for Wastes and Pollutants: Environmental and Industrial Applications* (pp. 371-421). M.A. Tarr, Editor. New York: Marcel Dekker.

16. Horst, J.F.*, et al.* (2002). Chlorobenzene NAPL Oxidation Using Potassium Permanganate: Bench and Field Scale Demonstration. In A. Gavaskar and A.S.C. Chen (Eds.), *Third International Conference on Remediation of Chlorinated and Recalcitrant Compounds, 20-23 May 2002, Monterey, CA* (2C-24). Monterey, CA: Battelle Press.

17. Hood, E.D. and N.G. Thompson. (2002). Impact of diffusion and natural oxidant demand on permanganate loss into low-permeability porous media. In A. Gavaskar and A.S.C. Chen (Eds.), *Third International Conference on Remediation of Chlorinated and Recalcitrant Compounds, 20-23 May 2002, Monterey, CA* (1A-11). Monterey, CA: Battelle Press.

18. Huang, K.-C., R.A. Couttenye, and G.E. Hoag. (2002). Kinetics of heat-assisted persulfate oxidation of methyl tert-butyl ether (MTBE). *Chemosphere*. **49**: 413-420.

19. Bruell, C.J.*, et al.* (2001). Kinetics of thermally activated persulfate oxidation of trichloroethylene (TCE) and 1,1,1-trichloroethane (TCA). In (Eds.), *1st International Conference on Oxidation and Reduction Technologies for In-Situ Treatment of Soil and Groundwater, 25-29 June 2001* (pp. 133-136). Niagara Falls, Ontario, Canada.

20. Carus Chemical Company. (2004). In-Situ Chemical Oxidation (ISCO) with Permanganate: Effective Application. In *Technical Information Disk: Groundwater & Soil Remediation, vol. 1.4*. LaSalle: Carus Chemical Company.

21. Siegrist, R.L.*, et al.* (2001). *Principles and Practices of In Situ Chemical Oxidation Using Permanganate*. Columbus: Batelle Press.

22.   Schroth, M.H., *et al.* (2001). In-situ oxidation of trichloroethene by permanganate: effects on porous medium hydraulic properties. *Journal of Contaminant Hydrology*. **50**: 79-98.

23.   Siegrist, R.L., *et al.* (2002). Genesis and Effects of Particles Produced during In Situ Chemical Oxidation Using Permanganate. *Journal of Environmental Engineering*. **128**(11): 1068-1079.

24.   Li, X.D. and F.W. Schwartz. (2002). Permanganate oxidation schemes for the remediation of source zone DNAPLs and dissolved contaminant plumes. In *Chlorinated Solvent and DNAPL Remediation. Innovative Strategies for Subsurface Cleanup.* (pp. 73-85). S.M. Henry and S.D. Warner, Editors. Washington D.C.: American Chemical Society Press.

25.   Lowe, K.S., F.G. Gardner, and R.L. Siegrist. (2002). Field evaluation of in situ chemical oxidation through vertical well-to-well recirculation of NaMnO4. *Ground Water Monitoring and Remediation*. **22**(1): 106-115.

26.   Lowe, K.S., *et al.* (1999). Field pilot test of in situ chemical oxidation through recirculation using vertical wells at the Portsmouth gaseous diffusion plant. In (Eds.), *Abiotic In Situ Technologies for Groundwater Remediation, 31 Aug - 2 Sept, 1999, Dallas, TX* (pp. 42-49). Dallas, TX: U.S. Environmental Protection Agency.

27.   Stewart, R. (1965). Oxidation by permanganate. In *Oxidation in Organic Chemistry* (pp. 1-68). K.B. Wiberg, Editor. New York: Academic Press.

28.   Wiberg, K.B. and K.A. Saegebarth. (1957). The mechanisms of permanganate oxidation. IV. Hydroxylation of olefins and related reactions. *Journal of the American Chemical Society*. **79**(11): 2822-2824.

29.   Lee, D.G. and N.S. Srinivasan. (1981). Oxidation of hydrocarbons. X. Concerning the formation of ketols and diones during the oxidation of alkenes by permanganate ion. *Canadian Journal of Chemistry*. **59**: 2146-2149.

30.   Mata-Perez, F. and J.F. Perez-Benito. (1985). Identification of the product from the reduction of permanganate ion by trimethylamine in aqueous phosphate buffers. *Canadian Journal of Chemistry*. **63**: 988-992.

31.   Stewart, J.J.P. (2004). Comparison of the accuracy of semiempirical and some DFT methods for predicting heats of formation. *Journal of Molecular Modeling*. **10**: 6-12.

32.   Klamt, A. and G. Schüürmann. (1993). COSMO: A new approach to dielectric screening in solvents with explicit expressions for the screening energy and its gradient. *Journal of the Chemical Society Perkin Transactions 2*. 799-803.

33.   Perez-Benito, J.F. and C. Arias. (1992). Occurrence of colloidal manganese dioxide in permanganate reactions. *Journal of Colloid and Interface Science*. **152**(1): 70-84.

34. Lee, D.G. and J.F. Perez-Benito. (1985). Oxidation of hydrocarbons. 14. Autocatalysis during the oxidation of 1-tetradecene by methyltributylammonium permanganate. *Canadian Journal of Chemistry*. **63**(6): 1275-1279.

35. Gardner, K.A. (1996). *Permanganate oxidations of aromatic hydrocarbons in aqueous and organic solution.* Doctoral dissertation. University of Washington.

36. Skoog, D.A., F.J. Holler, and T.A. Nieman. (1998). *Principles of Instrumental Analysis*. 5th ed. Philadelphia: Harcourt Brace College Publishers.

37. Morrey, J.R. (1963). Isosbestic points in absorbance spectra. *Journal of Physical Chemistry*. **57**: 1569.

38. Damm, J.H*., et al.* (2002). Kinetics of the oxidation of methyl tert-butyl ether (MTBE) by potassium permanganate. *Water Research*. **36**(14): 3638-3646.

39. Huang, K.C*., et al.* (2001). Oxidation of chlorinated ethenes by potassium permanganate: a kinetics study. *Journal of Hazardous Materials*. **87**: 155-169.

40. Hinshelwood, C.N. and C.A. Winkler. (1936). The oxidation of cyclic compounds by potassium permanganate. *Journal of the Chemical Society*. 368-370.

41. Matthess, G. (1982). *The Properties of Groundwater*. New York: Wiley.

42. Thurman, E.M. (1986). *Organic Geochemistry of Natural Waters*. Dordrecht: Nijhoff/Junk.

43. Nurmi, J.T. and P.G. Tratnyek. (2002). Electrochemical properties of natural organic matter (NOM), fractions of NOM, and model biogeochemical electron shuttles. *Environmental Science and Technology*. **36**(4): 617-624.

44. Gu, B*., et al.* (1995). Adsorption and desorption of different organic matter fractions on iron oxide. *Geochimica et Cosmochimica Acta*. **59**(2): 219-229.

45. Gu, B*., et al.* (1996). Competitive adsorption, displacement, and transport of organic matter on iron oxide: I. Competitive adsorption. *Geochimica et Cosmochimica Acta*. **60**(11): 1943-1950.

46. Gu, B*., et al.* (1994). Adsorption and desorption of natural organic matter on iron oxide: mechanisms and models. *Environmental Science and Technology*. **28**(1): 38-46.

47. Chen, J*., et al.* (2002). Spectroscopic characterization of structural and functional properties of natural organic matter fractions. *Chemosphere*. **48**: 59-68.

48. Chen, J*., et al.* (2003). The roles of natural organic matter in chemical and microbial reduction of ferric iron. *Science of the Total Environment*. **307**: 167-178.

49. Chen, J., B. Gu, and E.J. LeBoeuf. (2003). Fluorescence spectroscopic studies of natural organic matter fractions. *Chemosphere*. **50**: 639-647.

50. Mumford, K.G., N.R. Thompson, and R.M. Allen-King. (2002). Investigating the kinetic nature of natural oxidant demand during ISCO. In A. Gavaskar and A.S.C.

Chen (Eds.), *Third International Conference on Remediation of Chlorinated and Recalcitrant Compounds, 20-23 May, 2002, Monterey, CA* (2C-37). Monterey, CA: Battellle Press.

51.   Tratnyek, P.G. (1998). Correlation analysis of the environmental reactivity of organic substances. In *Perspectives in Environmental Chemistry* (pp. 167-194). D.L. Macalady, Editor. New York: Oxford.

52.   Canonica, S. and P.G. Tratnyek. (2003). Quantitative structure-activity relationships (QSARs) for oxidation reactions of organic chemicals in water. *Environmental Toxicology and Chemistry*. **22**(8): 1743-1754.

53.   Karelson, M. (2000). *Molecular descriptors in QSAR/QSPR*. New York: John Wiley & Sons, Inc.

54.   Miehr, R.*, et al.* (2004). The diversity of contaminant reduction reactions by zero-valent iron: role of the reductate. *Environmental Science and Technology*. **38**(1): 139-147.

55.   Watanabe, K., T. Nakayama, and J. Mottl. (1962). Ionization potentials of some molecules. *Journal of Quantitative Spectroscopy and Radiative Transfer*. **2**: 369-382.

56.   Kobayashi, T. and S. Nagakura. (1974). Photoelectron spectra of substituted benzenes. *Bulletin of the Chemical Society of Japan*. **47**(10): 2563-2572.

57.   Kobayashi, T. and S. Nagakura. (1975). Photoelectron spectra of nitrophenols and nitroanisoles. *Journal of Electron Spectroscopy and Related Phenomena*. **6**: 421-427.

58.   Hoigné, J. and H. Bader. (1983). Rate constants of reactions of ozone with organic and inorganic compounds in water—I. Non-dissociating organic compounds. *Water Research*. **17**(2): 173-183.

59.   Hoigné, J. and H. Bader. (1983). Rate constants of reactions of ozone with organic and inorganic compounds in water—II. Dissociating organic compounds. *Water Research*. **17**(2): 185-194.

60.   Hoigné, J.*, et al.* (1985). Rate constants of reactions of ozone with organic and inorganic compounds in water—III: Inorganic compounds and radicals. *Water Research*. **19**(8): 993-1004.

61.   Freeman, F. (1975). Possible criteria for distinguishing between cyclic and acyclic activated complexes and among cyclic activated complexes in addition reactions. *Chemical Reviews*. **75**(4): 439-490.

62.   Larson, R.A. and E.J. Weber. (1994). Chapter 4. Environmental Oxidations. In *Reaction Mechanisms in Environmental Organic Chemistry* (pp. 217-273. Chelsea, MI: Lewis.

63.   Tratnyek, P.G. and J. Hoigné. (1991). Oxidation of substituted phenols in the environment: a QSAR analysis of rate constants for reaction with singlet oxygen. *Environmental Science and Technology*. **25**(9): 1596-1604.

64.   Suatoni, J.C., R.E. Snyder, and R.O. Clark. (1961). Voltammetric studies of phenol and aniline ring substitution. *Analytical Chemistry*. **33**(13): 1894-1897.

65.   Exner, O. (1988). *Correlation Analysis of Chemical Data*. New York: Plenum.

66.   Tratnyek, P.G. and J. Hoigné. (1994). Photooxidation of 2,4,6-trimethylphenol in aqueous laboratory solutions and natural waters: kinetics of reaction with singlet oxygen. *Journal of Photochemistry and Photobiology. A: Chemistry*. **84**(2): 153-160.

67.   Pankow, J.F. (1991). *Aquatic Chemistry Concepts*. Chelsea, MI: Lewis.

68.   Baumbach, J.I., *et al.* (2003). Detection of the gasoline components methyl tert-butyl ether, benzene, toluene, and m-xylene using ion mobility spectrometers with a radioactive and UV ionization source. *Analytical Chemistry*. **75**(6): 1483-1490.

69.   Rudakov, E.S. and V.L. Lobachev. (2000). The first step of oxidation of alkylbenzenes by permanganates in acidic aqueous solutions. *Russian Chemical Bulletin*. **49**(5): 761-777.

70.   U.S. Environmental Protection Agency. (2004). *2004 Edition of the Drinking Water Standards and Health Advisories* (EPA 822-R-04-005). U.S. Environmental Protection Agency: Washington D. C.

71.   Pankow, J.F. and J.A. Cherry. (1996). *Dense Chlorinated Solvents and Other DNAPLs in Groundwater: History, Behavior, and Remediation*. Portland, OR: Waterloo Press.

72.   Barter, R.M. and J.S. Littler. (1967). Hydride ion transfer in oxidations of alcohols and ethers. *Journal of the Chemical Society (B)*. 205-210.

73.   Jaky, M., J. Szammer, and E. Simon-Trompler. (2000). Kinetics and mechanism of the oxidation of ketones with permanganate ions. *Journal of the Chemical Society-Perkin Transactions 2*. (7): 1597-1602.

74.   Jin, Z., L. Gui-bai, and M. Jun. (2003). Effects of chlorine content and position of chlorinated phenols on their oxidation kinetics by potassium permanganate. *Journal of Environmental Sciences*. **15**(3): 342-345.

75.   Gardner, K.A. and J.M. Mayer. (1995). Understanding C-H bond oxidations: H• and H⁻ transfer in the oxidation of toluene by permanganate. *Science*. **269**(5232): 1849-1851.

76.   Stewart, R. and M.M. Mocek. (1963). The mechanisms of permanganate oxidation. VII. The oxidation of fluoral hydrate. *Canadian Journal of Chemistry*. **41**: 1160-1169.

77.   Wiberg, K.B. and R.D. Geer. (1966). The kinetics of the permanganate oxidation of alkenes. *Journal of the American Chemical Society*. **88**: 5827-5832.

78.   Son, N.T., M. Jaky, and L.I. Simandi. (1976). Kinetics and mechanism of the permanganate oxidation of cis-2-butene-1,4-diol. *Inorganic Nuclear Chemistry Letters*. **12**: 291-296.

79.   Szammer, J., M. Jaky, and O.V. Gerasimov. (1992). Oxidation by permanganate in strong alkaline medium. Oxidation of ethane-1,2-diol, glycol aldehyde, glycollic acid, and glyoxylic acid. *International Journal of Chemical Kinetics*. **24**: 145-154.

80.   Wiberg, K.B. and R. Stewart. (1955). The mechanisms of permanganate oxidation. I. The oxidation of some aromatic aldehydes. *Journal of the American Chemical Society*. **77**: 1786-1795.

81.   Simandi, L.I. and M. Jaky. (1973). Mechanism of the permanganate oxidation of unsaturated compounds. Part IV. Kinetic investigation of the oxidation of maleic and fumaric acids. *Journal of the Chemical Society, Perkin Transactions 2*. **14**: 1856-60.

Appendix A: Experimental Conditions and Associated Rate Constants

COC	[COC] (mM)	[KMnO$_4$] (mM)	[COC]/ [KMnO$_4$]	[Phosphate Buffer] (mM)	$\mathcal{E}_{MnO_2}^{525\ a}$	k_{obs} (s^{-1})	k'' (M^{-1}s^{-1})[b]	R^2
Static Method								
Chloroform	30	0.1	300	100	0.19 ± 0.02	5.54E-06	1.32E-04	0.99
	40	0.1	400	100	0.16 ± 0.02	6.87E-06		
	50	0.1	500	100	0.15 ± 0.02	8.18E-06		
PCE	1	0.1	10	50	0.55 ± 0.01	4.58E-05	4.58E-02[c]	N/A
	1	0.1	10	50	0.55 ± 0.01	4.11E-05	4.11E-02[c]	N/A
TCE	1	0.1	10	50	0.355 ± 0.005	3.34E-02	0.76 ± 0.03	0.98
	1	0.1	10	50		3.30E-02		
	2	0.1	20	50	0.351 ± 0.002	9.10E-02		
	2	0.1	20	50		8.05E-02		
	3	0.1	30	50	0.350 ± 0.009	1.31E-01		
	3	0.1	30	50		1.29E-01		
	4	0.1	40	50	0.332 ± 0.005	1.77E-01		
	4	0.1	40	50		1.62E-01		
TCE	1	0.1	10	50	0.30 ± 0.02	4.68E-04	0.46 ± 0.05	0.96
	1	0.1	10	50		4.98E-04		
	2.5	0.1	25	50	0.34 ± 0.01	1.46E-03		
	2.5	0.1	25	50		1.33E-03		
	4	0.1	40	50	0.42 ± 0.01	1.93E-03		
	4	0.1	40	50		1.78E-03		

COC	[COC] (mM)	[KMnO$_4$] (mM)	[COC]/ [KMnO$_4$]	[Phosphate Buffer] (mM)	$\mathcal{E}_{MnO_2}^{525\ a}$	k_{obs} (s^{-1})	k'' (M^{-1}s^{-1})[b]	R^2
cis-DCE	3	0.3	10	50	0.376 ± 0.001	3.06E-03	0.71 ± 0.06	0.96
	3	0.3	10	50		3.16E-03		
	6	0.3	20	50	0.384 ± 0.002	4.54E-03		
	6	0.3	20	50		5.98E-03		
	9	0.3	30	50	0.388 ± 0.002	7.08E-03		
	9	0.3	30	50		8.10E-03		
	12	0.3	40	50	0.350 ± 0.003	9.32E-03		
	12	0.3	40	50		9.40E-03		
1,4-Dioxane	50	0.1	500	50	0.47 ± 0.01	4.37E-06	4.19E-05	0.992
	100	0.1	1000	50	0.34 ± 0.01	7.06E-06		
	200	0.1	2000	50	0.24 ± 0.01	1.14E-05		
	300	0.1	3000	50	0.11 ± 0.03	1.49E-05		
ETBE	40	0.1	400	50	-3.5 ± 0.5	2.02E-05	N/A[d]	N/A
	50	0.1	500	50	-1.7 ± 0.5	3.59E-05		
	5	0.1	50	50	-1.3 ± 0.1	3.47E-06		
	10	0.1	100	50	-2.7 ± 0.3	2.97E-06		
MEK	10	0.1	100	100	0.310 ± 0.004	1.21E-05	9.07E-04	0.993
	30	0.1	300	100	0.315 ± 0.007	3.38E-05		
	50	0.1	500	100	0.292 ± 0.004	3.98E-05		
MTBE	50	0.05	1000	50	0.28 ± 0.01	4.90E-06	9.8E-05[c]	N/A
	50	0.1	500	100	0.192 ± 0.006	5.48E-06	1.04E-04[c]	N/A
Toluene	4	0.1	40	50	0.17 ± 0.01	3.33E-06	8.32E-04[c]	N/A
2-Nitrophenol	2	0.05	5	50	-0.34 ± 0.05	1.22E-04	2.43E-01[c]	N/A
4-Nitrophenol	1	0.1	10	50	-0.37 ± 0.06	3.89E-05	3.70E-02	0.993
	2	0.1	20	50	-0.06 ± 0.03	7.75E-05		
	3	0.1	30	50	-0.02 ± 0.03	1.13E-04		
2,4-Dinitrophenol	1	0.1	10	50	-0.10 ± 0.04	6.43E-02	6.43E-02[c]	N/A
	0.5	0.1	5	50	-0.44 ± 0.06	2.80E-05	5.60E-02[c]	N/A
Picric acid	5	0.1	50	50	0.37 ± 0.01	2.81E-06	5.63E-04[c]	N/A

COC	[COC] (mM)	[KMnO$_4$] (mM)	[COC]/ [KMnO$_4$]	[Phosphate Buffer] (mM)	$\mathcal{E}_{MnO_2}^{525\ a}$	k_{obs} (s^{-1})	k'' (M^{-1}s^{-1})[b]	R^2
Stopped-flow								
TCE	1	0.1	10	50	0.45 ± 0.01	3.80E-02	0.67 ± 0.05	0.96
	1	0.1	10	50		3.70E-02		
	2	0.1	20	50	0.26 ± 0.01	5.85E-02		
	2	0.1	20	50		5.73E-02		
	3	0.1	30	50	0.35 ± 0.01	1.07E-01		
	3	0.1	30	50		1.01E-01		
	4	0.1	40	50	0.47 ± 0.02	1.52E-01		
	4	0.1	40	50		1.61E-01		
cis-DCE	3	~0.3	10	50	0.380 ± 0.001	3.60E-03	0.69 ± 0.1	0.85
	3	~0.3	10	50		3.82E-03		
	6	~0.3	20	50	0.340 ± 0.001	8.28E-03		
	6	~0.3	20	50		7.50E-03		
	9	~0.3	30	50	0.443 ± 0.002	9.43E-03		
	9	~0.3	30	50		8.90E-03		
	12	~0.3	40	50	0.431 ± 0.003	1.10E-02		
	12	~0.3	40	50		9.35E-03		
trans-DCE	2	~0.1	20	50	0.470 ± 0.001	6.15E-02	39 ± 3	0.95
	2	~0.1	20	50		5.99E-02		
	2	~0.1	20	50		5.21E-02		
	2	~0.1	20	50		5.02E-02		
	3	~0.1	30	50	0.650 ± 0.001	1.05E-01		
	3	~0.1	30	50		1.15E-01		
	3	~0.1	30	50		1.01E-01		
	4	~0.1	40	50	0.443 ± 0.001	1.36E-01		
	4	~0.1	40	50		1.30E-01		
	4	~0.1	40	50		1.35E-01		

COC	[COC] (mM)	[KMnO$_4$] (mM)	[COC]/ [KMnO$_4$]	[Phosphate Buffer] (mM)	$\mathcal{E}_{MnO_2}^{525\ a}$	k_{obs} (s^{-1})	k'' (M^{-1}s^{-1})[b]	R^2
2,3-Dichloropropene	1	~0.1	10	50		9.53E-02	77 ± 5	0.94
	1	~0.1	10	50	0.490 ±0.001	8.87E-02		
	1	~0.1	10	50		9.21E-02		
	1	~0.1	10	50		9.69E-02		
	1.5	~0.1	15	50		1.09E-02		
	1.5	~0.1	15	50	0.404 ± 0.001	1.09E-02		
	1.5	~0.1	15	50		1.12E-02		
	1.5	~0.1	15	50		1.14E-02		
	2	~0.1	20	50		1.69E-02		
	2	~0.1	20	50	0.797 ± 0.001	1.69E-02		
	2	~0.1	20	50		1.70E-02		
	2.5	~0.1	25	50		1.91E-02		
	2.5	~0.1	25	50	0.507 ± 0.002	1.80E-02		
	2.5	~0.1	25	50		1.79E-02		
	3	~0.1	30	50		2.18E-02		
	3	~0.1	30	50	0.543 ± 0.003	2.13E-02		
	3	~0.1	30	50		1.86E-02		
2-Chlorophenol	0.75	~0.1	~7.5	50	0.560 ± 0.002	6.08E-02	74 ± 7	0.97
	0.75	~0.1	~7.5	50		6.00E-02		
	1	~0.1	~10	50	0.727 ± 0.002	7.21E-02		
	1	~0.1	~10	50		7.98E-02		
	1.25	~0.1	~12.5	50	0.881 ± 0.004	9.69E-02		
	1.25	~0.1	~12.5	50		9.81E-02		

COC	[COC] (mM)	[KMnO$_4$] (mM)	[COC]/ [KMnO$_4$]	[Phosphate Buffer] (mM)	$\mathcal{E}_{MnO_2}^{525\ a}$	k_{obs} (s^{-1})	k'' (M^{-1}s^{-1})[b]	R^2
3-Chlorophenol	1	~0.1	~10	50		1.67E-02		
	1	~0.1	~10	50	0.532 ± 0.001	1.75E-02		
	1	~0.1	~10	50		1.81E-02		
	2	~0.1	~20	50		2.22E-02		
	2	~0.1	~20	50	0.319 ± 0.005	2.52E-02		
	2	~0.1	~20	50		2.47E-02		
	3	~0.1	~30	50		4.61E-02		
	3	~0.1	~30	50	0.643 ± 0.001	4.45E-02	13.4 ± 0.7	0.96
	3	~0.1	~30	50		4.60E-02		
	4	~0.1	~40	50		4.96E-02		
	4	~0.1	~40	50	0.411 ± 0.003	4.99E-02		
	4	~0.1	~40	50		4.78E-02		
	4	~0.1	~40	50		4.67E-02		
	6	~0.1	~60	50		8.58E-02		
	6	~0.1	~60	50	0.584 ± 0.001	8.58E-02		
	6	~0.1	~60	50		8.20E-02		
2,4 Dichlorophenol	1	~0.1	10	50		8.57E-02		
	1	~0.1	10	50	-0.050 ± 0.007	8.44E-02		
	1	~0.1	10	50		8.28E-02		
	2	~0.1	20	50		2.16E-01		
	2	~0.1	20	50	0.398 ±0.008	2.11E-01	142 ± 3	0.995
	2	~0.1	20	50		2.12E-01		
	3	~0.1	30	50		3.61E-01		
	3	~0.1	30	50	0.452 ± 0.003	3.70E-01		
	3	~0.1	30	50		3.76E-01		

COC	[COC] (mM)	[KMnO$_4$] (mM)	[COC]/ [KMnO$_4$]	[Phosphate Buffer] (mM)	$\mathcal{E}^{525\ a}_{MnO_2}$	k_{obs} (s^{-1})	k'' (M^{-1}s^{-1})[b]	R^2
2,4,6 Trichlorophenol	0.5	~0.1	5	50		3.32E-02		
	0.5	~0.1	5	50	-0.104 $\pm$ 0.003	3.37E-02		
	0.5	~0.1	5	50		3.39E-02		
	1	~0.1	10	50		7.27E-02		
	1	~0.1	10	50	0.207 $\pm$ 0.003	7.39E-02	120 $\pm$ 9	0.96
	1	~0.1	10	50		7.60E-02		
	1.5	~0.1	15	50		1.53E-01		
	1.5	~0.1	15	50	0.232 $\pm$ 0.003	1.57E-01		
	1.5	~0.1	15	50		1.51E-01		
m-Cresol	1	~0.1	10	50		7.99E-02		
	1	~0.1	10	50	0.198 $\pm$ 0.002	8.63E-02		
	1	~0.1	10	50		8.27E-02		
	1	~0.1	10	50		8.45E-02		
	2	~0.1	20	50		2.06E-01		
	2	~0.1	20	50	0.383 $\pm$ 0.006	2.03E-01	98 $\pm$ 4	0.98
	2	~0.1	20	50		1.95E-01		
	3	~0.1	30	50		2.73E-01		
	3	~0.1	30	50	0.300 $\pm$ 0.008	2.74E-01		
	3	~0.1	30	50		2.88E-01		
p-Cresol	1	~0.1	10	50		1.24E-01		
	1	~0.1	10	50	0.250 $\pm$ 0.009	1.23E-01		
	1	~0.1	10	50		1.18E-01		
	1.5	~0.1	15	50		2.39E-01		
	1.5	~0.1	15	50	0.075 $\pm$ 0.009	2.42E-01	237 $\pm$ 3	0.99
	1.5	~0.1	15	50		2.31E-01		
	2	~0.1	20	50		3.56E-01		
	2	~0.1	20	50	0.101 $\pm$ 0.007	3.61E-01		
	2	~0.1	20	50		3.58E-01		

COC	[COC] (mM)	[KMnO$_4$] (mM)	[COC]/ [KMnO$_4$]	[Phosphate Buffer] (mM)	$\mathcal{E}^{525\ a}_{MnO_2}$	k_{obs} (s^{-1})	k'' (M^{-1}s^{-1})[b]	R^2
Dichlorvos	1	~0.1	10	50		1.71E-02	15.7 $\pm$ 0.4	0.99
	1	~0.1	10	50	0.5895 $\pm$ 0.0001	1.70E-02		
	1	~0.1	10	50		1.68E-02		
	2	~0.1	20	50		3.09E-02		
	2	~0.1	20	50	0.4483 $\pm$ 0.0002	3.04E-02		
	2	~0.1	20	50		3.01E-02		
	3	~0.1	30	50		5.01E-02		
	3	~0.1	30	50	0.4894 $\pm$ 0.0001	4.75E-02		
	3	~0.1	30	50		4.93E-02		
	4	~0.1	40	50		6.44E-02		
	4	~0.1	40	50	0.3062 $\pm$ 0.0001	6.25E-02		
	4	~0.1	40	50		6.28E-02		
Aldicarb	1	~0.1	10	50		3.51E-03	2.4 $\pm$ 0.2	0.93
	1	~0.1	10	50	0.444 $\pm$ 0.001	2.54E-03		
	1	~0.1	10	50		2.80E-03		
	2	~0.1	20	50		5.93E-03		
	2	~0.1	20	50	0.552 $\pm$ 0.001	5.58E-03		
	2	~0.1	20	50		5.01E-03		
	2	~0.1	20	50		5.01E-03		
	3	~0.1	30	50		6.74E-03		
	3	~0.1	30	50	0.535 $\pm$ 0.002	7.85E-03		
	3	~0.1	30	50		8.56E-03		

a) Value obtained from a global fit of the individual experiments at the same conditions.
b) k'' obtained from the slope of a k_{obs} vs. [COC] plot unless otherwise noted.
c) The second-order-rate constants were calculated from the equation: $k'' = k_{obs} /$ [COC].
d) No k'' was obtained for this compound. See section 4.5, "Variability in the effective absorptivity of MnO$_2$."

Appendix B: Experimental and Literature Values Used in Figure 20

COC	k" (M^{-1}s^{-1})	pH	Temp °C	Reference
Chlorinated Alkanes				
Carbon Tetrachloride	< 1E-04	7	25	This Study
Chloroform	5.63E-04	7	25	This Study
Dichloromethane	< 1E-04	7	25	This Study
1,1,1-TCA	< 1E-04	7	25	This Study
1,2-DCA	< 1E-04	7	25	This Study
Chlorinated Ethylenes				
PCE	4.08E-02	5.2	21	[7]
PCE	3.60E-02	7	20	[39]
PCE	3.50E-02	7	20	[39]
PCE	5.10E-02	7	25	[39]
PCE	3.30E-02	7	20	[39]
PCE	3.20E-02	7	20	[39]
PCE	3.70E-02	7	20	[39]
PCE	3.03E-02		23	[9]
PCE	4.56E-02		23	[9]
PCE	8.40E-03	8		[2]
PCE	4.50E-02	7.1		[3]
PCE	4.58E-02	7	25	This Study
PCE	4.11E-02	7	25	This Study
TCE	8.80E-01	7	20	[6]
TCE	8.90E-01	7	20	[6]
TCE	9.50E-01	7	20	[39]
TCE	9.30E-01	7	20	[39]
TCE	1.19E+00	7	25	[39]

COC	k" (M^{-1}s^{-1})	pH	Temp °C	Reference
TCE	8.40E-01	7	20	[39]
TCE	7.40E-01	7	20	[39]
TCE	7.80E-01	7	20	[39]
TCE	8.90E-01	7	20	[39]
TCE	7.67E-01			[10]
TCE	6.45E-01		23	[9]
TCE	6.63E-01		23	[9]
TCE	4.42E-01		23	[9]
TCE	4.61E-01		23	[9]
TCE	8.90E-01	6.9	20	[21]
TCE	6.83E-01	6.3		[1]
TCE	6.07E-01	8		[1]
TCE	6.86E-01	6.3		[1]
TCE	6.10E-01	8		[1]
TCE	6.60E-01	7.1		[3]
TCE	6.60E-01	7.1		[4]
TCE	6.70E-01			[4]
TCE	6.80E-01			[4]
TCE	6.10E-01			[4]
TCE	4.40E-01			[4]
TCE	6.80E-01	4		[5]
TCE	6.50E-01	6		[5]
TCE	6.50E-01	8		[5]
TCE	7.60E-01	7	25	This Study
TCE	6.70E-01	7	25	This Study
cis-DCE	1.47E+00	7	20	[39]

COC	k" (M^{-1}s^{-1})	pH	Temp °C	Reference
cis-DCE	1.42E+00	7	20	[39]
cis-DCE	1.78E+00	7	25	[39]
cis-DCE	1.53E+00	7	20	[39]
cis-DCE	1.54E+00	7	20	[39]
cis-DCE	1.53E+00	7	20	[39]
cis-DCE	1.14E+00		23	[9]
cis-DCE	9.20E-01	7.1		[3]
cis-DCE	9.20E-01	7.1		[4]
cis-DCE	6.90E-01	7	25	This Study
cis-DCE	7.10E-01	7	25	This Study
trans-DCE	4.80E+01	7	20	[39]
trans-DCE	4.74E+01	7	20	[39]
trans-DCE	5.68E+01	7	25	[39]
trans-DCE	4.91E+01	7	20	[39]
trans-DCE	4.82E+01	7	20	[39]
trans-DCE	4.90E+01	7	20	[39]
trans-DCE	3.00E+01	7.1		[3]
trans-DCE	3.00E+01	7.1		[4]
trans-DCE	3.90E+01	7	25	[4]
1,1-DCE	2.08E+00	7	20	This Study
1,1-DCE	2.47E+00	7	25	[39]
1,1-DCE	2.08E+00	7	20	[39]
1,1-DCE	2.15E+00	7	20	[39]
1,1-DCE	2.07E+00	7	20	[39]
1,1-DCE	2.16E+00	7	20	[39]
1,1-DCE	2.38E+00	7.1		[39]

COC	k" $(M^{-1}s^{-1})$	pH	Temp °C	Reference
1,1-DCE	2.38E+00	7.1		[4]
2,3-Dichloropropene	7.70E+01	7	25	This Study
Oxygenates				
Ethanol	1.67E-03	4.6	20	[72]
Ethanol	4.03E-03	4.6	30	[72]
MTBE	6.26E-05	7.6	23	[38]
MTBE	9.80E-05	7	25	This Study
MTBE	1.04E-04	7	25	This Study
Diisopropyl Ether	9.00E-04	4.6	20	[72]
Diisopropyl Ether	1.79E-03	4.6	30	[72]
1,4-Dioxane	3.09E-05	4.6	20	[72]
1,4-Dioxane	7.85E-05	4.6	30	[72]
1,4-Dioxane	8.73E-05	7	25	This Study
Methyl Ethyl Ketone	2.60E-03	4.8	25	[73]
Methyl Ethyl Ketone	9.07E-04	7	25	This Study
Substituted Phenols				
Phenol	3.54E+01	7.2	1.60E+01	[74]
2-Chlorophenol	7.40E+01	7.0	2.50E+01	This Study
3-Chlorophenol	1.34E+01	7.0	2.50E+01	This Study
4-Chlorophenol	5.92E+01	7.2	16	[74]
2,4-Dichlorophenol	4.38E+01	7.2	16	[74]
2,4-Dichlorophenol	1.42E+02	7.0	25	This Study
2,6-Dichlorophenol	3.19E+01	7.2	16	[74]
2,4,6-Trichlorophenol	1.20E+02	7.0	25	This Study
m-Cresol	9.80E+01	7.0	25	This Study
p-Cresol	2.37E+02	7.0	25	This Study

COC	k" $(M^{-1}s^{-1})$	pH	Temp °C	Reference
2-Nitrophenol	2.43E-01	7.0	25	This Study
4-Nitrophenol	3.70E-02	7.0	25	This Study
2,4-Dinitrophenol	6.43E-02	7.0	25	This Study
2,4-Dinitrophenol	5.42E-02	7.0	25	This Study
Picric Acid	5.63E-04	7.0	25	This Study
BTEX				
Benzene	7.00E-06	5.0 - 7.0	70	[69]
Ethylbenzene	1.13E-02	5.0 - 7.0	30	[69]
Ethylbenzene	3.90E-03	7.0	25	[35]
Toluene	2.30E-04	5.0 - 7.0	20	[69]
Toluene	6.10E-04	5.0 - 7.0	30	[69]
Toluene	7.00E-04	7.0	20	[75]
Toluene	8.32E-04	7.0	25	This Study
o-Xylene	8.90E-04	5.0 - 7.0	20	[69]
o-Xylene	2.05E-03	5.0 - 7.0	30	[69]
m-Xylene	6.00E-04	5.0 - 7.0	20	[69]
m-Xylene	1.49E-03	5.0 - 7.0	30	[69]
p-Xylene	1.15E-03	5.0 - 7.0	20	[69]
p-Xylene	2.94E-03	5.0 - 7.0	30	[69]
Pesticides				
Aldicarb	2.4E+00	7.0	25	This Study
Dichlorvos	1.57E+01	7.0	25	This Study

Appendix C: Values Used in QSARs

COC	E_{HOMO} (eV) PM5/H$_2$O	E_{LUMO} (eV) PM5/H$_2$O	E_{Gap} (eV) PM5/H$_2$O	pH	Temp °C	k" KMnO$_4$ (M^{-1}s^{-1})	KMnO$_4$ Ref	k" Ozone (M^{-1}s^{-1})	Ozone Ref	IP[a] (eV)
Chlorinated Ethylenes										
PCE	-9.68	-1.244	-8.436	5.2	21	4.08E-02	[7]	1.00E-01	[58]	9.32
PCE	-9.68	-1.244	-8.436	7.0	20	3.60E-02	[39]	1.00E-01	[58]	9.32
PCE	-9.68	-1.244	-8.436	7.0	20	3.50E-02	[39]	1.00E-01	[58]	9.32
PCE	-9.68	-1.244	-8.436	7.0	25	5.10E-02	[39]	1.00E-01	[58]	9.32
PCE	-9.68	-1.244	-8.436	7.0	20	3.30E-02	[39]	1.00E-01	[58]	9.32
PCE	-9.68	-1.244	-8.436	7.0	20	3.20E-02	[39]	1.00E-01	[58]	9.32
PCE	-9.68	-1.244	-8.436	7.0	20	3.70E-02	[39]	1.00E-01	[58]	9.32
PCE	-9.68	-1.244	-8.436		23	3.03E-02	[9]	1.00E-01	[58]	9.32
PCE	-9.68	-1.244	-8.436		23	4.56E-02	[9]	1.00E-01	[58]	9.32
PCE	-9.68	-1.244	-8.436	8.0		8.40E-03	[2]	1.00E-01	[58]	9.32
PCE	-9.68	-1.244	-8.436	7.1		4.50E-02	[4]	1.00E-01	[58]	9.32
PCE	-9.68	-1.244	-8.436	7.0	25	4.58E-02	This Study	1.00E-01	[58]	9.32
PCE	-9.68	-1.244	-8.436	7.0	25	4.11E-02	This Study	1.00E-01	[58]	9.32
TCE	-9.828	-0.803	-9.025	7.0	20	8.80E-01	[6]	1.70E+01	[58]	9.45
TCE	-9.828	-0.803	-9.025	7.0	20	8.90E-01	[6]	1.70E+01	[58]	9.45
TCE	-9.828	-0.803	-9.025	7.0	20	9.50E-01	[39]	1.70E+01	[58]	9.45
TCE	-9.828	-0.803	-9.025	7.0	20	9.30E-01	[39]	1.70E+01	[58]	9.45
TCE	-9.828	-0.803	-9.025	7.0	25	1.19E+00	[39]	1.70E+01	[58]	9.45
TCE	-9.828	-0.803	-9.025	7.0	20	8.40E-01	[39]	1.70E+01	[58]	9.45
TCE	-9.828	-0.803	-9.025	7.0	20	7.40E-01	[39]	1.70E+01	[58]	9.45
TCE	-9.828	-0.803	-9.025	7.0	20	7.80E-01	[39]	1.70E+01	[58]	9.45
TCE	-9.828	-0.803	-9.025	7.0	20	8.90E-01	[39]	1.70E+01	[58]	9.45
TCE	-9.828	-0.803	-9.025			7.67E-01	[10]	1.70E+01	[58]	9.45

COC	E_{HOMO} (eV) PM5/H_2O	E_{LUMO} (eV) PM5/H_2O	E_{Gap} (eV) PM5/H_2O	pH	Temp °C	k" $KMnO_4$ ($M^{-1}s^{-1}$)	$KMnO_4$ Ref	k" Ozone ($M^{-1}s^{-1}$)	Ozone Ref	IP^a (eV)
TCE	-9.828	-0.803	-9.025		23	6.45E-01	[9]	1.70E+01	[58]	9.45
TCE	-9.828	-0.803	-9.025		23	6.63E-01	[9]	1.70E+01	[58]	9.45
TCE	-9.828	-0.803	-9.025		23	4.42E-01	[9]	1.70E+01	[58]	9.45
TCE	-9.828	-0.803	-9.025		23	4.61E-01	[9]	1.70E+01	[58]	9.45
TCE	-9.828	-0.803	-9.025	6.9	20	8.90E-01	[21]	1.70E+01	[58]	9.45
TCE	-9.828	-0.803	-9.025	6.3		6.83E-01	[1]	1.70E+01	[58]	9.45
TCE	-9.828	-0.803	-9.025	8.0		6.07E-01	[1]	1.70E+01	[58]	9.45
TCE	-9.828	-0.803	-9.025	6.3		6.86E-01	[1]	1.70E+01	[58]	9.45
TCE	-9.828	-0.803	-9.025	8.0		6.10E-01	[1]	1.70E+01	[58]	9.45
TCE	-9.828	-0.803	-9.025	7.1		6.60E-01	[3]	1.70E+01	[58]	9.45
TCE	-9.828	-0.803	-9.025	7.1		6.60E-01	[4]	1.70E+01	[58]	9.45
TCE	-9.828	-0.803	-9.025	4.0 - 8.0		6.70E-01	[4]	1.70E+01	[58]	9.45
TCE	-9.828	-0.803	-9.025			6.80E-01	[4]	1.70E+01	[58]	9.45
TCE	-9.828	-0.803	-9.025			6.10E-01	[4]	1.70E+01	[58]	9.45
TCE	-9.828	-0.803	-9.025			4.40E-01	[4]	1.70E+01	[58]	9.45
TCE	-9.828	-0.803	-9.025	4.0		6.80E-01	[5]	1.70E+01	[58]	9.45
TCE	-9.828	-0.803	-9.025	6.0		6.50E-01	[5]	1.70E+01	[58]	9.45
TCE	-9.828	-0.803	-9.025	8.0		6.50E-01	[5]	1.70E+01	[58]	9.45
TCE	-9.828	-0.803	-9.025	7.0	25	7.60E-01	This Study	1.70E+01	[58]	9.45
TCE	-9.828	-0.803	-9.025	7.0	25	6.70E-01	This Study	1.70E+01	[58]	9.45
Cis-DCE	-9.975	0.067	-10.042	7.0	20	1.47E+00	[39]	8.00E+02	[58]	9.65
Cis-DCE	-9.975	0.067	-10.042	7.0	20	1.42E+00	[39]	8.00E+02	[58]	9.65
Cis-DCE	-9.975	0.067	-10.042	7.0	25	1.78E+00	[39]	8.00E+02	[58]	9.65
Cis-DCE	-9.975	0.067	-10.042	7.0	20	1.53E+00	[39]	8.00E+02	[58]	9.65
Cis-DCE	-9.975	0.067	-10.042	7.0	20	1.54E+00	[39]	8.00E+02	[58]	9.65

COC	E_{HOMO} (eV) PM5/H_2O	E_{LUMO} (eV) PM5/H_2O	E_{Gap} (eV) PM5/H_2O	pH	Temp °C	k" $KMnO_4$ ($M^{-1}s^{-1}$)	$KMnO_4$ Ref	k" Ozone ($M^{-1}s^{-1}$)	Ozone Ref	IP^a (eV)
Cis-DCE	-9.975	0.067	-10.042	7.0	20	1.53E+00	[39]	8.00E+02	[58]	9.65
Cis-DCE	-9.975	0.067	-10.042		23	1.14E+00	[9]	8.00E+02	[58]	9.65
Cis-DCE	-9.975	0.067	-10.042	7.1		9.20E-01	[3]	8.00E+02	[58]	9.65
Cis-DCE	-9.975	0.067	-10.042	7.1		9.20E-01	[4]	8.00E+02	[58]	9.65
Cis-DCE	-9.975	0.067	-10.042	7.0	25	6.90E-01	This Study	8.00E+02	[58]	9.65
Cis-DCE	-9.975	0.067	-10.042	7.0	25	7.10E-01	This Study	8.00E+02	[58]	9.65
Trans-DCE	-9.967	-0.418	-9.549	7.0	20	4.80E+01	[39]	5.70E+03	[58]	9.66
Trans-DCE	-9.967	-0.418	-9.549	7.0	20	4.74E+01	[39]	5.70E+03	[58]	9.66
Trans-DCE	-9.967	-0.418	-9.549	7.0	25	5.68E+01	[39]	5.70E+03	[58]	9.66
Trans-DCE	-9.967	-0.418	-9.549	7.0	20	4.91E+01	[39]	5.70E+03	[58]	9.66
Trans-DCE	-9.967	-0.418	-9.549	7.0	20	4.82E+01	[39]	5.70E+03	[58]	9.66
Trans-DCE	-9.967	-0.418	-9.549	7.0	20	4.90E+01	[39]	5.70E+03	[58]	9.66
Trans-DCE	-9.967	-0.418	-9.549	7.1		3.00E+01	[3]	5.70E+03	[58]	9.66
Trans-DCE	-9.967	-0.418	-9.549	7.1		3.00E+01	[4]	5.70E+03	[58]	9.66
Trans-DCE	-9.967	-0.418	-9.549	7.0	25	3.90E+01	This Study	5.70E+03	[58]	9.66
1,1-DCE	-10.113	-0.474	-9.639	7.0	20	2.08E+00	[39]	1.10E+02	[58]	
1,1-DCE	-10.113	-0.474	-9.639	7.0	25	2.47E+00	[39]	1.10E+02	[58]	
1,1-DCE	-10.113	-0.474	-9.639	7.0	20	2.08E+00	[39]	1.10E+02	[58]	
1,1-DCE	-10.113	-0.474	-9.639	7.0	20	2.15E+00	[39]	1.10E+02	[58]	
1,1-DCE	-10.113	-0.474	-9.639	7.0	20	2.07E+00	[39]	1.10E+02	[58]	
1,1-DCE	-10.113	-0.474	-9.639	7.0	20	2.16E+00	[39]	1.10E+02	[58]	
1,1-DCE	-10.113	-0.474	-9.639	7.1		2.38E+00	[3]	1.10E+02	[58]	
1,1-DCE	-10.113	-0.474	-9.639	7.1		2.38E+00	[4]	1.10E+02	[58]	
2,3-Dichloropropene	-10.197	-0.316	-9.881	7.0	25	7.70E+01	This Study			9.82

COC	E_{HOMO} (eV) PM5/H_2O	E_{LUMO} (eV) PM5/H_2O	E_{Gap} (eV) PM5/H_2O	pH	Temp °C	k" KMnO$_4$ ($M^{-1}s^{-1}$)	KMnO$_4$ Ref	k" Ozone ($M^{-1}s^{-1}$)	Ozone Ref	IP[a] (eV)
Oxygenates and Related Compounds										
1,1-Ethane Diol, 2,2,2-Trifluoro	-11.775	-0.825	-10.95	7.6	25	3.40E-03	[76]			
1,4-Dioxane	-10.15	0.693	-10.843	4.6	20	3.09E-05	[69]	4.50E-01	[58]	9.13
1,4-Dioxane	-10.15	0.693	-10.843	4.6	30	7.85E-05	[69]	4.50E-01	[58]	9.13
1,4-Dioxane	-10.15	0.693	-10.843	7.0	25	4.19E-05	This Study	4.50E-01	[58]	9.13
2-Methoxyethanol	-10.39	0.588	-10.978	4.6	20	5.73E-04	[69]			
2-Methoxyethanol	-10.39	0.588	-10.978	4.6	30	1.52E-03	[69]			
Acetone	-10.919	-0.223	-10.696	4.8	25	1.30E-03	[70]	3.20E-02	[58]	9.69
Allyl Alcohol	-9.974	1.138	-11.112	6.5	25	1.40E+02	[77]			9.67
Butane-2,3-Dione	-10.578	-1.536	-9.042	4.8	25	2.70E-03	[70]			9.23
Cis-2-Butene-1,4-Diol	-9.84	0.852	-10.692	4.2	25	2.10E+02	[78]			
Cis-2-Butene-1,4-Diol	-9.84	0.852	-10.692	4.6	25	2.30E+02	[78]			
Cis-2-Butene-1,4-Diol	-9.84	0.852	-10.692	4.2	25	2.10E+02	[78]			
Cis-2-Butene-1,4-Diol	-9.84	0.852	-10.692	4.6	25	2.30E+02	[78]			
Cyclohexanol	-10.402	1.632	-12.034	4.6	20	1.88E-03	[69]			
Cyclohexanol	-10.402	1.632	-12.034	4.6	30	4.35E-03	[69]			
Diisopropyl Ether	-10.253	1.07	-11.323	4.6	20	9.00E-04	[69]			
Diisopropyl Ether	-10.253	1.07	-11.323	4.6	30	1.79E-03	[69]			
Ethanol	-10.488	1.689	-12.177	4.6	20	1.67E-03	[69]	3.70E-01	[58]	10.5
Ethanol	-10.488	1.689	-12.177	4.6	30	4.03E-03	[69]	3.70E-01	[58]	10.5
Glycol Aldehyde	-10.846	-0.475	-10.371	4.6	25	1.30E-01	[79]			
Hydroxyacetone	-10.945	-0.436	-10.509	4.8	25	3.10E-02	[70]			
Methyl Ethyl Ketone	-10.726	-0.185	-10.541	4.8	25	2.60E-03	[70]	7.00E-02	[58]	9.53
Methyl Ethyl Ketone	-10.726	-0.185	-10.541	7.0	25	9.07E-04	This Study	7.00E-02	[58]	9.53
Methanol	-10.708	1.753	-12.461	4.6	20	4.46E-05	[69]	2.40E-02	[58]	10.9

COC	E_{HOMO} (eV) PM5/H_2O	E_{LUMO} (eV) PM5/H_2O	E_{Gap} (eV) PM5/H_2O	pH	Temp °C	k" $KMnO_4$ ($M^{-1}s^{-1}$)	$KMnO_4$ Ref	k" Ozone ($M^{-1}s^{-1}$)	Ozone Ref	IP^a (eV)
Methanol	-10.708	1.753	-12.461	4.6	30	1.18E-04	[69]	2.40E-02	[58]	10.9
MTBE	-10.321	1.151	-11.472	7.6	23	6.26E-05	[38]			9.24[d]
MTBE	-10.321	1.151	-11.472	7.6	23	7.37E-05	[38]			9.24[d]
MTBE	-10.321	1.151	-11.472	7.6	23	5.89E-05	[38]			9.24[d]
MTBE	-10.321	1.151	-11.472	7.6	23	5.59E-05	[38]			9.24[d]
MTBE	-10.321	1.151	-11.472	7.6	23	6.93E-05	[38]			9.24[d]
MTBE	-10.321	1.151	-11.472	7.6	23	6.58E-05	[38]			9.24[d]
MTBE	-10.321	1.151	-11.472	7.6	23	5.77E-05	[38]			9.24[d]
MTBE	-10.321	1.151	-11.472	7.0	25	9.80E-05	This Study			9.24[d]
MTBE	-10.321	1.151	-11.472	7.0	25	1.04E-04	This Study			9.24[d]
Substituted Phenols										
2-Chlorophenol	-9.238	0.028	-9.266	7.0	25	7.40E+01	This Study	9.50E+06	[59]	
3-Chlorophenol	-9.317	-0.013	-9.304	7.0	25	1.34E+01	This Study			
2,4-Dichlorophenol	-9.214	-0.232	-8.982	7.0	25	1.42E+02	This Study	1.60E+09	[59]	
2,4,6-Trichlorophenol	-9.337	-0.651	-8.686	7.0	25	1.20E+02	This Study	8.90E+07	[59]	
m-Cresol	-9.12	0.269	-9.389	7.0	25	9.80E+01	This Study	1.20E+04	[59]	8.52[b]
p-Cresol	-8.925	0.262	-9.187	7.0	25	2.37E+02	This Study	8.10E+03	[59]	8.38[b]
2-Nitrophenol	-9.75	-2.012	-7.738	7.0	25	2.43E-01	This Study			9.29[c]
4-Nitrophenol	-9.771	-2.008	-7.763	7.0	25	3.70E-02	This Study	6.20E+06	[59]	9.38[c]
2,4-Dinitrophenol	-10.305	-2.205	-8.1	7.0	25	6.43E-02	This Study			
2,4-Dinitrophenol	-10.305	-2.205	-8.1	7.0	25	5.42E-02	This Study			
2,4,6-Trinitrophenol (Picric Acid)	-10.8	-2.479	-8.321	7.0	25	5.63E-04	This Study			
BTEX										
Benzaldehyde	-9.944	-0.989	-8.955	6.5	25	3.02E-01	[80]	2.50E+00	[58]	9.53
Benzaldehyde	-9.944	-0.989	-8.955	6.5	25	3.24E-01	[80]	2.50E+00	[58]	9.53

COC	E_{HOMO} (eV) PM5/H_2O	E_{LUMO} (eV) PM5/H_2O	E_{Gap} (eV) PM5/H_2O	pH	Temp °C	k" KMnO$_4$ (M^{-1}s^{-1})	KMnO$_4$ Ref	k" Ozone (M^{-1}s^{-1})	Ozone Ref	IP[a] (eV)
Benzaldehyde	-9.944	-0.989	-8.955	6.5	25	3.22E-01	[80]	2.50E+00	[58]	9.53
Benzaldehyde	-9.944	-0.989	-8.955	6.5	25	3.30E-01	[80]	2.50E+00	[58]	9.53
Benzaldehyde	-9.944	-0.989	-8.955	6.5	25	3.57E-01	[80]	2.50E+00	[58]	9.53
Benzaldehyde	-9.944	-0.989	-8.955	6.5	25	3.84E-01	[80]	2.50E+00	[58]	9.53
Benzaldehyde	-9.944	-0.989	-8.955	5.2	25	4.75E-01	[80]	2.50E+00	[58]	9.53
Benzaldehyde	-9.944	-0.989	-8.955	5.9	25	3.94E-01	[80]	2.50E+00	[58]	9.53
Benzaldehyde	-9.944	-0.989	-8.955	6.8	25	3.70E-01	[80]	2.50E+00	[58]	9.53
Benzaldehyde	-9.944	-0.989	-8.955	7.7	25	3.70E-01	[80]	2.50E+00	[58]	9.53
Benzaldehyde	-9.944	-0.989	-8.955	6.5	25	3.24E-01	[80]	2.50E+00	[58]	9.53
Benzaldehyde	-9.944	-0.989	-8.955	6.5	30	4.31E-01	[80]	2.50E+00	[58]	9.53
Ethylbenzene	-9.282	0.478	-9.76	5.0 - 7.0	30	1.13E-02	[72]	1.40E+01	[58]	8.76
Ethylbenzene	-9.282	0.478	-9.76	7.0	25	3.90E-03	[35]	1.40E+01	[58]	8.76
Isopropyl Benzene	-9.398	0.495	-9.893	7.0	25	7.70E-03	[35]	1.10E+01	[58]	8.69
m-Xylene	-9.191	0.459	-9.65	5.0 - 7.0	20	6.00E-04	[72]	9.40E+01	[58]	8.56
m-Xylene	-9.191	0.459	-9.65	5.0 - 7.0	30	1.49E-03	[72]	9.40E+01	[58]	8.56
o-Xylene	-9.163	0.459	-9.622	5.0 - 7.0	20	8.90E-04	[72]	9.00E+01	[58]	8.56
o-Xylene	-9.163	0.459	-9.622	5.0 - 7.0	30	2.05E-03	[72]	9.00E+01	[58]	8.56
p-Xylene	-9.032	0.432	-9.464	5.0 - 7.0	20	1.15E-03	[72]	1.40E+02	[58]	8.45
p-Xylene	-9.032	0.432	-9.464	5.0 - 7.0	30	2.94E-03	[72]	1.40E+02	[58]	8.45
Toluene	-9.309	0.473	-9.782	5.0 - 7.0	20	2.30E-04	[72]	1.40E+01	[58]	8.82
Toluene	-9.309	0.473	-9.782	5.0 - 7.0	30	6.10E-04	[72]	1.40E+01	[58]	8.82
Toluene	-9.309	0.473	-9.782	7.0	20	7.00E-04	[73]	1.40E+01	[58]	8.82
Toluene	-9.309	0.473	-9.782	7.0	25	8.32E-04	This Study	1.40E+01	[58]	8.82

COC	E_{HOMO} (eV) PM5/H_2O	E_{LUMO} (eV) PM5/H_2O	E_{Gap} (eV) PM5/H_2O	pH	Temp °C	k" KMnO$_4$ (M^{-1}s^{-1})	KMnO$_4$ Ref	k" Ozone (M^{-1}s^{-1})	Ozone Ref	IP^a (eV)
Misc. Compounds Used Only in the Scatter Plot For All Compounds										
Chloroform	-11.076	0.548	-11.624	7.0	25	5.63E-04	This Study	1.00E-01	[58]	11.4
Fumaric Acid	-11.761	-1.657	-10.104	4.1	25	1.80E+03	[81]	6.00E+03	[59]	
Fumaric Acid	-11.761	-1.657	-10.104	4.5	25	1.50E+03	[81]	6.00E+03	[59]	
Fumaric Acid	-11.761	-1.657	-10.104	4.8	25	1.30E+03	[81]	6.00E+03	[59]	
Fumaric Acid	-11.761	-1.657	-10.104	5.3	25	1.30E+03	[81]	6.00E+03	[59]	
Glyoxylic Acid	-11.079	-1.641	-9.438	4.6	25	2.10E-01	[79]			
Maleic Acid	-11.798	-1.802	-9.996	4.1	25	1.84E+03	[81]	1.00E+03	[59]	
Maleic Acid	-11.798	-1.802	-9.996	4.3	25	1.72E+03	[81]	1.00E+03	[59]	
Maleic Acid	-11.798	-1.802	-9.996	4.4	25	1.73E+03	[81]	1.00E+03	[59]	
Maleic Acid	-11.798	-1.802	-9.996	4.8	25	1.66E+03	[81]	1.00E+03	[59]	
Maleic Acid	-11.798	-1.802	-9.996	4.8	25	1.57E+03	[81]	1.00E+03	[59]	
Maleic Acid	-11.798	-1.802	-9.996	4.8	25	1.47E+03	[81]	1.00E+03	[59]	
Maleic Acid	-11.798	-1.802	-9.996	5.2	25	1.45E+03	[81]	1.00E+03	[59]	
Maleic Acid	-11.798	-1.802	-9.996	5.3	25	1.51E+03	[81]	1.00E+03	[59]	
Maleic Acid	-11.798	-1.802	-9.996	5.3	25	1.48E+03	[81]	1.00E+03	[59]	
Maleic Acid	-11.798	-1.802	-9.996	5.7	25	1.28E+03	[81]	1.00E+03	[59]	
Maleic Acid	-11.798	-1.802	-9.996	5.8	25	1.10E+03	[81]	1.00E+03	[59]	
p-Chlorobenzaldehyde	-9.874	-1.139	-8.735	5.2	25	4.01E-01	[80]			
p-Chlorobenzaldehyde	-9.874	-1.139	-8.735	7.1	25	3.02E-01	[80]			
p-Chlorobenzaldehyde	-9.874	-1.139	-8.735	6.5	25	4.72E-01	[80]			
p-Methylbenzaldehyde	-9.658	-0.995	-8.663	5.2	25	5.52E-01	[80]			
p-Methylbenzaldehyde	-9.658	-0.995	-8.663	7.7	25	3.60E-01	[80]			
p-Methylbenzaldehyde	-9.658	-0.995	-8.663	6.5	25	3.41E-01	[80]			
p-Methyoxybenzaldehyde	-9.467	-1.054	-8.413	5.2	25	6.00E-01	[80]			

COC	E_{HOMO} (eV) PM5/H_2O	E_{LUMO} (eV) PM5/H_2O	E_{Gap} (eV) PM5/H_2O	pH	Temp °C	k" $KMnO_4$ ($M^{-1}s^{-1}$)	$KMnO_4$ Ref	k" Ozone ($M^{-1}s^{-1}$)	Ozone Ref	IP^a (eV)
p-Methyoxybenzaldehyde	-9.467	-1.054	-8.413	7.0	25	4.51E-01	[80]			
p-Methyoxybenzaldehyde	-9.467	-1.054	-8.413	6.5	25	3.85E-01	[80]			
p-Nitrobenzaldehyde	-10.438	-2.26	-8.178	5.2	25	3.48E-01	[80]			
p-Nitrobenzaldehyde	-10.438	-2.26	-8.178	7.3	25	2.88E-01	[80]			
p-Nitrobenzaldehyde	-10.438	-2.26	-8.178	6.5	25	2.24E-01	[80]			

a)   Unless otherwise noted, values for IP were obtained from [55].
b)   Value of IP obtained from [56].
c)   Value of IP obtained from [57].
d)   Value of IP obtained from [68].

Descriptors specific to the correlations with the substituted phenols

Substitued Phenol	$E_{1/2}{}^a$	σ^{-b}	$pK_a{}^c$
2-Chlorophenol	0.625	0.24	8.3
3-Chlorophenol	0.734	0.37	9.2
2,4-Dichlorophenol	0.645	0.48	7.8
246-Trichlorophenol	0.637	0.72	6.1
m-Cresol	0.607	-0.06	10.0
p-Cresol	0.543	-0.14	10.3
2-Nitrophenol	0.846	1.25	7.2
4-Nitrophenol	0.924	1.25	7.2
2,4-Dinitrophenol	1.137	2.50	4.1
Picric Acid	1.350	3.75	0.4

a)   Values obtained from [64].
b)   Values obtained from [65].
c)   Values obtained from [63, 66].

Biography

I was born on December 18, 1977 in St. Louis, MO. I was granted both a National Merit Scholarship and a Sigma/Dan Broida Scholarship to study at Iowa State University, where I received my Bachelor of Science degree in Biochemistry in May of 2000. After graduation, I worked for two years in a virology research lab at Oregon Health and Science University, where I created and studied drug-resistant strains of human cytomegalovirus.

In September of 2002, I began the Environmental Science and Engineering Master of Science degree program at the Oregon Graduate Institute (OGI). While at OGI, I gave an oral presentation at the Oregon Academy of Science (February 2004) and a poster presentation at the Fourth International Conference for the Remediation of Chlorinated and Recalcitrant Compounds in Monterey, CA (May 2004). Also in 2004, I received an American Chemical Society Graduate Student Award in Environmental Chemistry. The following is a list of my publications:

MacRae, A. F., R. M. Birch, R. H. Bange. 1999. Analysis of hexamer and pentamer motifs within a maize database: the presence of motif 'signatures' in functional gene categories. *Genetica.* **105:** 19-29.

Chou, S., R. H. Waldemer, A. E. Senters, K. S Michels, G. W. Kemble, R. C. Miner, and W. L. Drew. 2002. Cytomegalovirus UL97 phosphotransferase mutations that affect susceptibility to ganciclovir. *Journal of Infectious Diseases.* **185:** 162-169.

Waldemer, R. H. and P. G. Tratnyek. 2004. The efficient determination of rate constants for oxidation by permanganate. In *Proceedings of the Fourth International Conference on Remediation of Chlorinated and Recalcitrant Compounds, 24-27May 2004, Monterey, CA.* Monterey, CA: Battelle Press (in press).